Modeling Natural Attenuation of Wastewater-Contaminated Aquifers over Different Scales

by

Verónica C. Rojas Scheffer

A Thesis

Submitted to the Faculty of

WORCESTER POLYTECHNIC INSTITUTE

in partial fulfillment of the requirements for the

Degree of Master of Science

In

Environmental Engineering

By

Verónica C. Rojas Scheffer (signature)

Verónica C. Rojas Scheffer

July 2016

APPROVED:

Paul P. Mathisen (signature)

Professor Paul P. Mathisen, Ph.D., Major Advisor

John Bergendahl (signature)

Professor John Bergendahl, Ph.D., Committee Member

Abstract

Characterizing the effects of subsurface wastewater effluent discharges remains as a significant challenge impacting both ground-water and surface water resources. Important aspects of this challenge relate to the quantification of the main processes affecting oxygen consumption within a wastewater plume and to the ability of representing these conditions over a range of scales.

The goal of this research is to improve our understanding of the relevant processes affecting oxygen consumption and thus, controlling natural attenuation in wastewater contaminated aquifers, and also to characterize and quantify these processes through modeling approaches considering different scales. The analysis included consideration of restoration processes associated with a former sewage disposal discharge in Falmouth, MA. The discharge was removed in 1995, and the site has been experiencing natural restoration since removal.

A small-scale natural gradient tracer test, completed 6 years after cessation of sewage disposal, was used in previous research to develop parameters to characterize aerobic respiration and nitrification processes, key oxygen consuming processes for this site. In addition, field monitoring by the United States Geological Survey has provided a series of concentration profiles at different locations along the flowpath associated with the contaminant source. For this research, predictions obtained with the existing model were used in conjunction with these concentration profiles to assess the sensitivity and applicability in the parameters from this small-scale test, as well as their pertinence to the larger scale restoration process. By evaluating the applicability of this model to different scales and the associated variability of key model parameters, the approach provided an improved characterization of the primary processes affecting oxygen consumption.

Acknowledgements

Table of Contents

List of Figures

List of Tables

Abbreviations

Br^-	Bromide
Ca	Calcium
DO	Dissolved oxygen
DOC	Dissolved organic carbon
EPA	Environmental Protection Agency
K	Potassium
MMR	Massachusetts Military Reservation
Mg	Magnesium
Mn	Manganese
NH_4^+	Ammonium
NO_3^-	Nitrate
NO_2^-	Nitrite
NRC	National Research Council
SOC	Sorbed organic carbon
U.S. Geological Survey	United States Geological Survey
U.S.G.S.	United States Geological Survey

1   Introduction

1.1 Problem Statement

Subsurface disposal of treated wastewater effluent, originated from large municipal treatment facilities or from smaller, on-site household treatment systems, is an approach commonly taken for protecting surface water resources from the impacts of wastewater discharge (Mathisen, et al., 2010). However, the wastewater effluent discharge contains a mixture of organic and inorganic chemicals (LeBlanc, 1984), which contaminate the ground-water after infiltrating through the unsaturated zone. These practices can have severe impacts on ground-water quality, which may affect surface waters as well. Given the wide use of these facilities throughout the world, wastewater contaminated aquifers continue to be a widespread problem (Mathisen, et al., 2010; Repert, et al., 2006).

A well-known example illustrating the impacts of wastewater disposal practices is located in Cape Cod in Massachusetts, where wastewater disposal has resulted in ground-water contaminant plumes in an unconfined sand and gravel aquifer. After more than 60 years of disposal onto rapid infiltration beds, the source of treated wastewater was removed in 1995 (Repert, et al., 2006; Parkhurst, et al., 2003; Stollenwerk, et al., 1999; Smith, et al., 2013). For this study site, it was initially suggested that, after the contamination source was removed, the concentrations of dissolved oxygen in the plume would increase as uncontaminated ground-water flowed into the sewage contaminated zone from up-gradient areas (Hess, et al., 1996). However, more recent studies developed at this site indicated that oxygen entrainment into the contaminated zone was still slow, even after more than 15 years after the treated wastewater discharge was stopped. Previous research proposed that the movement of the front was controlled by the oxygen consumption related to the

aquifer solids (Smith, et al., 1999; Repert, et al., 2006; Smith, et al., 2013). Oxygen concentrations in ground-water regulate the geochemistry and microbiology of an aquifer (Smith, et al., 1999), and may be determinant to the natural attenuation evolution. This site shows that characterizing the effects of subsurface wastewater effluent discharges remains as a significant challenge impacting both, ground-water and surface water resources. Quantifying the main processes affecting oxygen consumption within a wastewater plume and representing these conditions over a range of scales is essential for quantifying natural attenuation.

1.2 Background

It is recognized that the impacts of the wastewater discharged from these facilities will be mitigated to some extent by natural attenuation. Natural attenuation includes the subsurface transport and transformation processes occurring at any contaminated site that naturally tend to reduce or mitigate the concentrations of contaminants of concern. The ability to understand these complex processes and their relevance in restoration of polluted aquifers is fundamental for addressing a proper management of contaminated sites. Natural attenuation is also viewed as a remediation technique which relies on natural physical, chemical and biological processes for the ground-water contaminant plume restoration, but it also involves careful and extended monitoring to ensure the site will eventually return to pre-contamination conditions. Its features make natural attenuation a non-intrusive and cost effective remediation approach for sites polluted by certain types of contaminants; however, the effectiveness of natural attenuation and overall impacts of the wastewater discharges on the environment are difficult to characterize, since the processes controlling the natural attenuation and ground-water restoration are still not completely understood.

The research at the Cape Cod site and other sites (Christensen, et al., 2000; Khan, et al., 2004; Schirmer, et al., 1999) demonstrates that detailed monitoring and extensive efforts to

characterize the contaminated site is a requirement for the application of natural attenuation. Furthermore, modeling of the fate and transport of the contaminants in the subsurface has been a widely applied tool for gaining insight into the processes and demonstrating the presence of natural attenuation at various study sites. Model development usually needs to be supported by a large amount of reliable data, which should be obtained, in many cases, throughout a long time period. Although it is recognized that simulation models provide a viable means for gaining insight into the processes in development at the subsurface, the model efficacy is, in many cases, limited by the availability of biological growth and decay rates as well as hydrogeologic data (e.g., porosity, hydraulic conductivity, and heterogeneities) (Kennedy, et al., 2004). Moreover, a wide range of spatial and temporal scales is involved in the study of ground-water problems, and usually small scale descriptions are aggregated into large scale models by applying averaging procedures. Even assumptions associated with the microscopic scale can have effects on the level of uncertainty in the modeling of a ground-water system (van der Heijde, et al., 1988).

Another approach that has been taken is to perform relatively short, small-scale experiments which may serve as a basis to develop and calibrate models, and to obtain parameters to characterize the main geochemical processes between the ground-water and the sediments. Six years after the treated wastewater disposal at the Cape Cod site was discontinued, a small-scale field experiment was conducted down-gradient of the abandoned disposal beds. Based on this field experiment, a one-dimensional reactive, advective transport model was developed using the PHREEQC software package (Mathisen, et al., in preparation). This model provided the base case for setting up a large scale model, aiming to investigate the variability in the parameters from the small-scale test when applied to extended spatial and temporal scales.

Chemical characteristics of the infiltrated effluent, as well as key processes occurring in the subsurface determine the evolution of the contaminant plume (Mathisen, et al., 2010). However, the mechanisms by which the sediment´s organic carbon and nitrogen pools contribute to oxygen consumption, and the relative relevance of each of these processes, are still not completely understood. Characterizing and quantifying the main processes controlling the natural attenuation of a wastewater plume, and the ability to accurately represent these processes over different scales through modeling approaches, is clearly an important question to be addressed.

1.3 Objective and Scope

The goal of this project is to characterize the main processes controlling the natural attenuation of a wastewater polluted aquifer, through the extension of an existing small-scale model, investigating the variability in the physical and geochemical parameters for fitting a large scale application. This was accomplished through the following specific objectives: 1) characterization of the variability in the parameters for different altitudes at the small-scale; 2) application of the existing small-scale model to an extended spatial and temporal scale; 3) calibration of the extended model to fit a set of field data; and 4) investigation of the variability in the parameters for the large scale. The existing model´s parameters are intended to describe the subsurface geochemical conditions and the interaction between the aquifer´s sediments and the dissolved constituents (sorption parameters), to represent the ammonium oxidation process and the related microbial activity (ammonium oxidation parameters), and to determine the features of the carbon oxidation process and of the aerobic respiring microorganisms responsible for this process (carbon oxidation parameters).

The characterization of variability in parameters at the small-scale was performed through the evaluation of the results of model applications to different sampling altitudes for the same site

and scale. Locations at different distances from the injection of the small-scale model were also examined, and the main processes contributing to oxygen consumption were quantified through the calculation of their corresponding rates.

For the extended application, the same small-scale model features and parameters were applied as a first step to assess the model capabilities and constraints at a larger scale. Then, calibration of the extended model was performed, based on field data originated from the long time monitoring of the wastewater plume by the U.S. Geological Survey. Afterwards, the parameters resulting from the large scale model calibration were evaluated in comparison to the small-scale parameters, and to previous research references. The main oxygen consuming processes at the extended scale were quantified, calculating the rates of development for these processes at the large scale. A characterization of the key processes controlling the natural attenuation of the wastewater plume at the large scale, based on the aforementioned elements, was finally proposed.

The sewage plume at the Massachusetts Military Reservation (MMR) in Cape Cod was selected for this study due to the amount of field and modeling data already in existence for this site (Savoie, et al., 2012; Savoie, et al., 2006). A variety of field and modeling efforts have been completed to characterize the plume after cessation (e.g. (Smith, et al., 2013; Stollenwerk, et al., 1999; Parkhurst, et al., 2003)) and a field tracer test has been completed in the discharge of this plume (e.g. (Mathisen, et al., in preparation)). The existing model is site-specific since it incorporates the effects of the physical and chemical characteristics of the site. However, its application and extension for a range of temporal and spatial scales provides valuable insight into the applicability of reactive transport models for characterizing natural attenuation processes.

Accordingly, the scope of this study includes the variation in the parameters as required to accurately simulate the relevant processes related to oxygen consumption for extended spatial and

temporal scales. This will lead to an improved understanding and ability to characterize the primary oxygen consuming processes associated with natural attenuation over different scales. A better comprehension about these parameters may also lead to recommendations for developing large scale models based on the performance of relatively short, small-scale studies, with consideration to the best ways to reduce costs and complexity in the development of modeling tools to support requirements for site monitoring. The development of a sensitivity analysis for the large scale version of the model may drive to a broader understanding of the uncertainty in model parameters and add greater scope for the study.

1.4 Report Outline

This thesis presents the background, methods, results and discussion, and conclusions and recommendations for an investigation about the use of a geochemical transport model to characterize natural attenuation of wastewater contaminated aquifers over different scales.

Chapter 2 provides background on natural attenuation definition and its related processes by describing these processes and indicating their role in contaminants remediation. Afterwards, a review about the scaling problem related to ground-water modeling is developed. The chapter continues with a detailed description of the selected site, and concludes with a summary of recent research and modeling approaches developed for this particular location.

Chapter 3 explains the overall approach of the research, followed by a brief overview of reactive transport modeling and a presentation of the code applied in this study. Then, the steps taken to develop the small-scale variability investigation, the approach selected for the model extension and its corresponding parameters' investigation are presented. Finally, the method followed for the characterization of the oxygen consuming processes is developed.

The results produced by the approach developed in Chapter 3 are presented and discussed in Chapter 4. This chapter is subdivided in two main sections. The first section presents the results of a small scale variability study, including assessments of the existing model´s performance at different locations and altitudes. The second section provides the results from the extended application of the model, focusing on model parameters discussion and main oxygen consuming processes characterization.

Conclusions and recommendations are presented in Chapter 5.

2   Background

The main goal of this project is to improve the understanding of the processes controlling natural attenuation, by extending an existing model and studying the key parameters over multiple scales. This chapter provides an overview of the literature and background information related to this research. First, a review of general concepts and processes regarding natural attenuation is presented. Next a brief discussion about scale considerations is developed, and finally the selected site of study is characterized in terms of its geological and hydrological features and along with the biogeochemical processes that are occurring at the site according to previous research.

2.1 Natural attenuation

Natural attenuation comprises processes experienced by all contaminant plumes, and it is also included as an option for remediation, management and control of polluted aquifers. Natural attenuation is also defined as an in situ treatment method which relies on natural processes to reduce the concentration and amount of contaminants at polluted sites (USEPA, 1996; Khan, et al., 2004). Another name for this treatment is monitored natural attenuation (Bekins, et al., 2001; USEPA, 2001). This term recognizes the dependence on natural processes, but also indicates that the approach is carried out in a carefully controlled context, within a reasonable time frame.

The concept of natural attenuation is not new. It was already referenced in the National Contingency Plan by the Environmental Protection Agency (EPA) in 1990 (NRC, 2000). Until 1996, EPA referred to natural attenuation mostly as a remediation approach for petroleum, TCE and other chlorinated solvents contamination, either as a combined or solely approach. Other ground-water polluted sites undergoing natural attenuation up to 1996 were landfills, refineries and recyclers (USEPA, 1996).

2.1.1　Natural attenuation as a remediation technique

Natural attenuation is recognized by the United States Environmental Protection Agency as a viable method of remediation for contaminated ground-water (USEPA, 2001; USEPA, 1996). It is selected due to its ability to achieve remediation goals in a reasonable time frame, and to its protection capabilities of human health and of the environment (Khan, et al., 2004), although its effectiveness depends on the geochemical conditions for the site and the types of contaminants.

Recently, the increased reliance and dependence on natural processes in site cleanup is a result of the wider recognition of its effectiveness under certain conditions and for specific contaminants, but it is also a result of the high costs of engineered systems (NRC, 2000).

Natural attenuation received increased interest in contaminated ground-water management due to an increase in the understanding of subsurface properties and of the ways in which natural processes impact plume migration. Moreover, the realization that many plumes exhibit little risk, combined with the limitations of pump and treat technologies commonly applied for ground-water remediation, have contributed to its broader consideration as remediation technique (Bedient, et al., 1997). The potential advantages and disadvantages of selecting natural attenuation as remediation approach are listed in Table 2-1.

Table 2-1 Potential advantages and disadvantages of monitored natural attenuation

Potential advantages	Potential disadvantages
Fewer remediation wastes, reduced potential for cross-media transfer of contaminants and reduced risk of human exposure to contamination (as any *in situ* process)	Longer time frames to achieve remediation objectives, compared to active remediation
Less intrusion	Complex and costly site characterization
Application to all or part of a given site	Toxicity of transformation products may exceed that of the parent compound
Use in conjunction with, or follow-up other remedial measures	Need for long-term monitoring
Lower overall remediation costs than active remediation	Need for institutional controls may be necessary to ensure long-term protectiveness
	Continued contamination migration, and/or cross-media transfer of contaminants

Source: based on data of EPA (1997), cited by Bedient (1997)

Natural attenuation focuses on the confirmation of occurrence of natural remediation processes rather than relying on 'engineered' remediation approaches (Khan, et al., 2004). Soil and ground-water samples must be collected and analyzed before natural attenuation can be proposed for a site. This is done in order to confirm and document that natural attenuation is actually occurring, as well as to estimate its effectiveness in decreasing the concentrations of contaminants over time (Khan, et al., 2004; Bedient, et al., 1997). In Table 2-2, key elements to demonstrate that natural attenuation is in development are shown.

Table 2-2 Key elements to demonstrate natural attenuation

Element	Application
Plume history	Demonstrate loss of contaminant mass that leaves the source. Define ground-water plume as stable, shrinking or expanding.
Geochemical indicators and rates	Demonstrate favorable conditions for contaminant mass loss. Indicator types: consumption of electron acceptors used for direct oxidative reactions; production of metabolic by-products.
Computer modeling	Demonstrate that site data are consistent with loss due to natural attenuation. Determine whether natural attenuation processes are sufficient to prevent further migration of the plume.

Source: prepared after Bedient, 1997

Natural attenuation processes are able to reduce contaminant mass and concentrations; or to bind contaminants to soil particles, preventing contaminant migration (Khan, et al., 2004; USEPA, 2001). Regarding the performance of natural attenuation, it is recognized as a relatively simple technology which implies little or no site disruption, although it can require more time than other remediation methods to achieve cleanup goals and is not considered an appropriate option for all sites (USEPA, 1996). Its cost lies mainly on the long-term monitoring program required, and depending of the attenuation rates, the plume could migrate. However, performance of natural attenuation is still difficult to predict (USEPA, 2001; USEPA, 1996).

2.1.2 Natural attenuation processes

In order to understand the potential implications for natural attenuation at any site, it is important to understand the processes that are included. The processes in a natural attenuation remediation approach might act, under favorable conditions, to reduce mass, toxicity, volume or concentrations of contaminants in ground-water (Khan, et al., 2004). These processes include physical, chemical and biological processes such as dispersion, diffusion, sorption, degradation (either biodegradation or abiotic processes such as hydrolysis), volatilization and dilution (Bedient, et al., 1997; USEPA, 1996; Khan, et al., 2004).

Natural attenuation processes can be categorized as destructive or non-destructive. Destructive processes destroy the contaminant, while non-destructive processes cause a reduction in contaminant concentrations (Khan, et al., 2004; USEPA, 1996). In many cases, a set of chemical reactions leads to contaminant transformation or immobilization. In other cases, the set of reactions prevents the contaminants from being transformed or immobilized, and may turn natural attenuation into an ineffective remediation strategy (NRC, 2000). In Table 2-3, a summary of the mentioned processes is presented. A more detailed discussion of natural attenuation processes is also presented in the following paragraphs.

As stated before, natural attenuation processes are often classified in physical, chemical and biological. Following this classification, a review of these processes is developed in the next paragraphs.

Table 2-3 Key Natural attenuation *in-situ* processes

	Process	Mechanisms	Description
Physical processes	Advection		Neither chemical nor biological reaction. Solute moves at seepage velocity of ground-water.
	Dispersion	Molecular diffusion Different water velocities in pores Tortuosity	Mixing of dissolved substance as the water moves, altering concentrations.
	Phase transfer	Sorption Volatilization	Sorption: slows movement of contaminants; is represented by a retardation factor. Volatilization: reduces total mass of contaminant in ground-water system.
	Dilution		Relatively clean water from ground surface can seep underground and mix with polluted ground-water; as well as clean ground-water flowing into contaminated areas.
Chemical processes	Degradation	Biodegradation Abiotic degradation	Biodegradation: contaminant can be the primary substrate, or it can degrade through co-metabolism. Abiotic degradation: acid-base, redox, precipitation and dissolution reactions, chemical sorption, hydrolysis, radioactive decay and aqueous complexation.

Source: prepared after Bedient (1997), U.S. EPA (1996) and National Research Council (2000)

Physical processes are the cause of contaminants to move in the subsurface. The relevant transport processes for subsurface contaminants can be categorized as advection, dispersion, or phase transfer, indicating transfer from one physical medium to another (NRC, 2000).

Advection: refers to the transport of a solute (a chemical species dissolved in water) occurring when the ground-water moves. In advection, the solute moves at the average velocity of the ground-water, without reacting chemically or biologically in the subsurface. Its concentration does not change from its initial value at the injection point; such chemicals are called "tracers" or "conservative solutes". The three key factors governing the velocity in the saturated zone are hydraulic gradient, conductivity, and porosity (NRC, 2000).

Dispersion: refers to mixing of substances dissolved in ground-water, which occurs as the water moves. The concentrations are different from those that would occur if advection were the only transport mechanism (NRC, 2000). The mixing is caused by ground-water movement and aquifer heterogeneities, and can occur in the longitudinal, transverse and vertical directions (Bedient, et al., 1997).

Molecular diffusion, different water velocities within individual pores, different water velocities between adjacent pores, and tortuosity of the subsurface flow path are the mechanisms leading to dispersion in the subsurface (NRC, 2000).

Dilution can be an important process for natural attenuation. Dilution may occur when a slowly moving ground-water plume flows into a zone with significant surface recharge; when contaminants migrate vertically through a low-permeability layer, and then mix with fast moving ground-water travelling horizontally through a more permeable underlying layer; and also when ground-water discharges to a surface water system with high flow rate relatively to the ground-water discharge (Bedient, et al., 1997). However, the National Research Council (NRC) was urged

to define natural attenuation as a process of degradation and/or transformation of contaminants that excludes dilution and dispersion processes. (NRC, 2000).

Phase transfer: relevant phases in the subsurface are ground-water, solids, NAPLs, and soil gas (air) in the vadose zone. Contaminants can be added to or removed from ground-water through their transfer between phases; this can increase or decrease the contaminant concentration in ground-water, depending on the mechanism, the contaminant, and the ground-water's chemical composition (NRC, 2000). The phase transfer processes are sorption and volatilization.

- The effect of *sorption* is to slow the movement of the contaminants, because the solids temporarily hold back some of the contaminant mass. The sorbed contaminants remain in the subsurface because the solids do not move, and can contaminate the water later by desorption (NRC, 2000). It is a non-destructive process in which organic compounds and metals are sorbed to the aquifer matrix, and it is often represented by a retardation factor, which indicates two processes: the degree to which a particular constituent moves slower than ground-water seepage velocity, and the ratio of total constituent mass per volume of aquifer matrix to the volume of dissolved constituents (Bedient, et al., 1997).

- *Volatilization* reduces the total mass of the contaminant in the ground-water system. The potential for volatilization is expressed by the contaminant's Henry's law constant. Volatilization does not permanently immobilize contaminant mass or destroy it. Instead, volatilized contaminants can biodegrade in some circumstances, but they can also re-dissolve in infiltrating ground-water, or be transported to the surface (NRC, 2000).

Degradation: Biodegradation and abiotic degradation involve chemical transformation of the constituent (Bedient, et al., 1997).

- In *biodegradation*, a wide range of reactions are able to be catalyzed by microorganisms, and these reactions are often considered the basis for natural attenuation. The chemical changes brought about by microorganisms can decrease the concentrations of contaminants (directly or indirectly) (NRC, 2000). Biodegradation can occur in two different ways: 1) biotransformation of a particular contaminant leads directly to energy generation and to growth of more microorganisms; in this case, the contaminant is named a "primary substrate"; 2) the fortuitous degradation of a contaminant when other materials are available to serve as the microorganisms' primary substrates is known as "co-metabolism" (NRC, 2000). Co-metabolism is considered not important under naturally occurring conditions (Bedient, et al., 1997).

- In *abiotic degradation*, many geochemical reactions can influence the potential for contamination control of natural attenuation. These types of reactions include acid-base, redox, precipitation and dissolution, chemical sorption, hydrolysis, radioactive decay, and aqueous complexation. Some of these reactions can decrease the hazards represented by contamination, while others can increase them. Furthermore, other reactions can influence processes affecting the fate of the contaminants (NRC, 2000).

Natural attenuation processes are contaminant specific, and the difference between organic and inorganic contaminants is particularly relevant. Another important feature to be taken into account is that mixtures of contaminants may present a different behavior compared to individual contaminants, due to several interconnecting processes. Natural attenuation success also depends on the hydrogeology and geochemistry of the site in question, as well as of environmental conditions which may vary with time (NRC, 2000; USEPA, 2001). Finally, some processes transform contaminants to forms that are less harmful to humans and the environment, but others form

products that are more hazardous or are more mobile in the environment than the parent contaminant (NRC, 2000).

2.1.2.1 Natural attenuation in wastewater contaminated aquifers

Contaminant plumes originated by subsurface disposal of treated wastewater effluent contain a wide range of pollutants that were introduced into ground-water. These constituents include organics, nutrients, metals and other constituents (Mathisen, et al., 2010; LeBlanc, 1984), and the transport and transformation processes associated with them as a mixture are still being object of study.

Transport of dissolved chemicals in a wastewater plume is influenced by processes causing retardation or restricting the movement, and by processes that cause spreading (LeBlanc, 1984). Downgradient of a site of treated wastewater discharge, biogeochemical transformations, aqueous complexation reactions, and reactions involving the aquifer´s sediments may occur. In regards to the biogeochemical transformations, dissolved oxygen concentrations are of great relevance in wastewater polluted aquifers. Some of the reactions in development may be associated to different oxidation-reduction zones, and likely include biodegradation process mediated by bacterial populations (Smith, et al., 1999; Smith, et al., 2013; Mathisen, et al., 2010).

Aqueous complexation reactions may occur between the treated sewage constituents and the aqueous solution. These reactions depend on many solution properties, and are frequently assumed to proceed to equilibrium in order to determine the speciation of the included constituents (Mathisen, et al., 2010). Finally, the contaminated ground-water´s interaction with the soil matrix may influence the processes taking place in the subsurface. These reactions are related to the sediment´s properties, but also to the properties of the aqueous solution, and include surface-

complexation and precipitation dissolution reactions (Mathisen, et al., 2010; Stollenwerk, et al., 1999; Parkhurst, et al., 2003).

Additionally, it was recognized that the dominance of the processes change significantly after the contaminant source is removed. For the wastewater plume at the Massachusetts Military Reservation area at Cape Cod, sorption, dispersion and denitrification were indicated as important processes before wastewater effluent discharge´s cessation. After the discharge was stopped, desorption, mobilization, oxidation and mineralization were suggested to be the main processes controlling the fate and transport of pollutants (Repert, et al., 2006).

2.2 Scale effects in ground-water modeling

Spatial and temporal scales are involved in the study of ground-water in a wide range. Spatial scales range from nanometers to hundreds of kilometers, whereas temporal scales may be classified in two major categories: steady state and transient state (van der Heijde, et al., 1988). It often happens that models are developed at a smaller scale than the one corresponding to other applications, which makes the upscaling necessary (Heuvelink, 1998). Small-scale processes are indicated as being highly variable in time and space, which difficult the use of local measurements directly, as well as the extrapolation of these measurements to large scale (Gelhar, 1993).

The potential problems related to scaling-up ground-water models examined for this research may be classified in two different categories: the implications of scale variation in ground-water heads prediction (Vermeulen, et al., 2006) and the variation of models from one scale to another regarding transport and reaction processes (Heuvelink, 1998; Carrera, 1993; Meile, et al., 2006). Since the goal of this study is to improve the understanding of the dominant processes contributing to oxygen consumption in wastewater contaminated aquifers, the following review is aimed to focus on the scale effects related to the latter. Additionally, the existing model on which

this investigation is based is a one dimensional model, and the ground-water heads are known at this particular site.

It is widely recognized that environmental processes, and among these, ground-water processes at large scales are the result of processes in development at smaller scales (van der Heijde, et al., 1988; Heuvelink, 1998). Despite this, it was also indicated that the models aimed to represent these processes can vary from one scale to another (Heuvelink, 1998; Carrera, 1993) and the errors and uncertainties related to the scaling problem have been classified in several ways for their study.

The causes of the uncertainties in model predictions may be attributed to uncertainties on future stresses, parameter values and conceptual models (Carrera, 1993). Among the conceptual uncertainties, the variation of the dominant processes at different scales is often indicated as being relevant for a successful model up-scaling (Carrera, 1993; Heuvelink, 1998); the quality and quantity of the available input data at a larger scale is also an important issue to be addressed (Gelhar, 1993), and the support of the inputs and outputs of a model may also change due to the change of scale (Heuvelink, 1998). Moreover, directional dependence of porosities and dispersivities obtained from field tracer tests, and the appropriate representation of breakthrough curves and pollutant plumes by the classical transport equation were also indicated as being related to conceptual difficulties in modeling transport processes at different scales (Carrera, 1993). The transport equation was indicated to be scale dependent, because the dispersion coefficient for field application is likely several orders of magnitudes larger than observed in laboratory experiments (Gelhar, 1993).

Aquifer heterogeneity was indicated as being related to scale effects in solute transport modeling, and the approaches to address this heterogeneity may be classified in stochastic and deterministic (Carrera, 1993). Stochastic approaches intend to treat the small-scale variability of

hydraulic properties as random, in a relatively simple and appropriate manner, combining the continuum description of small-scale physics with a probabilistic description of the variability (Gelhar, 1993). On the other hand, deterministic approaches are based on assumption that the advection-transport equation characterizes large heterogeneities and large velocity field variations, with the effects of smaller heterogeneities and small velocity field variations are represented implicitly as macrodispersion (Fitts, 1996).

This brief review is intended to recognize the effects of the subsurface heterogeneities in the up-scaling of a transport model, and to describe important considerations related to the application of a model to a larger scale compared to the scale for which it was originally developed. Since the intention of this investigation is not the development of a new model, but the application of an existing model to an extended scale, the considerations presented by Heuvelink (1998) were considered as appropriate to follow. The following subsections discuss these considerations concisely.

2.2.1   Variation of dominant processes at different scales

Modeling focusses on dominant processes, although ignoring other considered less important (Heuvelink, 1998). However, processes that are significant at a small scale may not be important at a larger scale and, on the other hand, different processes may emerge as a consequence of the increase in scale, which may affect the model structure (Carrera, 1993). Previous research indicated that the relevance of processes at different scales should be carefully considered. A certain process may not be only important at the scale at which it operates; instead, it may have relevance at other scales as well (Heuvelink, 1998).

2.2.2   Quality and quantity of available input data

There is the possibility that, at a large scale, measurements of input data are not available, and these inputs have to be derived from general information sources. The obtainment of the inputs in this way may involve some kind of transformation, which may cause a deterioration of the quality of the data and may lead to a model simplification (Heuvelink, 1998).

2.2.3   Inputs and outputs model support

Model support includes the size, shape and orientation of the model entities; this concept is related to the ´level of aggregation´ and ´sample volume´. A change of support may require modifications of the model, because it may imply a change in the relations between variables. In ground-water modeling, model parameters such as hydraulic conductivity and dispersivity change with this type of modifications, both in value and interpretation (Heuvelink, 1998).

It is important to indicate that a change of scale is not necessarily implying a change of support. In some cases, upscaling may reduce to spatial generalization or extrapolation, because the model entities retain the same support (Heuvelink, 1998).

2.2.4   Scale dependence of hydraulic conductivity and dispersivity

Differences between the real behavior of solutes and the one predicted by the advection-dispersion equation can be attributed to the spatial variability of hydraulic conductivity (Carrera, 1993). In subsurface hydrology, is simply assumed that the same small scale physical equation can be applied at the model grid with the same parameters, which may be related to problems due to the inherent spatial variability (Heuvelink, 1998).

The scale dependence of dispersivity was suggested to be explained by the growing size of heterogeneities (related to hydraulic conductivity) with the size of the model domain. The spatial

correlation of hydraulic conductivity may also address an explanation for the difference in shape of observed and computed breakthrough curves and solute plumes (Carrera, 1993).

2.2.5   Summary

In summary, models developed at the small scale must be adjusted for the applications at larger scale, for which the uncertainty analyses can be a helpful approach (Heuvelink, 1998). Furthermore, up-scaling a model should be done carefully, and the issues related to dominant processes, input data and parameters, model support, hydraulic conductivity and dispersivity should be properly addressed. These concepts provided a basis for the model development and parameter determinations completed for this investigation.

2.3 History of the site at the Massachusetts Military Reservation in Cape Cod, Massachusetts

As indicated previously, the site selected for this investigation is the Cape Cod Toxic-Substances Hydrologic Research Site, where a subsurface wastewater effluent discharge is has resulted in a large plume of wastewater-contaminated ground-water. The uncontaminated ground-water at this site was reported to be oxic, and to contain low concentrations of total dissolved solids, total nitrogen, nitrate, ammonium, total organic carbon, boton and chloride (Repert, et al., 2006).

Figure 2-1 shows the location of the Massachusetts Military Reservation in Cape Cod, Northeastern Massachusetts, and the location of the wastewater plume. The wastewater plume extends from former disposal beds at the Massachusetts Military Reservation´s municipal wastewater-treatment plant toward Ashumet Pond, other coastal ponds, and Vineyard Sound. For nearly 60 years, treated wastewater effluent was disposed onto rapid infiltration beds, until the discharge was stopped in December 1995. Since the cessation of the discharge, the site has been studied extensively by the USGS. (Savoie, et al., 2012; Smith, et al., 2013; Repert, et al., 2006; Parkhurst, et al., 2003).

2.3.1 Geology and hydrogeology

The study area is located on sand, gravel, silt and clay deposited during the retreat of the Pleistocene ice sheets from southern New England 14,000 years ago (LeBlanc, 1984). The site is located in an unconfined, non-calcareous, sand and gravel aquifer located on Cape Cod, Massachusetts (Smith, et al., 2013; Repert, et al., 2006). Two adjacent glacial lobes of the Wisconsin ice sheet provided meltwater for glacio-fluvial sedimentation, which currently makes up a large portion of Western Cape Cod. The glacial drift overlies Paleozoic crystalline bedrock, which surface ranges in altitude from approximately 75 ft below sea level near Cape Cod Canal to nearly 500 ft below sea level near Grand Island (Duncan, 1997). The advance and subsequent retreat of the Wisconsin ice sheet formed two recessional moraines, Buzzards Bay Moraine and Sandwich Moraine, composed predominantly by till. The Mashpee Pitted Plain lies between the two moraines, consisting on poorly sorted, fine to coarse grain outwash sands (Duncan, 1997; Gordon, 2001). Marine/lacustrine sediments and peats were reported in other geologic units, with peat layers tending to occur in kettle holes in the Mashpee Pitted Plain (Duncan, 1997).

Top altitudes of the aquifer were reported to be well sorted, brown, and medium to very coarse sand with some gravel. In the North portion, the outwash overlies fine sand and silt, whereas in the South, the outwash overlies fine to very fine sand and silt, and dense sandy till. Lenses of silt and clay, and of sand and gravel are contained in the till. Crystalline bedrock underlies these unconsolidated soils, and the bedrock slopes generally from west to east. The bedrock is assumed to be at the bottom of the aquifer (LeBlanc, 1984).
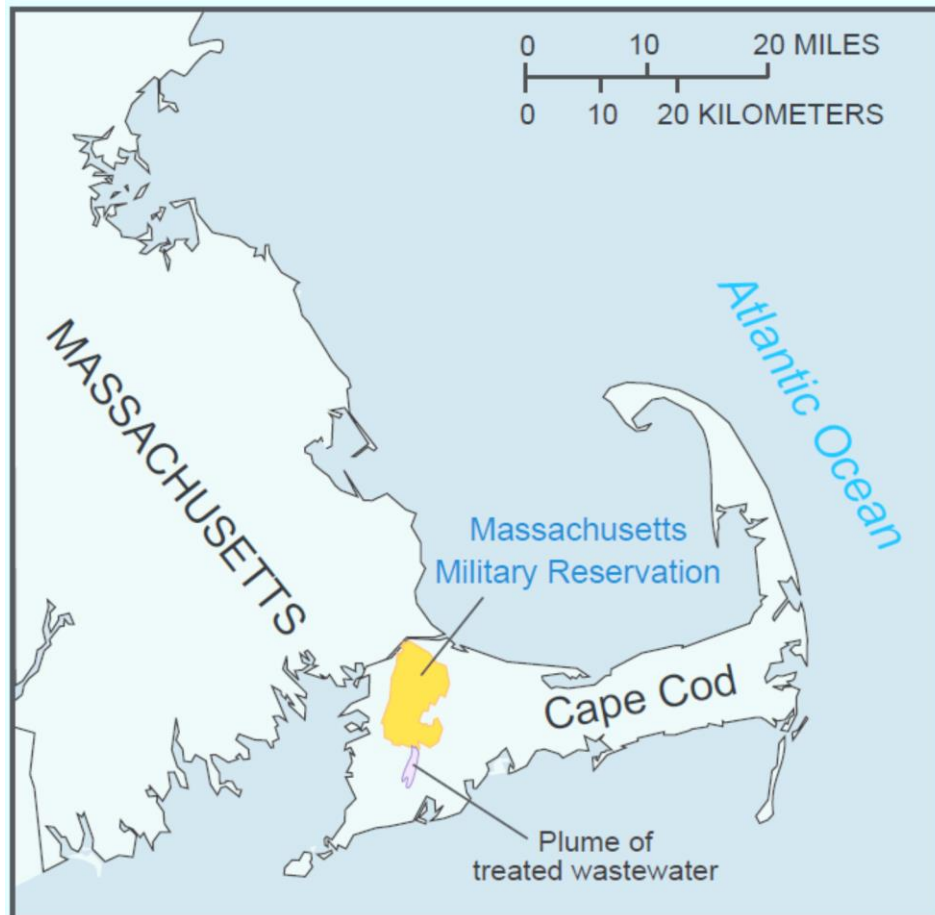
Figure 2-1 Location the Massachusetts Military Reservation in Cape Cod, Southeastern Massachusetts, and location of the wastewater plume.
Source: U.S. Geological Survey. Toxic Substances Hydrology Program

2.3.2 Natural attenuation processes at the contaminant plume in Cape Cod, Massachusetts

In order to approach the different processes in development at this particular plume, a review of previous research related to these processes was completed. This section summarizes previously investigated natural attenuation processes taking place at two specific locations in the wastewater plume, focusing on the variability of these processes along the plume, beneath and down-gradient of the former infiltration beds.

In order to improve the understanding of the processes controlling natural attenuation, the plume has been object of several studies. Oxygen consumption related processes at the wastewater

contaminant plume have been investigated through different methodologies, such as in situ tests (Smith, et al., 2006; Smith, et al., 1999), water samples analyses (Repert, et al., 2006; Smith, et al., 2006; Smith, et al., 1999; Smith, et al., 2013), isotope tracers (Bohlke, et al., 2006) and experiments with sediment cores (Smith, et al., 2013; Smith, et al., 1999). Several modeling approaches have also been developed in order to simulate the different processes occurring at this site (Stollenwerk, et al., 1999; Smith, et al., 2013; Parkhurst, et al., 2003; Bohlke, et al., 2006).

The ground-water contaminant plume was studied for more than 20 years and is estimated to be more than 8 km long, more than 25 m thick and over 1000 m wide (Stollenwerk, et al., 1999; Repert, et al., 2006; Smith, et al., 2013); it was found to be characterized by steep vertical gradients of dissolved constituents and includes an anoxic, ammonium-containing core surrounded by an oxic to sub-oxic nitrate-containing outer zone (Smith, et al., 2013; Smith, et al., 2006). The uncontaminated ground-water at this site was described as oxic, containing low concentrations of total dissolved solids, total nitrogen, nitrate, ammonium, total organic carbon and chloride (Repert, et al., 2006). Figure 2-2 depicts a plan view of Massachusetts Military Reservation area and the wastewater plume, as well as the location of the monitoring wells installed by the U.S. Geological Survey.

Figure 2-2 Plan view of the Massachusetts Military Reservation area and the wastewater plume. Black labels indicate sampling wells installed by the U.S. Geological Survey to monitor the contaminants along the plume.
Source: U.S. Geological Survey, map by Denis LeBlanc and Gillian Fairchild

Many research studies have been developed at this site since the treated wastewater discharge was stopped in 1995. Some of these studies were intended to determine the long-term evolution of the sewage plume (Stollenwerk, et al., 1999; Repert, et al., 2006; Smith, et al., 2013). Other studies focused on characterization and quantification of processes related to a particular constituent (Smith, et al., 2006; Parkhurst, et al., 2003; Smith, et al., 1999; Bohlke, et al., 2006; Miller, et al., 2009). A common observation among these different investigations is the absence or the very low level of dissolved oxygen in a large portion of the plume, despite the long time elapsed since the contaminant source removal.

After the wastewater discharge was stopped, uncontaminated (oxic) ground-water coming from up-gradient of the infiltration beds began to enter the contaminated zone (Stollenwerk, et al., 1999; Repert, et al., 2006; Smith, et al., 2013). Repert et al. (2006) reported that "a large portion of the plume core at S469 (10 to -3 m altitude, above mean sea level) remained anoxic after more than 8 years, suggesting that microbial processes and oxidation of reduced constituents, such as ammonium, were consuming oxygen entering the core of the plume underlying the infiltration beds." (p.1157).

The Cape Cod site was studied intensively after the cessation of the plume in order to get an insight into the biogeochemical processes related to natural attenuation. Two zones of the contaminant plume, the regions near Well S469 and Well F593 and F168, were studied in previous research, and thus may be considered as references regarding the processes occurring at the site (see Figure 2-2). Well S469 is located at the edge of the former treated wastewater infiltration beds. The processes in place at this well can be considered as a reference for understanding the oxygen consumption processes causing the permanence of the anoxic zone, despite the entrainment of uncontaminated ground-water beneath the infiltration beds. Another zone of the contaminant plume

that was intensively studied was between 2.4 and 2.5 km from the down-gradient edge of the

disposal location (well field F593 and well F168). This location may be considered representative

for the processes occurring down-gradient from the former infiltration beds. These locations can be

seen in Figure 2-3, which shows the location of the wells and multilevel samplers, the former treated

wastewater disposal beds, and the transect studied by the U.S. Geological Survey.
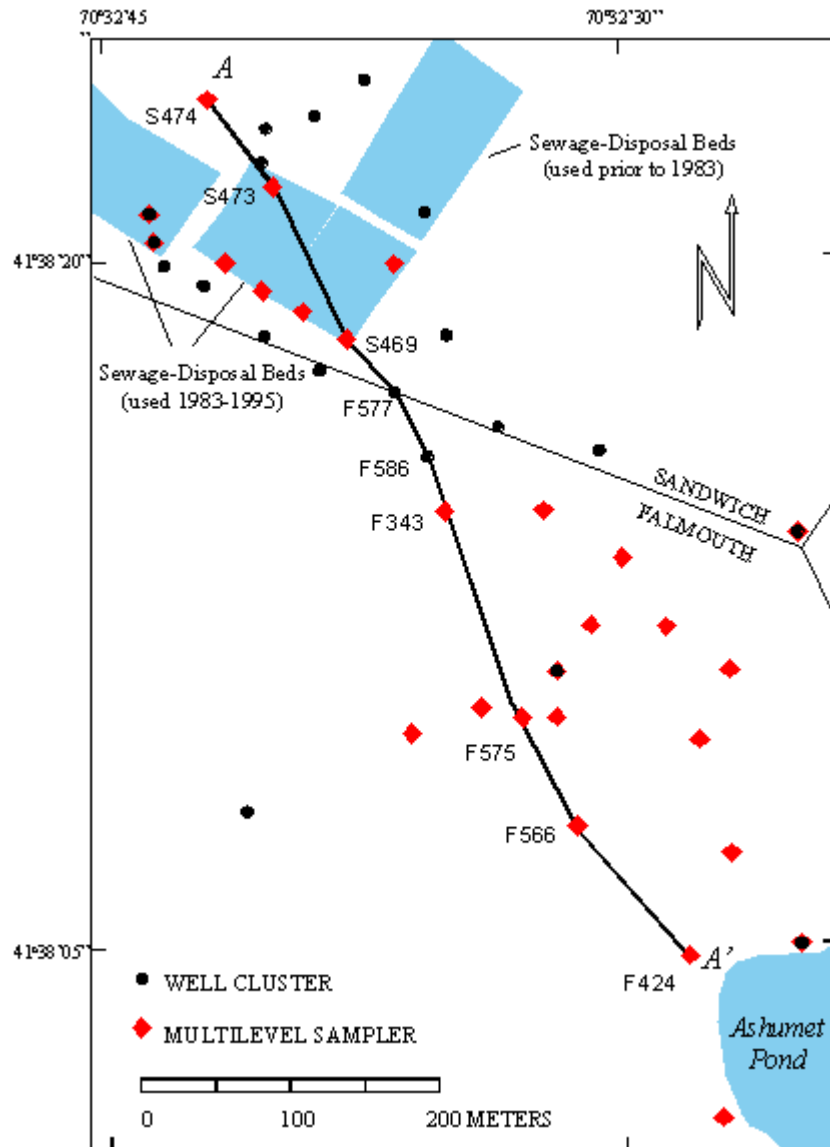
Figure 2-3 Map illustrating transect and well localities between sewage disposal beds and Ashumet
Pond.
Source: U.S. Geological Survey

 Researchers have identified two major processes occurring within this plume: ammonium oxidation (Repert, et al., 2006; Smith, et al., 2013; Smith, et al., 2006; Bohlke, et al., 2006; Miller, et al., 2009) and organic carbon oxidation (Smith, et al., 2013; Smith, et al., 1999). Oxygen consumption plays a main role in aquifer restoration, and it can be related to several processes. The processes were studied focusing on the vertical concentrations gradients observed for oxygen, dividing the plume in two main zones, anoxic and sub-oxic (indicating that dissolved oxygen concentration is less than the concentration in water in equilibrium with the atmosphere) (Smith, et al., 2006; Smith, et al., 1999; Bohlke, et al., 2006). As stated previously, the processes at the plume were also studied in regard to the direction of ground-water flow, identifying two major zones in this approach: one zone beneath the former rapid infiltration beds for wastewater discharge and another zone down-gradient of these infiltration beds (Stollenwerk, et al., 1999; Repert, et al., 2006; Smith, et al., 2013; Smith, et al., 2006; Parkhurst, et al., 2003; Bohlke, et al., 2006).

2.3.2.1 Ammonium transport and reaction, and related processes

Ammonium, which entered ground-water through treated wastewater discharge, was found to undergo two major processes: transport and oxidation. The movement of ammonium in the wastewater plume has been suggested to experience retardation due to physical-chemical processes such as sorption (Smith, et al., 2013), or to biological processes such as microbial induced transformations (Bohlke, et al., 2006).

Sorption slows the movement of the contaminants, because the aquifer´s solids temporarily store some of the contaminant mass; this difference in transport velocity of the constituents is represented by a retardation factor. After the wastewater discharge was stopped, the clean ground-water entering the zone caused desorption of the contaminants from the sediments. A sediment-associated source for the continued persistence of elevated concentrations of dissolved inorganic

nitrogen in the contaminant plume has been suggested by previous studies (Repert, et al., 2006; Smith, et al., 2013), and paired samples of ammonium in ground-water and ammonium extracted from core samples were approximately consistent with a linear sorption coefficient (K_{0d}) of 0.46 g H2O/g solid (Bohlke, et al., 2006).

Microbial oxidation of ammonium to nitrate (nitrification) is usually related to oxygen reduction, and it has been indicated that could be associated with the reduction of manganese oxides as well (Bohlke, et al., 2006). Previous studies conducted at different sites have concluded that nitrification does occur in ground-water. However, the form in which the nitrification process relates to other biogeochemical processes in ground-water to affect the transport and attenuation of ammonium is still under discussion (Smith, et al., 2006).

Nitrification was also likely to have been occurring at well S469, and it was suggested that nitrification was important in the conversion of sorbed ammonium to nitrate under the infiltration beds (Repert, et al., 2006; Miller, et al., 2009). After the treated wastewater source was removed, ammonium loss was documented over a ten-year period. Field experiments suggested that nitrification was active at this location during wastewater disposal, and that the nitrification potential persisted for a relatively long time after the discharge was discontinued (Miller, et al., 2009).

The wastewater plume was also likely undergoing nitrification at the end of the ammonium zone at well F593 (about 2.4 km from the removed contamination source) characterized by inversely vertical gradients of oxygen and ammonium, downgradient from the former infiltration beds. Moreover, clear evidence was also found for aerobic nitrification potential at a lower, anoxic depth which might have not received oxygen for several decades (Smith, et al., 2006). However, a deep isotope tracer test experiment in 1997 indicated no detectable nitrification was occurring within the

anoxic core of the ammonium cloud at the same location. Other nitrogen (N) species that coexist with ammonium (NH_4^+) are nitrate (NO_3^-) and nitrite (NO_2^-), but NH_4^+ and the other major dissolved N species in any given ground-water sample may not have come from the same source at the same time, and they may not be related to each other biogeochemically (Bohlke, et al., 2006). Previous research in this site indicated that a small part of the nitrate could have been produced by nitrification; instead, it was interpreted that most of the nitrate was recharged with the wastewater and partially denitrified within the aquifer up-gradient from the ammonium cloud (Bohlke, et al., 2006).

Additionally, the presence of a bacterial nitrifying community in the contamination plume has been reported after examination of aquifer cores at the two aforementioned locations (Well S469 and Well F168). However, Miller and Smith (2009) found that the nitrifying communities at these widely separated areas may be different (i.e. the nitrifying communities at the two aforementioned locations were indicated to differ due to the absence of Betaproteobacteria nitrifiers at S469 and their dominance at F168) (Miller, et al., 2009).

As mentioned before, ammonium transport at the wastewater plume was experiencing retardation, due to sorption and microbial induced transformations. Nitrification was suggested as the possible mechanism to explain the loss or sorbed ammonium at Well S469, although other investigations carried on at Well F593 indicated that the most part of the nitrate may have been introduced through the wastewater effluent discharge. The previous findings about different nitrifying communities at this two separated zones may also indicate that different processes may be in development in each of this mentioned areas.

2.3.2.2 Organic carbon oxidation and related processes

High organic carbon loads entered the ground-water through the treated wastewater discharge as well. Organic carbon coatings have accumulated on the surface of the aquifer´s sediments as a result of contaminant sorption during wastewater disposal (Stollenwerk, et al., 1999; Repert, et al., 2006; Smith, et al., 2013). As was the case for the ammonium, once the contaminant source was removed and oxic ground-water entered the contaminated zone, it was indicated that the organic carbon was being released from the sediments (Stollenwerk, et al., 1999; Repert, et al., 2006; Smith, et al., 2013; Smith, et al., 1999).

In regards to the organic carbon´s role in oxygen consumption, previous investigations proposed that the primary biogeochemical reaction in the sewage plume may be the oxidation of organic carbon by a succession of electron acceptors: O_2, NO_3, MnO_2 (manganese oxide), and FeOOH (iron oxy hydroxide) (Stollenwerk, et al., 1999). Elevated dissolved organic carbon (DOC) concentrations beneath the former infiltration beds, were interpreted to be related to desorption of sediment´s organic carbon and bacterial biomass associated with the sediments. The high and sustained DOC concentrations after the discharge´s cessation were associated to low dissolved oxygen concentrations more than 8 years after removal of the contaminant source (Repert, et al., 2006). However, in recent studies, oxygen consumption resulting from biodegradation of the DOC pool was assumed to be limited in the vicinity of well S469, but it was reported that the total sediment carbon content, although it was relatively low, was positively correlated with oxygen consumption rates in laboratory incubations (Smith, et al., 2013). Consequently with these approaches, other studies have linked oxygen uptake with aerobic respiration (Smith, et al., 1999).

Dissolved organic carbon concentrations prior to the discharge cessation, at the center of the plume (anoxic zone), were about 25 times greater than the typical uncontaminated concentrations

for the ground-water near this site. However, at the deepest part of the S469 vertical profile, the DOC concentrations were only 3 times these values (Parkhurst, et al., 2003). DOC concentrations recovered first at the deepest portion of the vertical profile, and this was attributed to the lesser amounts of sorbed organic carbon at the lower points (Parkhurst, et al., 2003; Smith, et al., 2013). The suggested decrease in the sorbed organic carbon pool with depth may be linked with the observed return of dissolved oxygen concentrations to pre-contamination conditions occurring first in the deeper ports (Repert, et al., 2006; Smith, et al., 2013), as can be stated in the published concentration profiles for this site (Savoie, et al., 2012; Savoie, et al., 2006).

The differences in concentrations trends for DOC and other soluble conservative constituents indicated that a sediment source might be responsible of the elevated concentrations of DOC along the plume throughout the years (Smith, et al., 2013). The oxidation of sorbed and dissolved organic carbon to inorganic carbon (DIC) was suggested by a markedly post-cessation increase in DIC concentrations at S469, and was proposed to be related to the sustained anoxic conditions beneath the former infiltration beds (Repert, et al., 2006). On the other hand, at the down-gradient zone at F168, observed concentrations of DOC and DIC were quite low and not as variable with depth (Miller, et al., 2009).

Many of these studies have related the sustained oxygen consumption capacity of the contaminated aquifer to two major processes: aerobic oxidation of ammonium to nitrate by bacterial communities (Smith, et al., 2006; Bohlke, et al., 2006; Miller, et al., 2009) and organic carbon oxidation due to aerobic respiration of bacteria (Stollenwerk, et al., 1999; Smith, et al., 2013; Smith, et al., 1999). These investigations also indicate that the dominance of either of both processes for oxygen consumption relates to several geochemical conditions and might change depending of the

zone of the aquifer considered and the time elapsed since the treated wastewater discharge was stopped.

Smith et al. (2013) affirmed that "degradation and desorption of sediment-associated organic contaminants after the source is removed are important components of natural attenuation, but this is a phase of the process that is poorly understood" (p.41). Thus, an important question that remains involves the mechanisms by which the sediment´s organic carbon and nitrogen pools contribute to oxygen consumption, and the relative relevance of one of these processes upon the other. Therefore, the present investigation is intended to contribute to the clarification of these questions.

3   Methods

This project included a series of model simulations to characterize the processes taking place at different scales, in a wastewater plume. The analyses made use of a combination of results from a previously completed tracer test and field data published by the U.S. Geological Survey (Savoie, et al., 2012; Savoie, et al., 2006). An extended application of the model at a larger scale was performed in order to evaluate the model capabilities and constraints related to scale effects.

This chapter describes the methods used for the research, including a brief description of the PHREEQC software package, the small-scale variability study, and the extended application of the model to a selected altitude within the wastewater plume. Furthermore, the methodology applied for the calibration of the large scale model and its sensitivity analysis are presented.

3.1 Overall approach

The investigation was performed considering two different scales: the small-scale from the natural gradient tracer test developed in previous research, and the large scale selected for modeling the section from Well S473 to Well S469 (as indicated in Figure 2-3).

Figure 3-1 displays a flow chart indicating the steps followed in the development of this research. First, a variability study was performed at the small-scale. This study was intended to assess the small-scale model results when applied to different locations and altitudes sampled during the test. The findings in regards to characterization and quantification of the oxygen consuming processes in development were taken as a basis for the further extension of the model to a larger scale.

The extended application of the model included the investigation of scale related effects on physical and geochemical parameters, the characterization and quantification of the main oxygen consuming processes likely to be occurring at this scale, and the evaluation of the model capabilities and constraints when applied to a different, extended spatial and temporal scale.
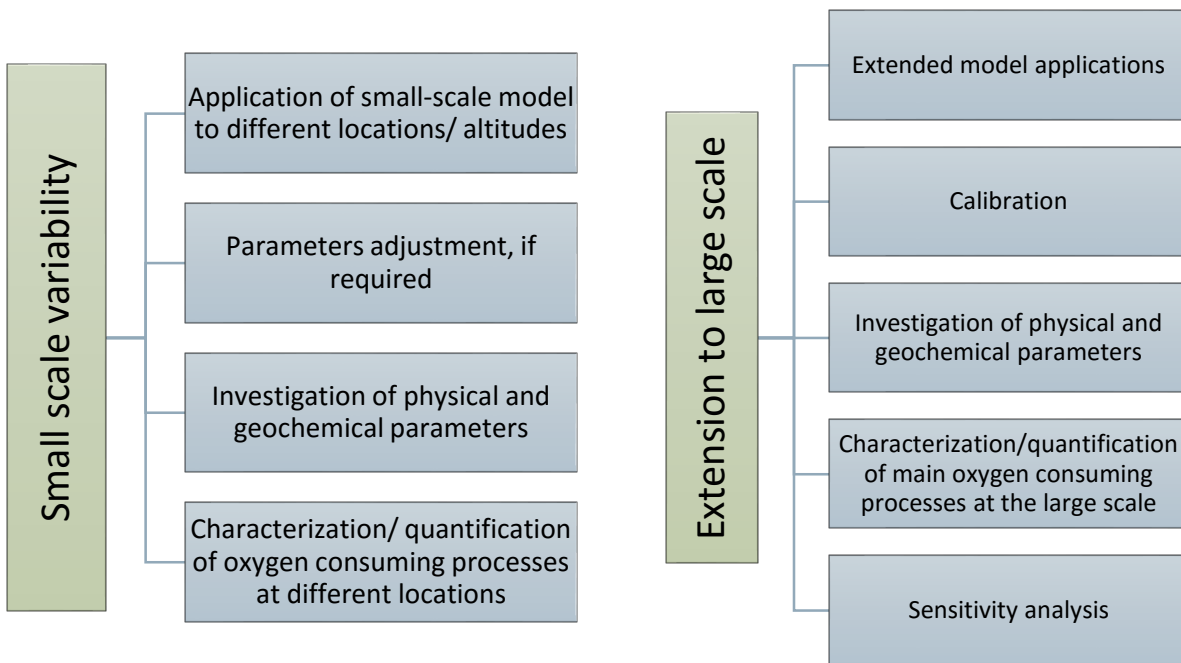
Figure 3-1 Overall approach taken for the investigation

3.2 Reactive-transport modeling

Forward modeling and reactive transport modeling attempt to predict the evolution of the water quality of ground-water, assuming specified hydrodynamic processes and reactions (Bundschuh, et al., 2012).

In this investigation, forward reactive transport modeling was applied in order to simulate the evolution of the wastewater plume, to investigate the parameters regarding different scales and to characterize the oxygen consuming processes likely to be in development. This section briefly describes the capabilities of the software package used for developing the previously existing small-

scale model and applied for the large scale version as well, and considerations in regards to the main processes assumed to be responsible of oxygen consumption in the simulations.

3.2.1 PHREEQC software package

The code used for the development of the existing small-scale model was PHREEQC version 3. This computer program allows simulation of chemical reactions and transport processes in natural or polluted water, and it includes equilibrium chemistry of aqueous solutions interacting with minerals, gases, solid solutions, exchangers, and sorption surfaces. The program also includes the capability to model kinetic reactions and 1D (one-dimensional) transport. Rate equations are user-specifiable and kinetic and equilibrium reactants can be interconnected by linking the number of surface sites to the amount of a kinetic reactant that is consumed (or produced) in a model period. A 1D transport algorithm simulates dispersion and diffusion (Parkhurst, et al., 2013).

The transport algorithms in PHREEQC use an operator splitting technique, where advection is modeled by shifting cell contents from one cell to the next at every time step or "shift". Dispersion and/or diffusion are simulated by mixing the aqueous contents of each cell with that of adjacent cells. This algorithm gives the code the advantage (over most typical finite-difference and finite-element codes) of being able to simulate not only an advective-dispersive transport process or a diffusive transport process, but also a purely advective, one-dimensional, transport process (Bundschuh, et al., 2012).

In regards to batch-reaction calculation, this software package is oriented toward system equilibrium rather than aqueous equilibrium, distributing the moles of each element in the system among the different phases to attain system equilibrium. Non-equilibrium reactions, temperature effects and pressure effects can also be modeled (Parkhurst, et al., 2013).

Sorption and desorption can be modeled as surface complexation reactions or as ion exchange reactions, and PHREEQC applies two models for surface complexation. One of these is based on the Dzombak and Morel (1990) database for complexation of heavy metal ions on hydrous ferric oxide, and the other model is CD-MUSIC (Charge Distribution MUltiSIte Complexation), which allows multiple binding sites for each surface. Ion exchange can also be modeled, and kinetically controlled reactions can be defined; rate expressions can be included in the input file. It is also possible to precipitate solid solutions from supersaturated conditions with no preexisting solid, and to dissolve solid solutions (Parkhurst, et al., 2013).

This code provides a numerically efficient method for simulating movement of solutions through a column, or one dimensional (1D) flow path, with or without dispersion effects. Initial composition of aqueous, gas and solid phases in the column are defined, and the changes due to advection and dispersion, and (or) diffusion, coupled with reversible and irreversible chemical reactions can be modeled (Parkhurst, et al., 2013).

3.2.2 Small-scale model considerations

A small-scale model developed in previous research, based on a natural gradient injection experiment, performed 6 years after the discharge's cessation, was used for characterizing the processes within the sewage plume. The experiment consisted in the injection of oxic ground-water at a location beneath the former treated wastewater infiltration beds, and was intended to assess the contribution for oxygen consumption of different processes (Mathisen, et al., in preparation).

This model was set and calibrated for a sampling altitude of 4.72 m (referred to mean sea level) in a Multi-Level Sampler (MLS). A one-dimensional model was considered to be appropriate for these simulations, because bromide (Br-) distributions indicated that dispersion was small and also, concentration distributions at this altitude, at 1.0, 4.6, and 6.2 m from the injection point were

considered representative of a single flow-path (Mathisen, et al., in preparation). Figure 3-1 shows the location of this small-scale experiment, and the well array used in the experiment. In this figure, the injection well and the monitoring wells considered to be in the modeled flow path are indicated.

The biodegradation processes considered in the existing small-scale model were nitrification of sorbed ammonium, and aerobic respiration using sorbed organic carbon as source. Nitrification (ammonium oxidation) was represented as two step reaction process (see equations 3-1 and 3-2), in which the oxidation of ammonium to nitrite was described by a rate-limited reaction using a Monod rate expression, and an equilibrium reaction was used to describe the subsequent oxidation of nitrite to nitrate (Mathisen, et al., in preparation). Aerobic respiration was assumed to be responsible of sorbed organic carbon oxidation (see equation 3-3), which was also described by a Monod rate expression.
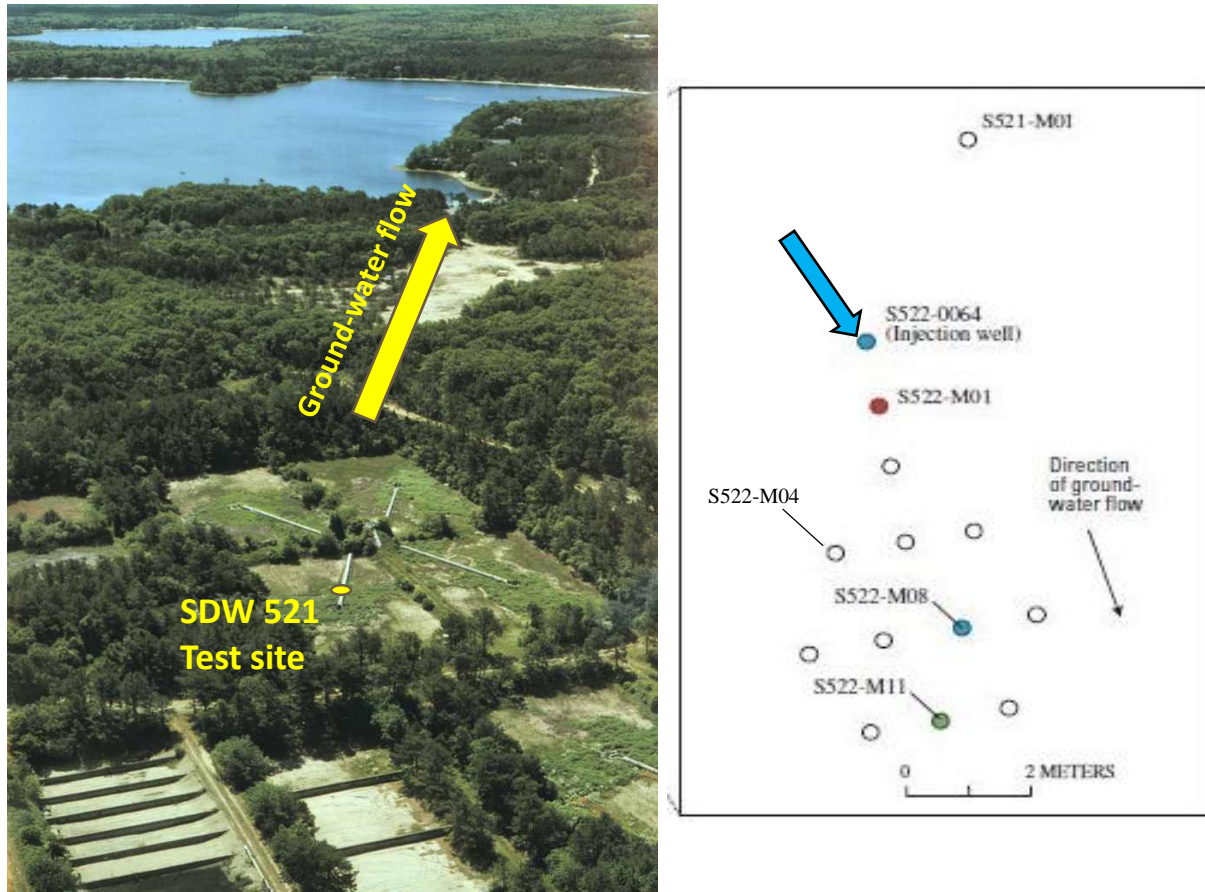
Figure 3-2 Left: location of the small-scale, natural gradient tracer test developed in previous research. Picture by Dennis LeBlanc for the U.S. Geological Survey. Right: Small-scale experiment setting.
Source: Mathisen et al., in prep.

The expression for oxidation of ammonium to nitrite is:

$$2NH_4^- + 3O_2 = 2NO_2^- + 4H^+ + 2H_2O \qquad \text{(Equation 3-1)}$$

and the oxidation of nitrite to nitrate is given by:

$$2NO_2^- + O_2 = 2NO_3^- \qquad \text{(Equation 3-2)}$$

The reaction for sorbed organic carbon oxidation is given by:

$$O_2 + CH_2O = CO_2 + H_2O \qquad \text{(Equation 3-3)}$$
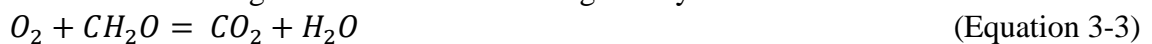
Reactions of ammonium and other cations with mineral surfaces were also considered in the model, and local equilibrium was assumed for reactions of aqueous and surface species. The initial chemical conditions derive from the equilibrium of the sediments with the background solution (Mathisen, et al., in preparation).

The selected model domain for the small scale test was a 6.5 m long section, and flux boundary conditions were used at the up-gradient and down-gradient ends of the section. The simulations followed the experiment´s setting, which consisted of an injection of oxic ground-water with a bromide tracer for a 75 day-period, followed by a shutdown period of injection of background-water for 25 days (Mathisen, et al., in preparation).

The small-scale model set up included varying injection concentrations, which allowed representing the actual injection conditions of the small-scale experiment. The injection was changed regarding the dissolved oxygen concentrations, which were considered to be in a range of 257.5 µmol/L to 287.5 µmol/L during the course of the test.

3.3 Small-scale variability study

In order to assess the variability in the parameters at the small-scale, and to investigate the processes occurring at different altitudes within the wastewater plume, the small-scale model was applied to two altitudes, at the same site. These altitudes were different from the calibration altitude to allow for an objective comparison with the calibration.

3.3.1   Small-scale model application to different altitudes

Field data were examined for altitudes of 4.27 m (designated as the green port) and 4.95 m (designated as the grey port) and compared with results from the calibration altitude of 4.72 m (designated as the yellow port). First, Br$^-$ concentration and specific conductance data were examined to determine if those sampling points could be considered within the injection cloud, at its edge or outside it. Starting with the existing model, simulations were performed for these two altitudes at four locations (1 m, 3.1 m, 4.6 m and 6.2 m from the injection point, named M01, M04, M08, M11, respectively) and then compared with the corresponding experiment's field data.

The simulations were compared by examining the concentrations of dissolved oxygen, dissolved organic carbon, ammonium, nitrate, pH, iron, and manganese at the four locations and the two altitudes. The concentrations of total dissolved inorganic carbon (TCO_2) used for comparison with the simulations were calculated with bases on pH, alkalinity and temperature data from the experiment, following the procedure reported by Mathisen et al. (in prep.), citing Kent et al. (2007). Moreover, the simulated sorbed organic carbon concentrations were examined, in order to assess the development of the aerobic respiration process, which is considered to be responsible for the sorbed organic carbon oxidation in this case.

In addition, simulations assuming only the nitrification (and no aerobic respiration process) to be in development, and after wards only the aerobic respiration process (and no nitrification process) were performed for selected locations considered to be within the injection cloud path, in order to investigate the fraction of oxygen consumption accounted for by each process.

3.3.2   Investigation of parameters

Parameters of interest for this step of the investigation include physical parameters and geochemical parameters. The physical parameters considered in the model were flow velocity, dispersivity and dispersion coefficient, whereas the geochemical parameters were divided into sorption parameters, ammonium oxidation parameters and carbon oxidation parameters.

Besides the small-scale model application to these altitudes and locations, simulations considering different values for the flow velocity were performed. The assumed velocities were based on the Br^- breakthrough plots obtained from the field data set, and considered the range of flow velocities for this site reported in previous research (Bohlke, et al., 1999). The corresponding parameters for dispersivity and dispersion coefficient were maintained for all small scale simulations. In regards to the geochemical parameters, the sorption coefficients, ammonium

oxidation parameters and carbon oxidation parameters were maintained for all the simulations corresponding to the small scale variability study.

3.3.3   Characterization of processes

At each of the examined well locations for the two selected altitudes, oxygen consumption rates were calculated. This was done by comparing the minimum dissolved oxygen concentration simulated within the duration of the experiment, to the corresponding concentration of dissolved oxygen from the injection. The porosity was assumed as 0.39 (Mathisen, et al., in preparation; Smith, et al., 2013), the travel time was calculated based on the assumed flow velocity for each altitude, and the dry solids content considered was 1864 g of dry sediments per liter of aquifer (Smith, et al., 2013). Additionally, the oxygen consumption rates for each of the biodegradation processes were considered separately and calculated assuming the same parameters, to quantify the contribution of each process to oxygen consumption.

Nitrification rates were calculated for the locations in each altitude that may be considered to be within the injection plume. The maximum nitrate concentration for each location during the experiment time course was compared to the nitrate injection's concentration assumed in the model (27.0 µmol/L), and the nitrification rate was then calculated based on the aforementioned values of porosity, travel time and dry solids content. Then, an oxygen consumption rate related to nitrification was determined, following equation 3-1 and equation 3-2.

Carbon oxidation rates for each of the selected locations were calculated as well. The maximum concentration of total dissolved inorganic carbon for each case was compared to the injection concentration of 246.1 µmol/L, corresponding to the concentration in location S522-0054, up-gradient from the experiment's injection point (Mathisen, et al., in preparation). Finally, oxygen

consumption rates corresponding to these carbon oxidation rates were calculated, following the equation 3-3.

3.4 Extended application

After assessing the variability of the small-scale model, the small-scale model was applied (or "extended") to a larger scale, using the same calibrated parameters obtained from the field experiment, as a first step. In order to calibrate the model to fit the extended spatial and temporal scales, the model parameters were adjusted following model upscaling recommendations developed in previous research (Carrera, 1993; Heuvelink, 1998) and also on the basis of comparisons with concentration profiles provided by the U.S. Geological Survey (Savoie, et al., 2012; Savoie, et al., 2006). The selected model domain comprises from Well S473 to Well S469 (see Figure 2.3).

For this investigation, the dominant processes from small-scale were assumed for the large scale application, because the large scale model was intended to be applied to the same site and the same zone for which the small-scale model was developed. The variability in the parameters and their applicability to the large scale were goals for this research, and the input data were reliable and abundant because of the extensive studies previously performed at the study site. In regard to the model support (interpreted here as the selected cell size), no major adjustments were made. Finally, the dispersivity value was taken from previous research developed at the same site (Hess, et al., 2002), through tracer tests that considered similar scales as the large scale corresponding for the present application.

3.4.1   Data review and selection for larger scale

The domain of the large scale model was selected to include the location where the small-scale tracer test was performed. The zone beneath the former infiltration beds for treated wastewater

was intensively studied, which assured the availability of reliable input parameters for the extended application of the model.

The selected altitude of -5.8 m was examined in previous research (Repert, et al., 2006; Smith, et al., 2013), and it corresponds to one of the lowest ports from the multilevel sampler at Well S469. This altitude was considered of interest because it was reported to be in the anoxic zone of the wastewater plume for several years, but the arrival of the oxygen breakthrough for this altitude was indicated in year 2004 (Savoie, et al., 2012).

The concentration profiles for different constituents used in this investigation were published by the U.S. Geological Survey (Savoie, et al., 2006; Savoie, et al., 2012). Additionally, alkalinity, pH, and temperature measurements were used to calculate total inorganic carbon (TCO_2) concentrations for samples corresponding from 1999 to 2007, because the data were not available. These calculations followed procedures applied in previous research (Kent, et al., 2007; Mathisen, et al., in preparation).

3.4.2   Large scale model considerations

At the larger scale, a one dimensional reactive transport model was considered to represent the flow path as well. The selected model domain for the section was 110 m long, beneath the former infiltration beds. Flux boundary conditions were used at the up-gradient and down-gradient ends of the section in order to maintain the small-scale model features. The extended model's starting point was Well S473, and the model domain extended up to Well S469 (at the edge of the infiltration beds) as depicted in Figure 3-3. The section was divided into 250 cells of 0.5 m each. This cell dimension was selected to match the average ground-water flow rate of 0.5 m/day (Smith, et al., 2013; Bohlke, et al., 1999) for a time step of 1 day.

The processes considered to be responsible for oxygen consumption in the extended application were the same as for the small-scale model, sorbed ammonium oxidation and sorbed organic carbon oxidation.

Four different representations were set up and calibrated in order to get the best fit to the concentration profiles for studied constituents, during the selected time course of 12 years:

1) Background from 1995: the first representation considered, as background solution, the concentrations from a sample taken at Well S469 in 1995, and as injection the concentrations from a sample taken at Well S474 (up-gradient of the former infiltration beds) in the same year;

2) Background from 1996: the second representation considered the background injection from Well S469, but in July 1996, and the same injection from Well S474, 1995;

3) Two different background solutions: the third representation considered two different background solutions, one from Well S469 in 1995 and the other from Well S469 in year 1999, changing from the first to the second background in 1999, and the same injection solution from the two aforementioned cases;

4) Two successive injection solutions: the last representation considered one background solution, from Well S469 in 1995, and two successive injections, the first one from Well S473 in 1995, and the second one from Well S474 in 1995.
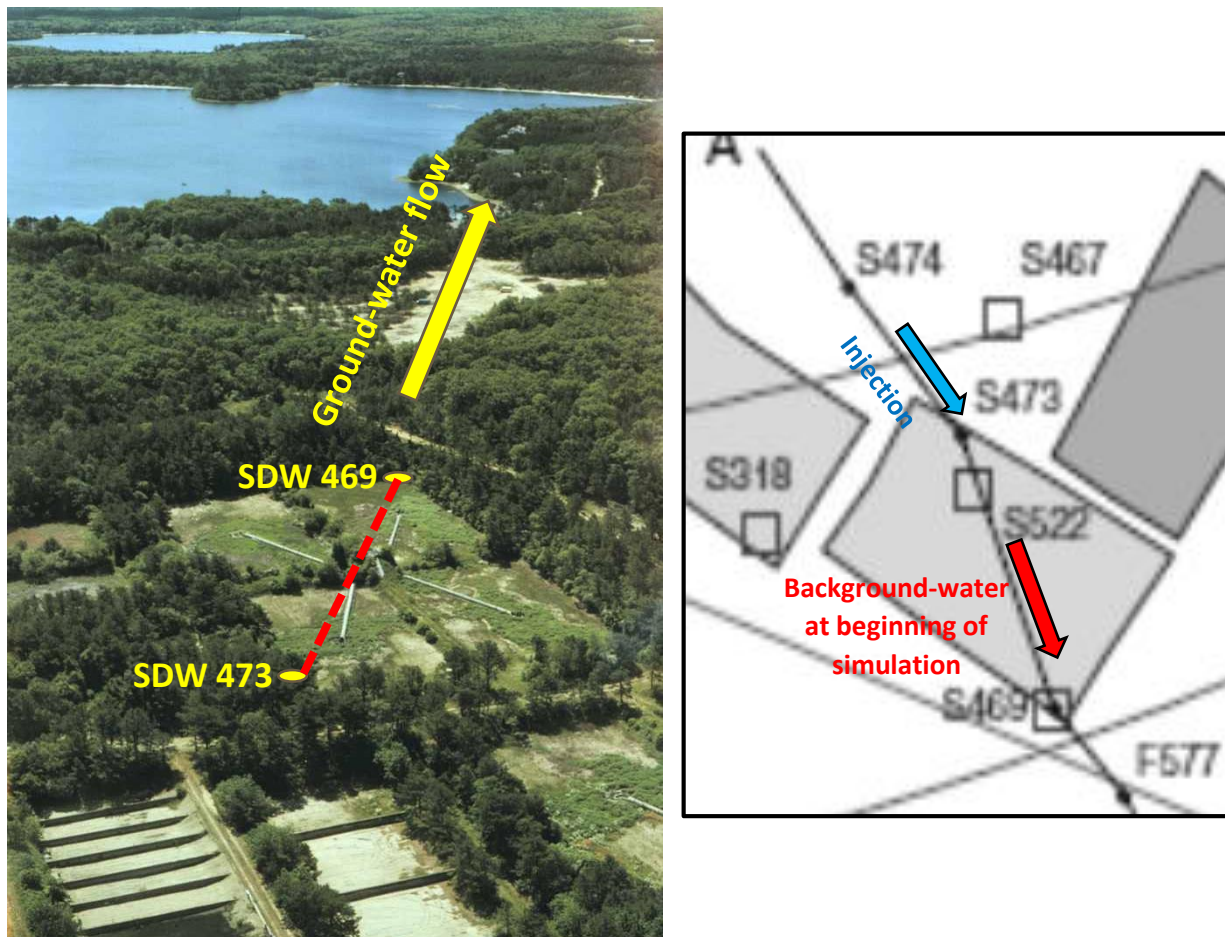
Figure 3-3 Left: Flow path considered for the large scale model application. Picture by Dennis LeBlanc for the U.S. Geological Survey. Right: Representation of large scale model setting, showing the location of the wells.
Source: Smith et al. (2013)

3.4.3   Extended model application

For the application of the existing model to an extended scale, the simulations were performed for an altitude of -5.8 m (referred to sea level), considered to be at the lower edge of the wastewater contaminant plume (Smith, et al., 2013; Repert, et al., 2006). The background and injection waters chemical conditions were based on published data for the considered altitude (Savoie, et al., 2006). In Table 3-1, the background and injection concentrations considered for the large scale simulations are shown. In this table, the different concentrations in the input constituents

are displayed. Note the high cation concentrations from background solution corresponding to year 1995, which is consistent with pre-cessation discharge concentrations.

For the concentration profiles from before 1999, alkalinity data were estimated for the background and injection water based on electroneutrality calculations included in the model, due to lack of data for the selected locations and times. Temperatures for input in the model were also estimated, based on temperature values of samples taken at similar times of subsequent years, for the same altitude and location.

The initial physical and chemical parameters for the extended simulations were assumed to be the same as for the small-scale case. These comparisons of the simulations with the field data (Savoie, et al., 2012; Savoie, et al., 2006) served as basis for the large scale model calibration.

Subsequent adjustments were made based on the sensitivity analysis performed for the small-scale model in previous research (Mathisen, et al., in preparation), as well as on previous research considerations about dispersivity (Heuvelink, 1998), in order to calibrate the model for the application at the extended scale.

Additionally, the large scale simulations were performed stepwise, as recommended by the PHREEQC code developers (Parkhurst, et al., 2013). Each simulation was started with a coarser grid (1.00 m), in order to obtain results fast, and have an insight into the occurring hydrogeochemical reactions. Then, the simulations were run with the finer grid (0.5 m) to decrease the effects of numerical dispersion. The explicit finite difference algorithm included in the code for the calculations of one dimensional advective-dispersive transport may show numerical dispersion when the grid is coarse (Parkhurst, et al., 2013).

Table 3-1 Background ground-water and injection ground-water constituent´s concentrations used for large scale simulations

	Background			Injection	
Sampling date	09/27/1995	07/25/1996	7/1/1999	09/22/1995	09/28/1995
Location	SDW 469-M01-12R	SDW 469-M01-12R	SDW 469-M01-12R	SDW 474-M01-12R	SDW 473-M01-12R
Ph	5.55	5.85	5.73	5.51	5.84
Alkalinity (µeq/L)	120**	80.00**	80.00	58.8**	53.60*
Temperature (C)	11.70*	16.40*	13.70	11.80*	15.20*
Ca (µmol/L)	616.21**	209.26	177.20	44.81	81.78
Mg (µmol/L)	235.46	73.38	102.41	75.82	130.86
Na (µmol/L)	2420.39**	496.79	739.78	172.34	520.65
K (µmol/L)	119.00**	82.82	26.72	21.34	24.39
Fe (µmol/L)	0.78	0.2	1.69	0.02	0.2
Mn (µmol/L)	1.90	0.54	0.74	0.20	1.32
Al (µmol/L)	1.85	1.85	1.85	1.85	1.85
Ba (µmol/L)	0.00	0.00	0.00	0.00	0.00
Cd (µmol/L)	0.00	0.00	0.40	0.00	0.00
Sr (µmol/L)	0.00	0.00	0.25	0.00	0.00
Zn (µmol/L)	0.25	0.40	0.26	0.25	0.25
Si (µmol/L)	191.73	176.61	151.33	162.81	165.09
Cl (µmol/L)	664.67	632.45	976.46	132.85	230.76
S(6) (µmol/L)	185.92	108.73	110.79	90.51	84.19
N_amm (µmol/L)	19.61	18.74	32.01	5.00	21.91
N(3) (µmol/L)	0.96	0.70	0.70	0.70	0.70
N(5) (µmol/L)	907.03	5.00	5.15	19.31	5.00
P (µmol/L)	32.91	52.35	25.72	3.23	3.23
Br (µmol/L)	0.00	0.00	0.00	0.00	0.00
O (0) (µmol/L)	18.75	18.75	30.63	562.5	37.5
B (µmol/L)	33.38	3.96	2.24	0.62	0.93
DOC (µmol/L)	301.28	67.73	30.00	28.90	12.49

*Estimated, not available from field data or analysis

**Adjusted, based on electroneutrality of solution

3.4.4 Calibration

For the large scale model calibration process, the parameters were divided in the following groups: 1) physical parameters, which included flow velocity, dispersivity and diffusion coefficient; 2) geochemical parameters, subdivided in three sub-groups: 2.1) Sorption parameters, 2.2) Ammonium oxidation parameters and 2.3) Carbon oxidation parameters.

3.4.4.1 Physical parameters

The physical parameters were adjusted based on previous research at the study site (Bohlke, et al., 1999), and investigations about model-upscaling considerations (Carrera, 1993; Heuvelink, 1998).

3.4.4.2 Geochemical parameters

For the geochemical parameters, the sorption parameters were not adjusted because the same values from the small-scale model calibration were considered to be representative for the extended application as well. These parameters were in the same range in previous models, developed at the same study site for different objectives, and which considered larger scales than the one selected for this investigation (Stollenwerk, et al., 1999; Parkhurst, et al., 2003). The geochemical parameters for ammonium oxidation and organic carbon oxidation are summarized in the next paragraph.

Ammonium oxidation. The ammonium oxidation parameters from the small-scale model were not varied, because the simulation of dissolved nitrate concentrations for the extended application performed before the calibration matched the field concentrations' profile well. Although the simulated dissolved ammonium concentrations did not match the field data very well for some of the selected model configurations, an explanation for the lower fit is proposed in the results section.

Organic carbon oxidation. The carbon oxidation parameters were considered to require adjustments. The initial sorbed organic carbon pool was considered as a key parameter to attain a good fit to the field's dissolved oxygen concentrations profile, as well as the growth and decay rates of aerobic respiring microorganisms. The first simulation used the small-scale model's parameters for the organic carbon oxidation. Afterwards, the initial sorbed organic carbon pool, the growth rate and the decay rate or aerobic respiring microorganisms were varied individually and as a set, until

a good fit for the dissolved oxygen concentrations, dissolved inorganic carbon concentrations and

pH profiles was attained for the extended application. The simulated concentration profiles for

sorbed organic carbon were also evaluated, allowing for the interpretation of the amount of sorbed

organic carbon being consumed according to the model.

3.4.5   Investigation of physical parameters

Among the physical parameters considered (Table 3.1), flow velocity and dispersivity were

adjusted for the extended application. Flow velocity was set to 0.5 m/day, which is in accordance

with field measurements (Bohlke, et al., 1999)and was assumed as the average flow velocity for

this site in previous modeling efforts (Smith, et al., 2013). Dispersivity was set to 1.5 m, based on

experimental values obtained for similar scales, from natural gradient tracer tests performed in

previous investigations (Hess, et al., 2002).

3.4.6   Investigation of geochemical parameters

The parameters obtained from the calibration process for the extended application were

compared with the parameters from the small-scale model, and also with reported values from

previous models developed at the same site, for different scales.

3.4.7   Characterization of processes

In order to characterize the relevant oxygen consuming processes within the wastewater

plume, the maximum oxygen consumption rate for each alternative for the extended application was

calculated. For this calculation, the minimum dissolved oxygen concentration obtained from the

simulation was compared to the dissolved oxygen concentration from the clean ground-water

considered as the injection in the model. The porosity was assumed as 0.39 (Mathisen, et al., in

preparation; Smith, et al., 2013), the travel time between the injection point at Well S473 and the

observation point at Well S469 was assumed to be 222 days, and the dry solids content of 1864 g

of dry sediments per liter of aquifer (Smith, et al., 2013). Additionally, the oxygen consumption rates for each of the biodegradation processes considered were calculated based on the same parameters, to quantify the contribution of each process to oxygen consumption at the large scale. A representative nitrification rate was also determined for the large scale application. For this calculation, the maximum nitrate concentration generated along the process was compared to the corresponding injection concentrations. An organic carbon oxidation rate was determined based on the simulations. In this case, the maximum generated concentration of dissolved inorganic carbon was compared to the injection concentration for dissolved inorganic carbon.

3.5 Sensitivity Analysis

The sensitivity analysis of the large scale model to selected parameters was performed by individually perturbing the model parameters to which the original small-scale model was found to be sensitive. Additionally, parameters that were considered relevant to the scaling-up process were included. The effects of nine model parameters were simulated, and the maximum oxygen consumption at Well S469 during the modeled time frame was calculated for each of these simulations. The parameters were increased and decreased by 20% to evaluate their effect on oxygen consumption, and the maximum oxygen consumption for each case was calculated following the same procedure as written in section 3.4.7.

From the sorption parameters, the one selected for this analysis was the sorption equilibrium constant for NH_4^+; from the ammonium oxidation parameters: half saturation constant for NH_4^+, microbial yield, and microbial growth rate; and from the carbon oxidation parameters: half saturation constant for O_2, microbial yield, and microbial growth and decay rates. Furthermore, the initial sorbed organic carbon pool was included in the sensitivity analysis, due to the dependence of

the timing for the oxygen front breakthrough on this parameter, which was detected during the large scale model calibration.

In summary, the investigation of the variability in the parameters and the characterization of the main oxygen consuming processes at the Cape Cod site were performed in two stages:

1. through model applications at different altitudes and locations for the small-scale, and comparisons to data sets sampled during the small-scale tracer test developed in previous research; and afterwards

2. through a model application to a larger scale which required calibration of the parameters to fit the concentrations distribution from the U.S. Geological Survey field data. The results corresponding to each of these stages is presented in the following chapter.

4   Results and Discussion

The goal of this investigation was to characterize and quantify the main oxygen consuming processes controlling the natural attenuation of the wastewater plume. This was achieved through a small-scale variability study, and through the analysis of the extended model application. In this chapter, results to characterize variability in the small scale test are provided first, in section 4.1. These results include the comparison of the simulated concentration profiles to the field data, and the calculation of rates for each of the assumed biodegradation processes, based on the simulations and the field data. Next, in section 4.2, results of the application of the model to an extended scale are presented. In this section, simulated concentration profiles for different constituents are compared with the corresponding concentrations from the field data. Then, the calculations of rates for the assumed biodegradation processes, based on the simulations, and the investigation of the variability in the model parameters are developed.

4.1 Small-scale variability

The following results focus on the small-scale application of the model for two studied sampling altitudes, one located above the calibration altitude for the small-scale model (4.95 m, Grey port) and another below the calibration altitude (4.27 m, Green port). At each of these altitudes, the model was applied at four locations, at 1 m, 3.1 m, 4.6 m and 6.2 m from the injection point. As a reference, results from the calibration altitude (4.72 m, Yellow port), developed by Mathisen et al. (in prep.) are included in Appendix A.

The simulations performed for the two altitudes closely matched the data for most of the studied locations. Thus, the model was found to effectively reproduce the processes occurring at the small scale. The Br$^-$ concentrations and specific conductance data indicate that the plume is sinking in the down-gradient direction, in which case some of the studied locations should be considered to

be at the edge of the injection cloud. These conditions might explain the poorer match of the simulations to field data for farthest locations at the 4.95 m altitude (6.2 m from injection point), because these points are likely to be showing a mixing between the injection and the background-water.

Variation of geochemical parameters was not required to attain good match to field data for the simulations at different altitudes. However, by varying the flow velocity to match arrival times, a better fit to field data could be obtained for the lower of the two investigated altitudes (i.e. 4.27 m). Previous investigations developed for this plume in the vicinity of the present study site mention that horizontal flow velocities may vary between 120 and 240 m/year, and flow velocities for 4.5 m elevation were estimated in 100 m/year (Bohlke, et al., 1999). Thus, these results are consistent with the selection of a lower flow velocity for the sampling altitude of 4.27 m (Grey port) below the original calibration altitude of 4.72 m (Yellow port).

4.1.1   Altitude 4.95 m (Grey port)

Figures 4-1 to 4-3 show observed and simulated concentration distributions for selected constituents for the 4.95 m altitude, at locations of 3.1 m, 4.6 m and 6.2 m from the injection point for the small-scale tracer test experiment, as well as plots from field data for specific conductance and bromide injection concentrations. Recognizing that the model was calibrated using data from the 4.72 m altitude, this location is selected to illustrate the variability for a region well within the plume. The bromide injection concentrations and the specific conductance data in these figures suggest that the locations at 3.1 m, 4.6 m and 6.2 m can be generally considered to be within the injection cloud, which is not the case for the location at 1.0 m from the injection point. It is noted that the injected bromide concentrations were variable, and zero from the period after 75 days. The injection included some periods with widely varying amounts of NaBr, and the Br- and specific

conductance varied significantly. The plots of Br- and specific conductance are still included to show the nature of the sampled water in relation to the plume of injected water. Since these short-term variations were not included in the model, the simulated model results for these parameters are not included for these figures.

The simulated dissolved oxygen concentrations accurately match the dissolved oxygen concentrations for the location at 4.6 m. A slight underestimation of oxygen consumption is shown for the first days at the location at 3.1 m. The simulations underestimate the oxygen consumption before 25 days at the farthest location (6.2 m), and overestimate oxygen consumption after 75 days. Considering that these two locations are within the injection cloud, a possible explanation for these inaccuracies may be the manganese peaks and subsequent depletion observed at these locations. Therefore, a manganese oxidation process is suggested as a possible explanation for the additional oxygen consumption in this time period. This process was not included in the model, and is recommended for future study.

The decrease in ammonium concentrations and the corresponding increase in nitrate concentrations, indicate that nitrification was occurring at the three locations considered to be within the plume. The simulations present a good fit to the corresponding data, although the nitrate generation is slightly underestimated for the location at 3.1 m and to a greater extent for the location at 6.2 m. Nevertheless, the simulated distributions correspond closely with the observations, and it may be concluded that the nitrification process is likely contributing to oxygen consumption at these three locations.
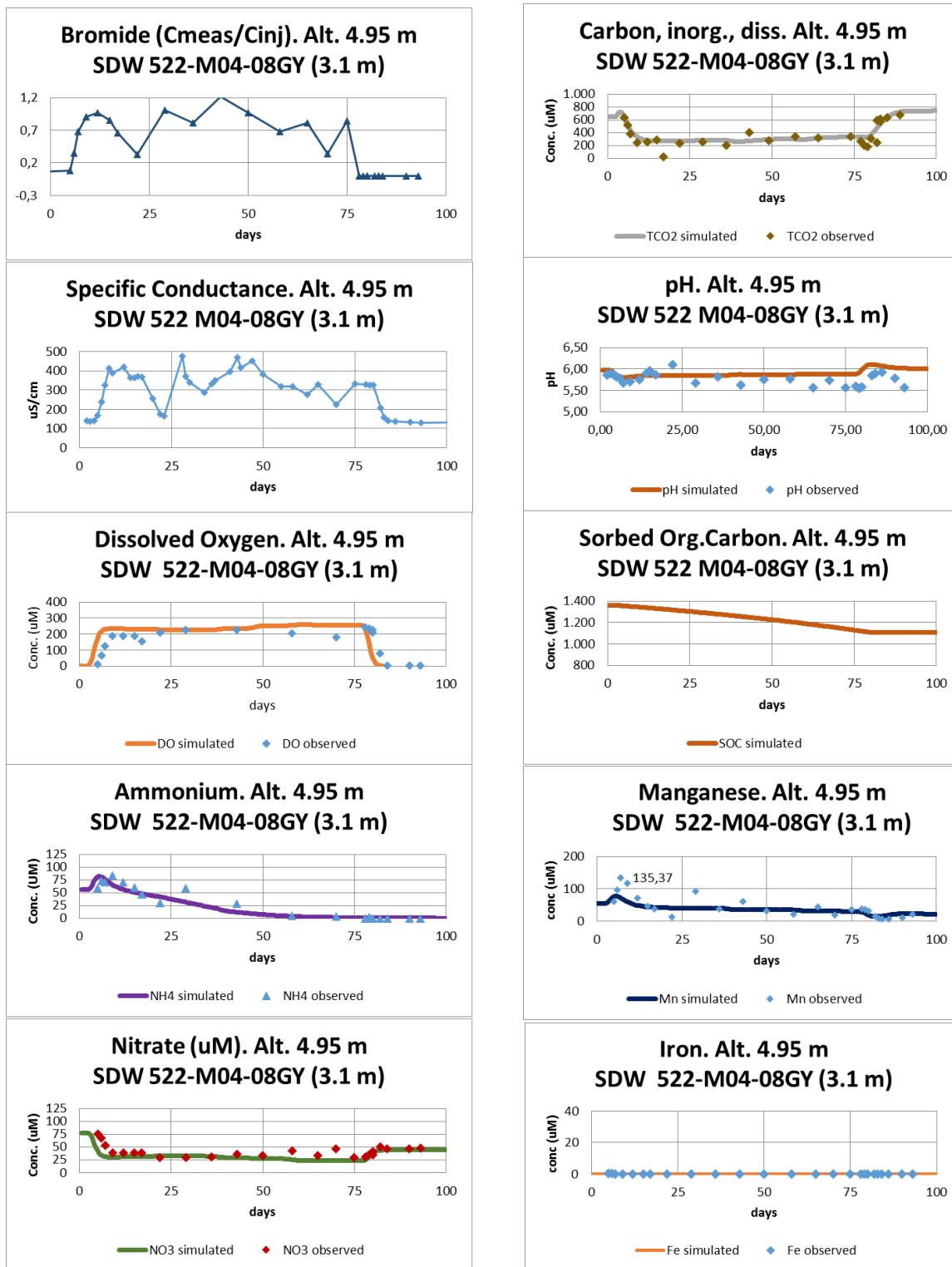
Figure 4-1 Simulated and observed concentrations for selected constituents during the experiment's time course, at altitude 4.95 m, for the location at 3.1 m from the injection well

Figure 4-2 Simulated and observed concentrations for selected constituents during the experiment's time course, at altitude 4.95 m, for the location at 4.6 m from the injection well

Figure 4-3 Simulated and observed concentrations for selected constituents during the experiment's time course, at altitude 4.95 m, for the location at 6.2 m from the injection well

The organic carbon oxidation process may be assessed by considering pH and inorganic carbon (TCO_2). The simulations of dissolved inorganic carbon concentrations present a good fit to the field data for all considered locations, at 3.1 m, 4.6 m, and 6.2 m. Moreover, for these three locations, simulated and observed pH concentrations match closely, which supports the likely development of organic carbon oxidation. In addition, the simulations of sorbed organic carbon concentrations indicate that organic carbon is being utilized throughout the duration of the tracer test.

Since the TCO_2 concentrations are variable, and a small amount of TCO_2 is required to account for the observed dissolved oxygen consumption, it is difficult to confirm the total amount of carbon oxidation based solely on the observed TCO_2 generation. Therefore, to gain a better understanding of the role of aerobic respiration and nitrification, simulations were performed by taking each of these biodegradation processes into account separately. Figure 4-4 shows the simulation results for locations at 4.6 m and at 6.2 m, including comparisons to field observations with oxygen consumption due to nitrification only, aerobic respiration only, and both nitrification and carbon oxidation. These plots show that nitrification, when considered separately, represents the oxygen consumption trends well, but underestimates oxygen consumption. Thus, the addition of carbon oxidation can account for the remaining consumption. The results suggest that both nitrification and organic carbon oxidation are required to account for the observed oxygen consumption.

Figure 4-4 Simulated and observed dissolved oxygen concentrations at altitude 4.95 m, for locations at 4.6 and 6.2 m from the injection point. Simulation results considering only the aerobic respiration process, and only the nitrification process are also included.

4.1.2   Altitude 4.27 m (Green port)

Figures 4-5 to Figure 4-7 show observed and simulated concentrations for selected constituents for the altitude of 4.27 m at locations 3.1 m, 4.6 m and 6.2 m from the injection point for the small-scale tracer test, and corresponding plots from field data for specific conductance and bromide injection concentrations. This sampling elevation is located 0.45 m below the elevation of the yellow port (i.e. of the sampling port used for calibration), and 0.68 m below the grey port (which was summarized in Section 4.1.1).

For this altitude, the location at 4.6 m from the injection point may be considered within the injection cloud. The location at 6.2 m seems to be in the cloud for some time periods and out of the cloud for other periods, based on the specific conductance and bromide injections plots presented in Figure 4-7. Moreover, the locations at 1.0 m and 3.1 m are considered to be out of the cloud at this altitude (see Figure 4-5). Therefore, the subsequent discussions do not consider the 3.1 m locations.

Comparisons between the simulated and observed concentrations of dissolved oxygen for the locations within the cloud and at the edge of the cloud (i.e. the 4.6 m and 6.2 m locations), reveal

that oxygen consumption is underestimated before 40 days for the location at 4.6 m, and before 50 days at the location at 6.2 m. However, the dissolved oxygen concentrations are effectively represented by the simulations after 50 days. Considering the peaks and subsequent depletion for the observed manganese concentrations, which do not match well with the simulations, a possible explanation for the oxygen consumption that is not accounted for by the model may be a manganese oxidation process. The variation in manganese concentrations is larger at the location at 4.6 m, where also the simulated pH concentrations are higher than the observed ones. Another possible interpretation is that some mixing of the injection with background-water could be occurring at this altitude before 40 days.

Nitrification should be indicated by the nitrate generation and its corresponding ammonium depletion. Ammonium concentrations present a good fit of the simulated to the observed concentrations. As such, nitrification is considered to be accounting for a fraction of the oxygen consumption at these locations. However, simulated nitrate concentrations are greater than the observed concentrations for the 4.6 m and 6.2 m locations. At 4.6 m, nitrification is likely occurring at a very low rate, whereas at 6.2 m, the nitrification process appears to increase significantly at day 50, and the simulated nitrate concentrations become similar in magnitude to the observed concentrations after 50 days.
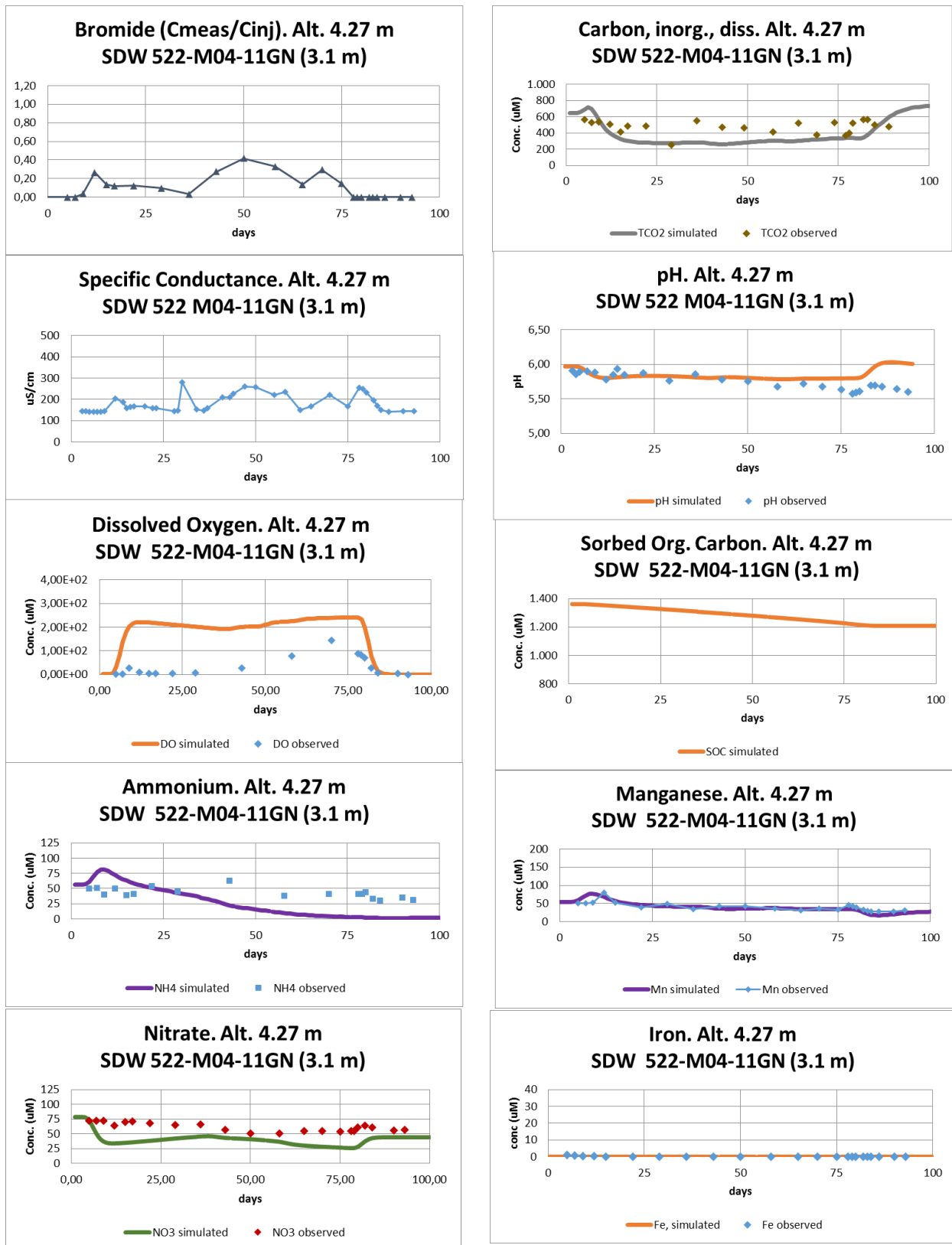
Figure 4-5 Simulated and observed concentrations for selected constituents during the tracer test experiment, at altitude 4.27 m, for the location at 3.1 m from the injection well
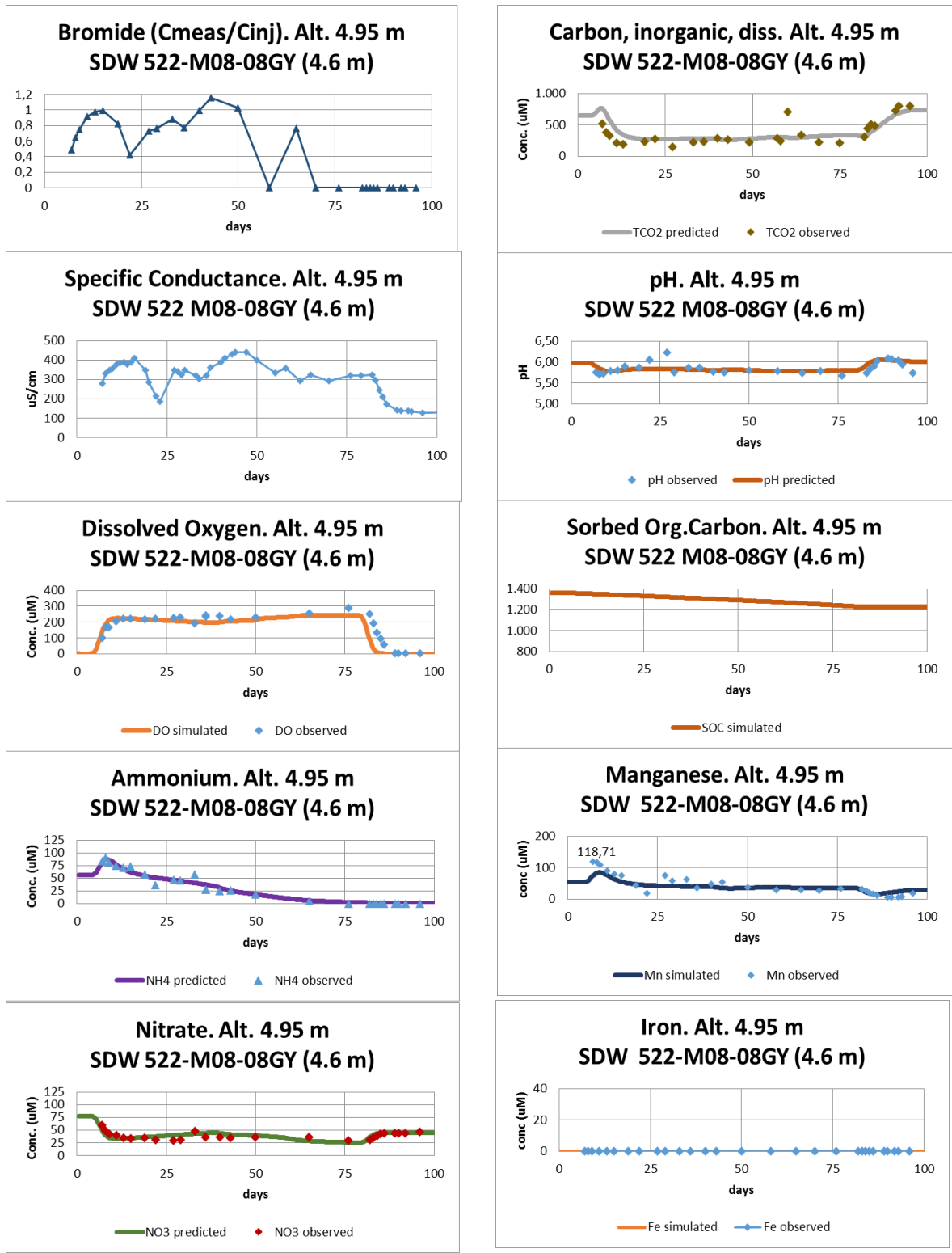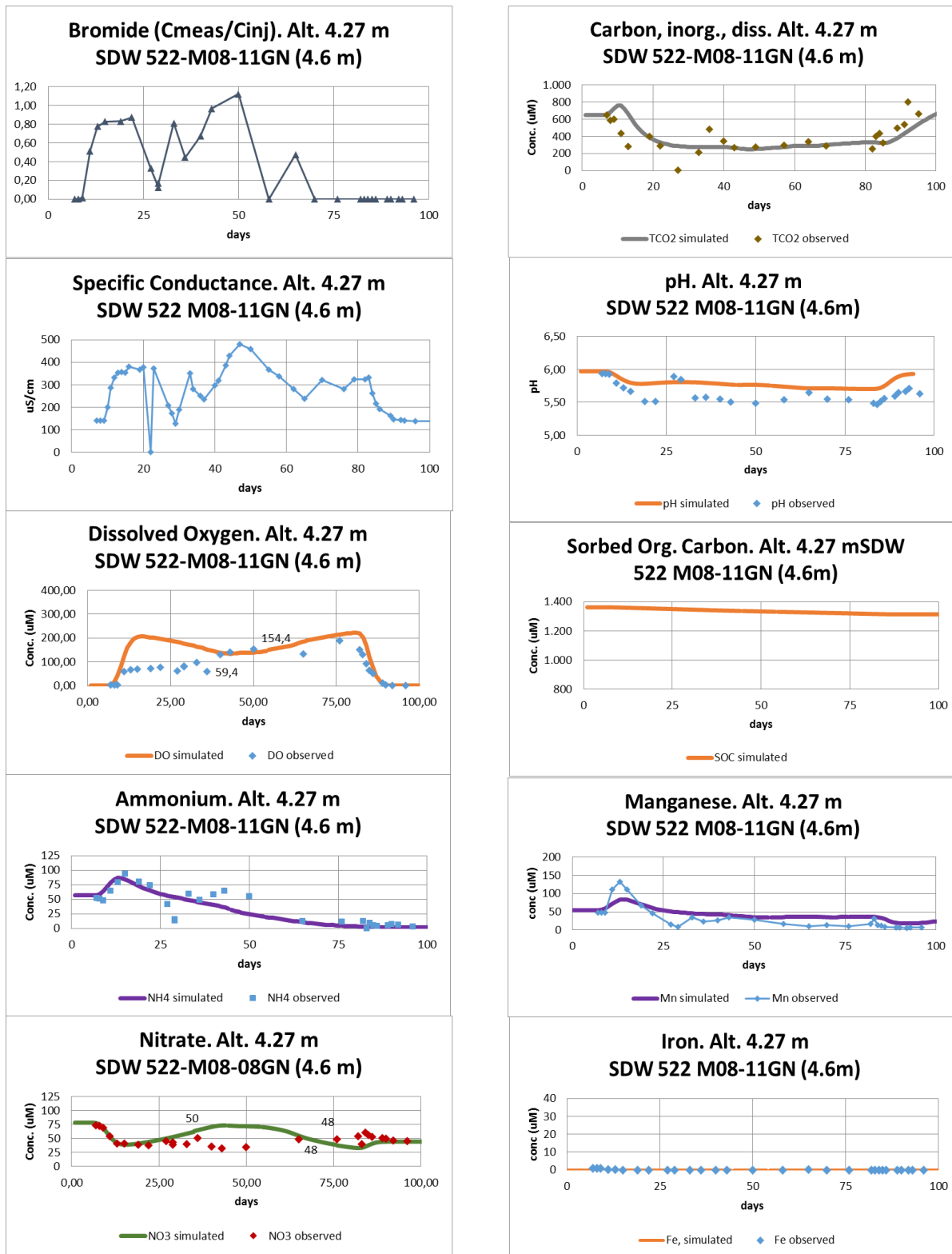
Figure 4-6 Simulated and observed concentrations for selected constituents during the tracer test experiment, at altitude 4.27 m, for the location at 4.6 m from the injection well
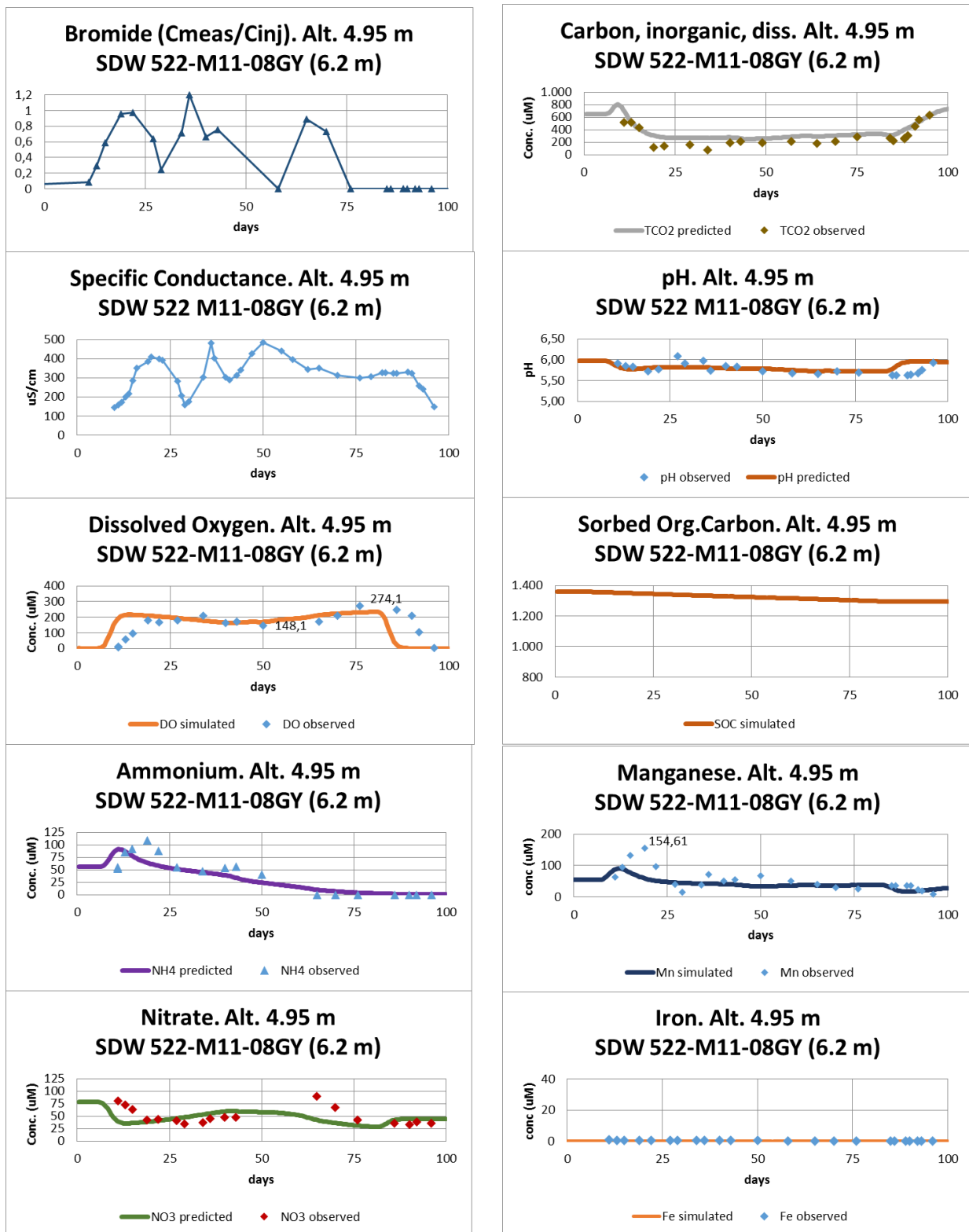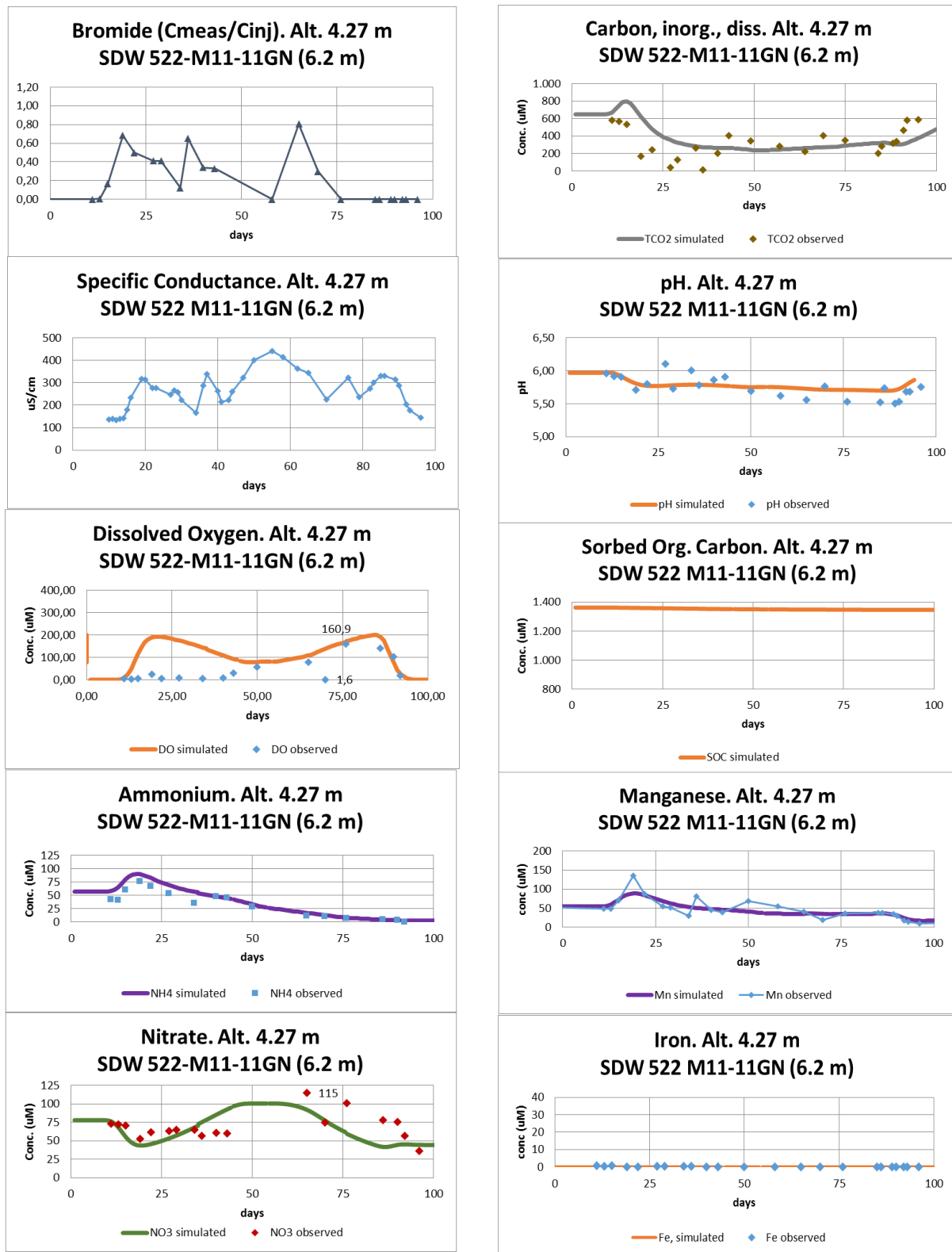
Figure 4-7 Simulated and observed concentrations for selected constituents during the tracer test experiment, at altitude 4.27 m, for the location at 6.2 m from the injection well

In general, simulations for dissolved inorganic carbon concentrations closely match the observed concentrations. Although the increase in concentrations for dissolved inorganic carbon is too small to formally verify that organic carbon oxidation is taking place at this altitude, the separated simulations performed considering each biodegradation process suggest that the aerobic respiration process is likely occurring, and that it may account for a fraction of the oxygen consumption. Figure 4-8 depicts simulated and observed dissolved oxygen concentrations when nitrification and aerobic respiration are assumed to occur simultaneously, and when each of the two processes is assumed to occur separately. The nitrification captures the trend of the oxygen concentrations well after 40 days for the location at 4.6 m, and after 50 days for the location at 6.2 m, but is not able to account for the entire observed oxygen consumption.
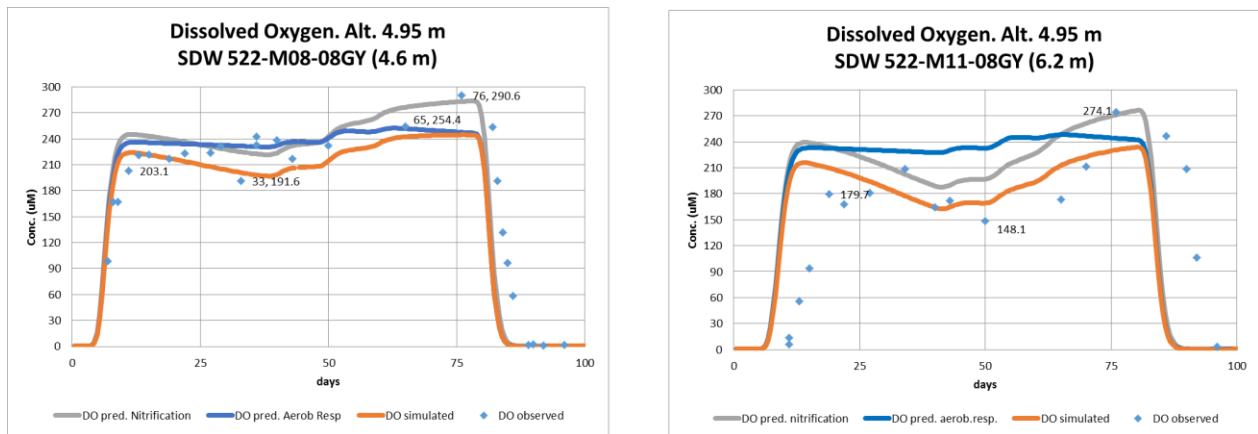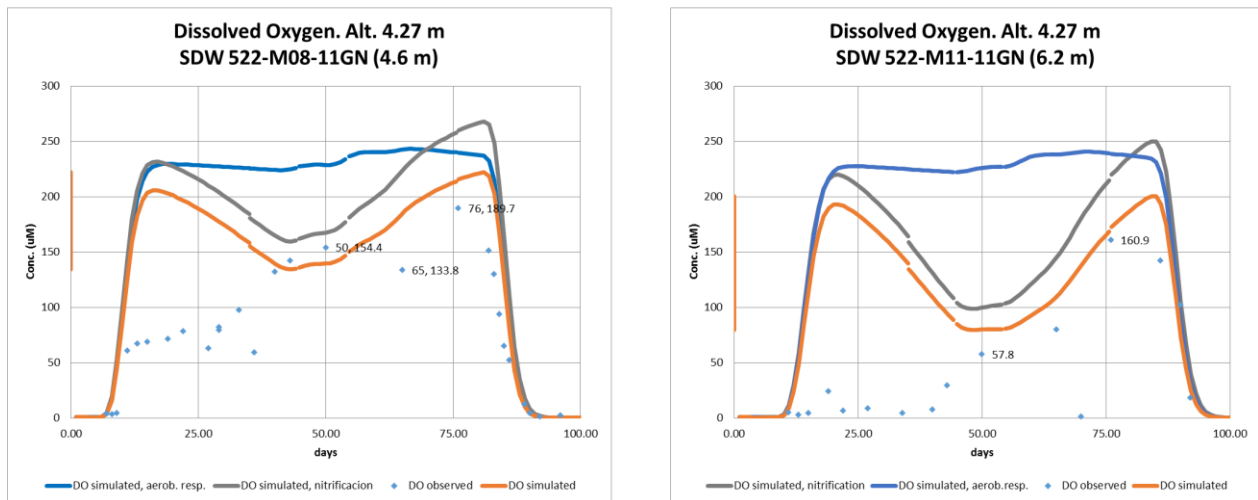

Figure 4-8 Simulated and observed dissolved oxygen concentrations at altitude of 4.27 m, for locations at 4.6 and 6.2 m from the injection point. Simulation results considering only the aerobic respiration process and only the nitrification process are also included.

The organic carbon oxidation process is also likely indicated by the overall good correspondence between simulated and observed pH. However, the match between simulated and observed pH is not very good at the location at 4.6 m, which may be related to overestimation of the oxidation processes. Finally, the simulated sorbed organic carbon concentrations indicate

consumption of organic carbon for the analyzed locations at 4.27 m altitude, which is also consistent with the organic carbon oxidation occurrence.

In summary, the overall good fit between observed and simulated concentrations for the locations considered to be within the injection cloud indicates that both biodegradation processes, nitrification and organic carbon oxidation, are contributing to oxygen consumption. However, the slight discrepancies between simulated and observed dissolved oxygen concentrations at the altitude of 4.95 m, suggest that a manganese oxidation process may be also occurring. The greater extent of the discrepancies between simulated and observed dissolved oxygen concentrations at the altitude 4.27 m, observed at the beginning of the simulations, likely indicates some mixing with background-water, and potentially a manganese oxidation process as suggested previously.

4.1.3   Characterization of processes

These results provide a basis for calculating oxygen consumption rates, nitrification rates and organic carbon oxidation rates for the various locations and altitudes. The rates were calculated based on the simulations and on the field data, and compared to each other to evaluate the accuracy of the simulations at different altitudes. The rates obtained from the simulations were also compared to the corresponding values from the small-scale model calibration altitude (4.72 m, Yellow port), to assess the variability of the processes development at the small-scale (see Appendix A).

Table 4-1 presents the rates for oxygen consumption calculated from the simulations, compared to the rates determined using the field experiment data. The calculations were developed considering a dry solids weight of 1864 (g/L) (Smith, et al., 2013), and a porosity of 0.39 (Mathisen, et al., in preparation; Smith, et al., 2013).

Table 4-1 Calculated oxygen consumption rates, based on simulated and observed dissolved oxygen concentrations, for selected locations at altitudes 4.95 m and 4.27 m

	Altitude (m)	Distance from injection point (m)	Travel time (days) **	Maximum O_2 consumption (μmol/L)*	Max O_2 consumpt. nitrification (%)	Max O_2 consumpt. aerob. resp. (%)	O_2 consumption rate (μmol *g dry sedim^{-1}*day^{-1})
Simulations, small-scale variability Study	4.95	4.6	7	60.74	57.18%	42.82%	**0.0019**
	4.95	6.2	9	103.07	67.43%	32.57%	**0.0023**
	4.27	4.6	11	131.21	72.32%	27.68%	**0.0025**
	4.27	6.2	15	186.12	80.18%	19.82%	**0.0027**
Field experiment data (Mathisen et al.)	4.95	4.6	7	65.90			0.0020
	4.95	6.2	9	117.53			0.0027
	4.27	4.6	11	206.23			0.0040
	4.27	6.2	15	279.60			0.0040

*maximum consumption corresponding to minimum concentration during the simulation, compared to the injection concentration, shifted based on travel time
** based on simulated flow velocity

All simulated oxygen consumption rates are within the range 0.0019 to 0.0027 μmol (g $_{dry}$ $_{sediment}$ × day)$^{-1}$; which is consistent with the rate of 0.0017 to 0.0025 μmol (g $_{dry\ sediment}$ × day)$^{-1}$ obtained through the previous application of the small-scale model (Mathisen, et al., in preparation). Another previously reported rate was 1.1 μmol ($L_{aquifer}$ × day)$^{-1}$ for 5.5 m of transport (Smith, et al., 1999) obtained through a natural gradient tracer test. After the conversion of corresponding units, this value is approximately 25% of the values presented here. Additionally, the oxygen consumption by slurried aquifer core material was determined in the same investigation, yielding 0.2 μmol (g $_{dry\ sediment}$ × day)$^{-1}$ (Smith, et al., 1999), which is around 75 times of the values obtained here. Finally, values obtained through laboratory microcosm experiments with aquifer sediments from the anoxic zone (0.0116 to 0.0447 μmol (g $_{dry\ sediment}$ × day)$^{-1}$), were approximately 6 to 15 times the rates calculated in this investigation (Smith, et al., 2013). This variability among oxygen consumption rates suggests that microcosm experiments likely result in estimation of higher rates. Effects of aquifer heterogeneities, even at the small-scale, as well as disruptive effects of material's

extraction upon microbial communities were indicated in previous research (Smith, et al., 1999). Therefore, the values reported here are considered consistent with the range of values obtained in previous research applying different methodologies.

From the comparison between the rates calculated from the simulations and the rates calculated based on the field data, it may be concluded that the model presents a very good fit to the data regarding dissolved oxygen concentrations. The difference between the simulated and observed oxygen consumption at the 4.95 m altitude is between 7.8% and 12.3 %, whereas at the altitude 4.27 m, the difference is around 33%. It is interesting to indicate here that, for the locations at the lowest sampled altitude, the first 40 to 50 days of the simulations did not captured the dissolved oxygen concentrations accurately. This was proposed to be due to an additional oxidation process that may in development at this altitude and locations (see section 4.1.2).

For this test, it can also be observed that the oxygen consumption rate was higher at lower altitudes, and it also increased slightly when distance down-gradient from the injection point. The variation of the oxygen consumption rate with the altitude suggests that biodegradation may be enhanced in the lower ports, which is consistent with previous reports (Smith, et al., 2013; Repert, et al., 2006) and may indicate that these lower ports would recover their pre-contamination oxygen concentrations first than the ports above them.

In regards to the percentage of consumed oxygen corresponding to each of the considered biodegradation processes, it can be observed in Table 4-1 that nitrification appears to be the dominant oxygen consuming process for the small-scale test. At the 4.95 m altitude, the contribution of organic carbon oxidation process to the oxygen consumption is nearly the contribution of nitrification at the location closer to the injection point (4.6 m), and nitrification becomes more relevant at the farthest location (6.2 m). At the altitude of 4.27 m, nitrification clearly dominates at

the two locations, since its fraction of oxygen consumption is higher at the further location from the injection point.

Nitrate generation rates were calculated, in order to get an insight into the nitrification process. Table 4-2 shows the calculated nitrate generation rates, based on the simulations and on the field data, for selected locations at two altitudes.

Table 4-2 Calculated nitrification rates, based on simulated and observed nitrate concentrations, for selected locations at altitudes 4.95 m and 4.27 m

	Altitude (m)	Distance from inj.point (m)	Travel time (days)**	Max NO$_3^-$ concentration (μmol/L)	Max NO$_3^-$ generation (μM)*	NO$_3^-$ generation rate (μmol *g dry sedim $^{-1}$*day^{-1})
Simulations, small scale variability study	4.95 m	4.6	7	44.25	17.25	**0,0005**
	4.95 m	6.2	9	60.29	33.29	**0,0008**
	4.27 m	4.6	11	73.18	46.18	**0,0009**
	4.27 m	6.2	15	100.85	73.85	**0,0011**
Field experiment data (Mathisen et al., in prep.)	4.95 m	4.6	7	48.00	21.00	0,0006
	4.95 m	6.2	9	90.00	63.00	0,0014
	4.27 m	4.6	11	50.00	23.00	0,0004
	4.27 m	6.2	15	115.00	88.00	0,0013

* based on injection concentration of the model, 27.00 μmol/L
** based on simulated flow velocity

The nitrification rates based on the simulations and on the field data indicate that nitrate generation is lower at locations nearer to the injection point; although the calculations corresponding to the simulations, for each of the both altitudes, present an approximately steady rate. The increase of the nitrification rates with the distance from the injection point is likely related to the available dissolved oxygen concentrations, as interpreted by Smith and Baumgartner (2006) and also to the aquifer´s heterogeneity regarding the sorbed ammonium pool.

The simulated rates were in the range of 0.0005 to 0.0011 μmol (g $_{dry\ sediment}$ × day)$^{-1}$, which are consistent with the corresponding rate from the previous application of the model, which was

0.0009 μmol (g $_{dry\ sediment}$ × day)$^{-1}$, calculated after data from Mathisen et al., (in prep.). Nitrification

rates reported in previous studies for this site, obtained by single-well injection tests, were in the

range of 0.02 to 0.28 μmol (L $_{aquifer}$ × h)$^{-1}$ (Smith, et al., 2006). The rates obtained from the

simulations, when converted to the corresponding units, vary between 0.10 and 0.21 μmol

(L $_{aquifer}$ × h)$^{-1}$, and the rates calculated from the field experiment data are in a range of 0.09 to 0.28

μmol (L $_{aquifer}$ × h)$^{-1}$. Although it was indicated by previous investigations that the rates from single-

well injection tests yielded overestimates of *in situ* rates (Smith, et al., 2006), the results from the

simulations are in the same range as the ones based on field data and on results from previous

research.

The dissolved oxygen consumption attributed to nitrification can be estimated from the

nitrate generation results from Table 4-2, following the equations 3-1 and 3-2. For the simulations,

the fraction of oxygen consumption based on the nitrate generation exhibits the same trends as the

fraction of oxygen consumption obtained from the simulated dissolved oxygen concentrations (see

Table 4-1). However, the oxygen consumption estimated from the nitrate generation rates for the

field data present a different trend. The percentage of consumed oxygen due to the nitrification

process increases with distance from injection point, at each altitude, but decreases with depth at

each location. For the location at 4.6 m from injection point, at 4.27 m altitude (Green port), the

oxygen consumption for nitrification calculated from field data, results only in 22% of the total

oxygen consumption, whereas for the simulation, the corresponding value is 65%. In all other cases,

the observed and simulated fractions of oxygen consumption attributed to nitrate generation are

consistent.

Finally, rates for generation of dissolved inorganic carbon were calculated, as a mean to

assess the aerobic respiration process development at the small-scale. Table 4-3 displays the TCO$_2$

generation rates, calculated for the simulations and the field data at selected locations and two different altitudes. The corresponding rate obtained after data of the application of this model in the previous study (0.0038 µmol (g $_{dry\ sediment}$ × day)$^{-1}$) is somewhat higher than the presented rates, but these may still be considered consistent. As stated before, any increases in dissolved inorganic carbon concentration resulting from aerobic respiration were small relative to the accuracy of the analysis techniques. Therefore, the measurement of generated TCO_2 was difficult (Mathisen, et al., in preparation).

However, the rates calculated for the simulations are close to the ones corresponding to the actual field data for the two examined locations at the altitude 4.95 m and for the location closer to the injection point at the altitude 4.27 m. The second studied location at the lower altitude shows a rate value for the field data that is two-fold the value obtained for the simulations. This location was considered to be at the edge of the injection plume, and the TCO_2 concentrations in the background-water were higher than the TCO_2 injection concentrations. Thus, the TCO_2 concentration at this location obtained from the field data may result from background concentrations, and not from generation of inorganic carbon.

Previously reported aerobic respiration rates determined by different approaches (Smith, et al., 1999) were: ≤0.8 µmol (L $_{aquifer}$ × day)$^{-1}$, obtained through a $^{18}O_2$ tracer test; 0.2 µmol (g $_{dry\ sediment}$ × day)$^{-1}$, obtained through microcosm determination of aerobic respiration within a 30 µmol oxygen horizon; and 1.1 µmol (L $_{aquifer}$ × day)$^{-1}$, for 5.5 m of transport, determined by a natural gradient tracer test to assess aerobic respiration *in situ* within a 20 µmol oxygen horizon. The aerobic respiration rates obtained from the simulations in this research are in a range of 5.22 to 13.21 µmol (L $_{aquifer}$ × day)$^{-1}$. The reported rate from the isotope test corresponds to about 100 times greater than

the rates obtained from the simulations, and the values obtained by the other methods in previous research are about 10 times less the values presented here.

The dissolved oxygen consumption attributed to organic carbon oxidation was estimated following equation 3-3 and the TCO_2 generation results listed in Table 4-3. For the simulations, the fractions of oxygen consumption based on the inorganic carbon generation, result in percentages that are close to the corresponding fraction of oxygen consumption calculated from the simulated dissolved oxygen concentrations (see Table 4-1). At the location at 4.6 m from injection point and 4.27 m altitude (Green port), the nitrification and organic carbon oxidation processes, together, account only for 45% of the oxygen consumption (all O_2 consumptions based on field data), which suggest that the location may not have been within the injection cloud during the whole duration of the tracer test, or that other oxygen consuming process may be occurring. In all other cases, the fraction of oxygen consumption attributed to carbon oxidation in the simulations matched closely with the fraction obtained from the field data.

Table 4-3 Calculated inorganic carbon generation rates, based on simulated and observed dissolved inorganic carbon concentrations, for selected locations at altitudes 4.95 m and 4.27 m

	Altitude (m)	Distance from inj.point (m)	Travel time (days)***	Max TCO_2 concentration (μmol/L)	Max TCO_2 generation (μM)*	TCO_2 generation (μmol *g dry sedim^{-1}*day^{-1})
Simulations, small-scale variability study	4.95 m	4.6	7	336.79	90.69	**0.0028**
	4.95 m	6.2	9	301.66	55.56	**0.0013**
	4.27 m	4.6	11	332.24	86.14	**0.0017**
	4.27 m	6.2	15	322.26	76.16	**0.0011**
Field experiment data (Mathisen et al.)	4.95 m	4.6	7	343.58	97.48	**0.0030**
	4.95 m	6.2	9	281.95	35.85	**0.0008**
	4.27 m	4.6	11	338.00	91.90	**0.0018**
	4.27 m	6.2	15	402.64	156.54	**0.0022**

* based on concentration of S522-0054, 246.10 μmol/L (Mathisen et al., in prep.)

In general, the oxygen consumption rates for each of the assumed biodegradation processes, (calculated from the simulations and based on field data), are consistent with the assumption that nitrification and organic carbon oxidation account for the most part of the oxygen consumption. It is important to indicate that, at the location at 4.6 m from injection point for the 4.27 m altitude, both assumed processes, combined, account only for 45% of the oxygen consumption, based on field data. This may indicate some mixing of the injectate with background-water at this location, or may be related to the development of other oxidation processes, like the proposed manganese oxidation.

4.2 Extended model

In this section, simulated concentration profiles for the extended application of the model are compared with the corresponding concentration profiles from field data. Next, the variability in the parameters from the small-scale is analyzed, and the assumed biodegradation processes are characterized and quantified through the calculation of their oxygen consumption rates. Finally, the results from the sensitivity analysis are shown in order to get an insight into the model uncertainties.

The large scale simulations were performed for a 111 m long transect, extending from Well S473 to Well S469 (see Figure 2-3). The simulation period was 12 years (1995 to 2007), and the calibration was based on the -5.8 m altitude (referenced to mean sea level). The large scale model maintained the configuration from the small-scale model, considering a background solution in equilibrium with the aquifer´s sediments, and an injection of uncontaminated ground-water at the upper boundary of the domain.

4.2.1   Simulations for Well S469, altitude -5.8 m

Once the oxidation rates and variability were defined for the small-scale, the next step was to consider their applicability to the larger scale restoration process. All simulations performed for the large scale involved application and re-calibration of the small-scale model as required.

Four different representations were applied for simulating the conditions of the wastewater plume over 12 years for the Massachusetts Military Reservation (MMR) site. The differences were based on the selection of the background and injection ground-water, on the temporal nature of the injection (i.e. steady or varying), and on considerations of relevant background solutions. The four options considered were as follows:

- Simulation with steady injection and one background solution based on year 1995

- Simulation with steady injection and one background solution based on year 1996

- Simulation with steady injection and two different background solutions, one from 1995 and the other from 1999

- Simulation with varying injection and one background solution, from year 1995

4.2.1.1 Simulation with steady injection and one background solution based on year 1995

The background solution considered for this simulation was based on the concentrations from a sample taken at Well S469 in 1995, before the treated wastewater effluent discharge was stopped. Alkalinity and temperature data were not available for this solution. Consequently, the background solution was obtained by estimating the alkalinity based on electroneutrality and the temperature based on values for the same location and altitude for similar dates of following years. Concentrations for major cations (Na, Ca, K and Mg) were adjusted by less than 15% from the corresponding values published by the U.S. Geological Survey to achieve electroneutrality of the solution. The adjusted background solution still presented a relatively high electroneutrality error

(about 30%) despite the adjustments applied to the major cation concentrations, but still provided a basis for estimating the initial equilibrium conditions of the background solution.

The injection solution was based on concentrations of a well upstream of the former discharge zone where the ground-water was uncontaminated. Alkalinity and temperature data were estimated following the same procedure as for the background ground-water, although in this case cation concentration adjustments were not required, and electroneutrality presented an error less than 10%.

For this configuration, a first run of the model was performed utilizing the same parameter values from the small-scale model calibration. However, the dissolved oxygen concentrations for this simulation did not match the field concentration profiles mostly because the simulated arrival of the oxygen breakthrough occurred very early (at around 250 days). The early breakthrough of oxygen was attributed to a low amount of sorbed organic carbon and a low growth rate for the aerobic respiration process, which may be associated with the proximity of the tracer test site to the source after many years of flushing. Therefore, the results are not shown here. For these first simulations, ammonium concentrations were not captured well by the simulations between 500 and 1600 days, although nitrate concentrations exhibited a quite good match up to 1600 days. Dissolved inorganic carbon concentrations reached a good fit of simulations and field up to 1600 days, and pH was simulated reasonably well up to 2500 days.

Figure 4-9 displays observed and simulated concentrations for selected constituents for the -5.98 m altitude (referenced relative to mean sea level), during 12 years (1995 to 2007), at Well S469, after the parameters were adjusted for the first configuration. After calibration was performed, the model results match the overall trend of the observed dissolved oxygen concentrations. The parameters that required calibration were the growth and decay rate for microorganisms related to

organic carbon oxidation, and the initial content of sorbed organic carbon in the sediments. A good fit is observed between the simulated and observed concentrations for nitrate, dissolved organic carbon, dissolved inorganic carbon, pH and selected cations.

As can be seen in Figure 4-9, ammonium concentrations for the first years are not captured well by the simulations. The differences between predicted and observed ammonium concentrations may be due to model limitations related to the steady injection configuration. The large scale version of the model was set up considering steady concentrations for dissolved oxygen in the injection solution, which may not be quite accurate for the first year after source removal. The ammonium concentrations corresponding to the treated wastewater effluent disposed at the infiltration beds was reported to have a mean value of 329 µM, varying in a range of 51-800 µM across the years of the wastewater treatment plant operation (Repert, et al., 2006), and the ammonium transport was found to be retarded by cation exchange (Smith, et al., 2004; Repert, et al., 2006). Thus, around the first 222 days, the injection may not reproduce the concentrations of the up-gradient ground-water entering Well S469.

However, the simulations presented a good fit to observed nitrate concentrations (see Figure 4-9). The simulated sorbed ammonium utilization likely indicates that, at the studied location (Well S469), the nitrification process may be occurring at a very low rate, as was suggested in previous research (Bohlke, et al., 2006), or possibly stopped due to the very low dissolved oxygen concentrations after source removal (Repert, et al., 2006).

The simulations performed for this application at the extended scale indicate that aerobic respiration is likely to be the dominant oxygen consuming process affecting the oxygen concentration shown in Figure 4-9 for Well S469. This result may be confirmed by the comparison between observed and simulated concentrations for TCO_2, where generation of TCO_2 indicates the

likely occurrence of organic carbon oxidation due to aerobic respiration. Possible causes of the discrepancy between observed and simulated concentrations for total dissolved inorganic carbon might be due to the calculated TCO_2 concentrations for representing the observed values. The calculation was performed to obtain the TCO_2 values from 1999 (1354 days) and after, as was reported in section 3.4.1. These values were not available from analysis of field samples. Another possible explanation for the observed discrepancy may be variability in the injected TCO_2 concentrations.

Figure 4-9 Observed and simulated concentrations for selected constituents at Well S469, for the -5.98 m altitude (referred to sea level), during 12 years (1995 to 2007), considering steady injection concentrations and one background solution from 1995

4.2.1.2 Simulation with steady injection and one background solution based on 1996

In order to address the discrepancies that may be caused variability in conditions immediately after source removal (along with potential limitations associated with the high electroneutrality error determined for the background solution for the previous case), an additional simulation was completed with a selected background solution for which concentrations are intended to represent the conditions in Well S469 after the contaminant source was removed.

The background solution used in this case corresponds to a sample collected from Well S469 in 1996. Considering that the travel time from Well S473 to Well S469 is about 222 days, this background-water aims to represent the conditions after source removal. For this case, electroneutrality for the background and injection solutions exhibit an error less than 10%. Parameters from the first configuration did not required adjustments for this case (as shown in Table 4-5). Figure 4-10 shows observed and simulated concentrations for selected constituents for the - 5.98 m altitude (referred to sea level), during 12 years (1995 to 2007), at Well S469, for the second case considered.

Simulated dissolved oxygen concentrations presented a very good fit to field data, with a slight underestimation of oxygen consumption. Dissolved ammonium concentrations were still not captured well, and the interpretation for these results is likely the same as that developed for the first large scale model configuration (i.e. related to the variability in ammonium concentrations in the treated effluent throughout the years of disposal). Nitrate concentrations of the first 228 days were not accurately simulated in this case, which can be attributed to the differences between concentrations of the selected background-water (Well S469, 1996) and the actual concentration profiles for Well S469 in 1995. Nitrification is likely occurring at very low rates, as was proposed for the first scenario.

If the concentrations after the first 230 days are considered, the simulations presented a good fit to the data for dissolved organic carbon, pH, calcium, potassium, magnesium, iron and manganese.

However, the inorganic carbon concentrations were not captured well for this case. The observed overestimation of dissolved inorganic carbon concentrations may be related to higher dissolved oxygen (DO) concentrations from the simulated injection of uncontaminated ground-water. The actual DO concentration was associated with ground-water that came from the region that was up-gradient of the contaminant source. For the first year after the cessation of the effluent discharge, this DO was likely lower as the DO concentration in the selected injection water, as explained for the first model configuration.

In general, from this simulation, it can be argued that aerobic respiration is likely the main oxygen consuming process, which can be supported by the good match between observed and simulated concentrations for dissolved oxygen, inorganic carbon and pH. Nitrification may be occurring at very low rates, or stopping after the first 228 days, which can be interpreted from the simulated and observed concentration profiles for ammonium and nitrate (see Figure 4-10).
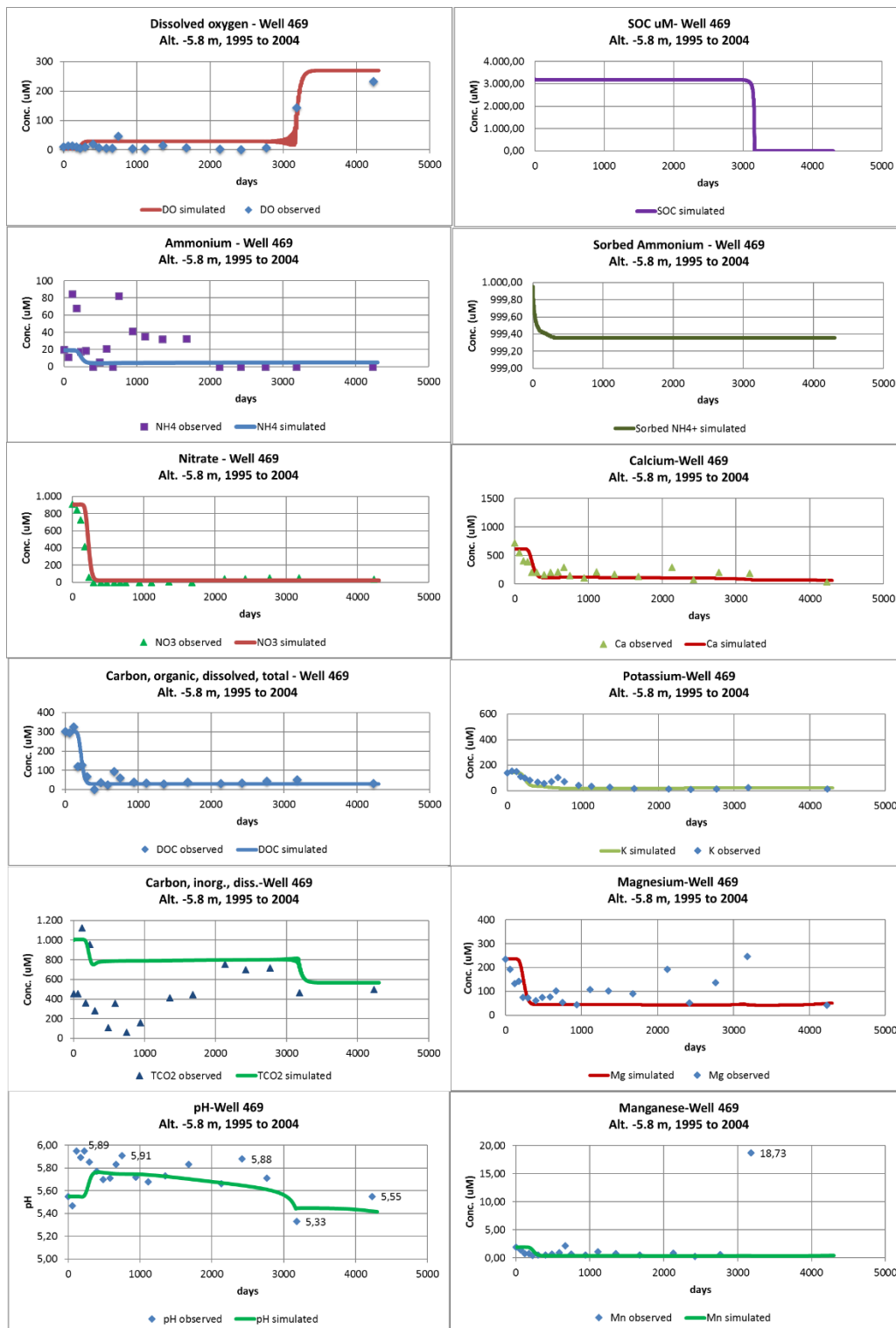
Figure 4-10 Observed and simulated concentrations for selected constituents at Well S469, for the -5.98 m altitude (referenced to sea level), during 12 years (1995 to 2007), considering steady injection concentrations and one background solution from year 1996

4.2.1.3 Simulation with steady injection and two different background conditions

The next simulation included a steady injection as before, but included two different conditions to represent the equilibrium background geochemistry for the region between the source and Well S469. This configuration for the large scale model application is proposed in order to evaluate the effect of the changes that the background solution for the modeled flow path likely experiences during the simulation time. A new calibration was needed in order to obtain a good fit between simulated and observed concentration profiles for the different constituents.

This simulation used a first background solution based on a sample collected in 1995, from Well S469 at an altitude of -5.8 m, and a second background solution based on a sample collected in 1999 for the same location and altitude. The considered injection solution was from a sample collected from Well S474 (up-gradient from the contaminant source) in 1995. The electroneutrality error for the first background solution was relatively high, as for the second background and injection was less than 10%. Figure 4-11 shows observed and simulated concentrations for selected constituents for the -5.98 m altitude (referred to sea level), during 12 years (1995 to 2007), at Well S469, for this model set up. For this case, the dissolved oxygen concentrations presented a good fit to the data, with a slight underestimation of oxygen consumption. The time of the change of the background solution concentrations presented an increase in the simulated dissolved oxygen concentration, as expected.

Ammonium concentrations were captured accurately after 1300 days. The trend of nitrate concentrations also exhibited a very good fit after 1300 days, where the model and the field data apparently indicate low nitrate generation. The simulations captured the concentrations for dissolved organic carbon, pH, iron, manganese, sodium, calcium, and magnesium well. The simulated dissolved inorganic carbon concentrations presented a good fit to data after 1300 days.

Before 1300 days, inaccuracies in the dissolved carbon concentrations (which would be related to the error in electroneutrality from the initial background solution) may cause the discrepancy. It is important to clarify that the plots (see Figure 4-11) present some discontinuities derived from the approach of using two different background solutions for the modeled flow path.

Although a nitrification process is likely present after 1300 days, where ammonium is being utilized and there may be some nitrate generation (see the plots for ammonium and nitrate concentration profiles showed in Figure 4-11), the aerobic respiration process seems to account for the main part of the observed oxygen consumption. This interpretation is supported by the good fit between observed and simulated inorganic carbon concentrations and pH concentrations, and also by the simulated sorbed organic carbon utilization presented in Figure 4-11.
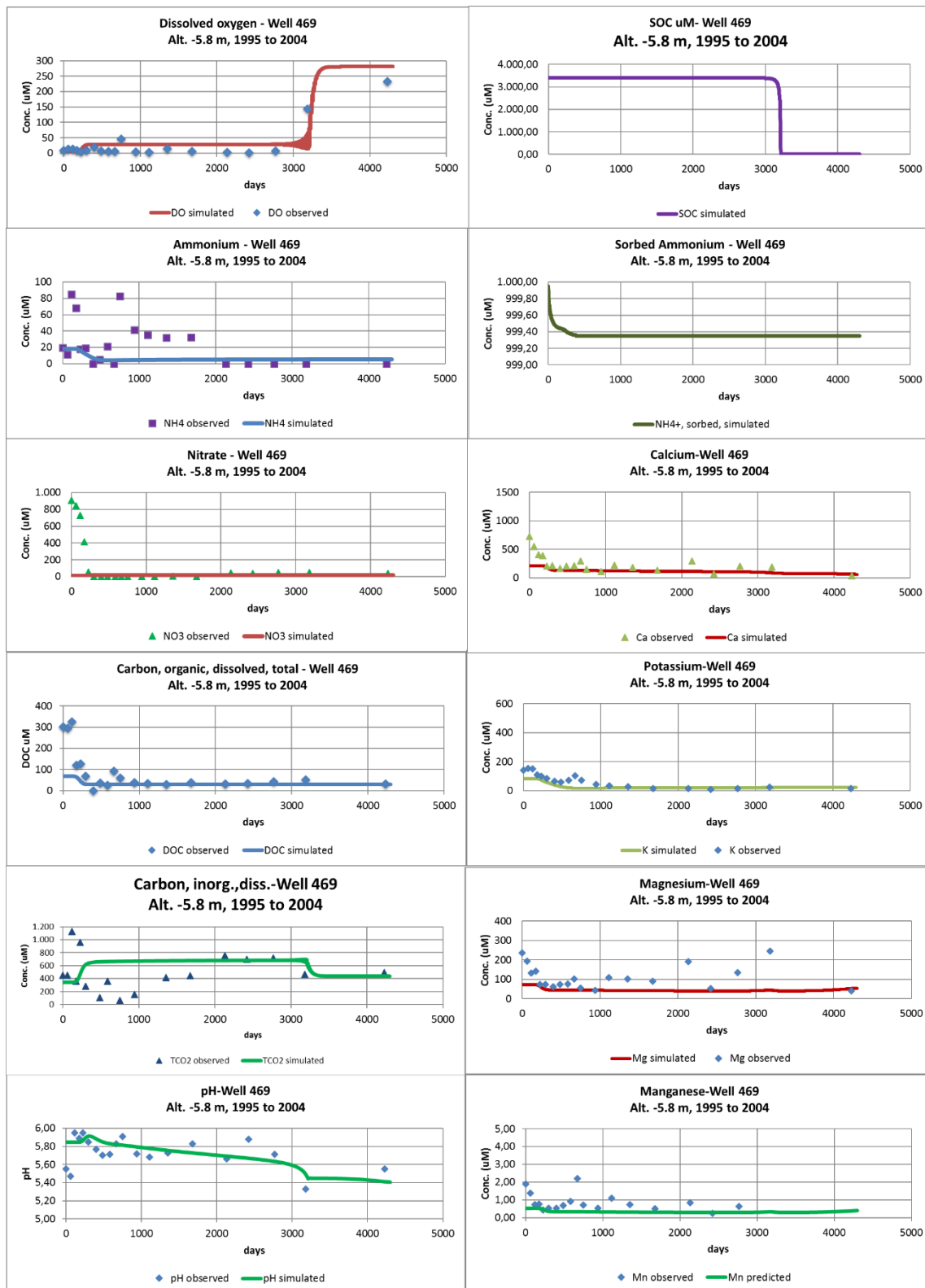
Figure 4-11 Observed and simulated concentrations for selected constituents at Well S469, for the -5.98 m altitude (referred to sea level), during 12 years (1995 to 2007), considering steady injection concentrations and two different background solutions

4.2.1.4 Simulation with varying injection and one background solution

The final simulation included a varying injection (consisting of two different injection conditions) and a single representative background condition). This configuration was intended to address the discrepancies observed in the first three model set ups presented previously, in sections 4.2.1.1 to 4.2.1.3. The background solution was selected in order to maintain the actual concentration profiles from Well S469 in 1995, and the two successive injections were selected to represent the possible variation in the concentrations related to the initial time period after the discharge was stopped, and the subsequent time period after uncontaminated ground-water from up-gradient entered the zone of Well S469. A new calibration was also performed, and geochemical parameters (growth and decay rates for the organic carbon oxidation process and initial sorbed organic carbon pool) were adjusted. Figure 4-12 displays observed and simulated concentrations for selected constituents for the -5.98 m altitude (referenced to mean sea level), during 12 years (1995 to 2007), at Well S469, for the case where two injections were considered.

In this case, one background solution based on the sample from Well S469 from 1995, the same solution used for the configurations 1 and 3 was selected. Two successive injection solutions, the first one based on concentrations from Well S473 from 1995, and the second one based on a sample from Well S474 from 1995, for the -5.8 m altitude, were considered (Savoie, et al., 2006). The background solution and the injection considered for the first time period for this simulation had a relatively high electroneutrality error, around 30%, but for the injection considered for the second time period this error was low, less than 10%.

Simulated and observed dissolved oxygen concentrations showed a very good fit, although oxygen consumption after 3000 days was slightly underestimated. The underestimation of the DO

may be related to the high DO concentration used in the injection solution for the second time period (see Figure 4-8).

The trend for the ammonium concentration distribution was effectively captured by these simulations, and the nitrate concentration was effectively captured as well. A small nitrate generation is observed after 3000 days, for both the observed and the simulated concentrations (see Figure 4-12).

These simulations also captured the concentrations for dissolved organic carbon, pH, iron, manganese, sodium, calcium, magnesium quite well. The simulated dissolved inorganic carbon concentrations presented a very good fit to data after 1300 days. Before this time, the error in electroneutrality from the first background solution may be related to the discrepancy.

According to these simulations, the aerobic respiration process is likely the dominant process responsible for oxygen consumption, which can be interpreted from the concentration distributions for inorganic carbon and pH, and supported by the simulated sorbed organic carbon concentrations (Figure 4-8). Nitrification is likely occurring after 1300 days, but at very low rates, which can be considered by the good fit between observed and simulated ammonium and nitrate concentrations and the slight increase in nitrate concentration after 1300 days (see Figure 4-12).
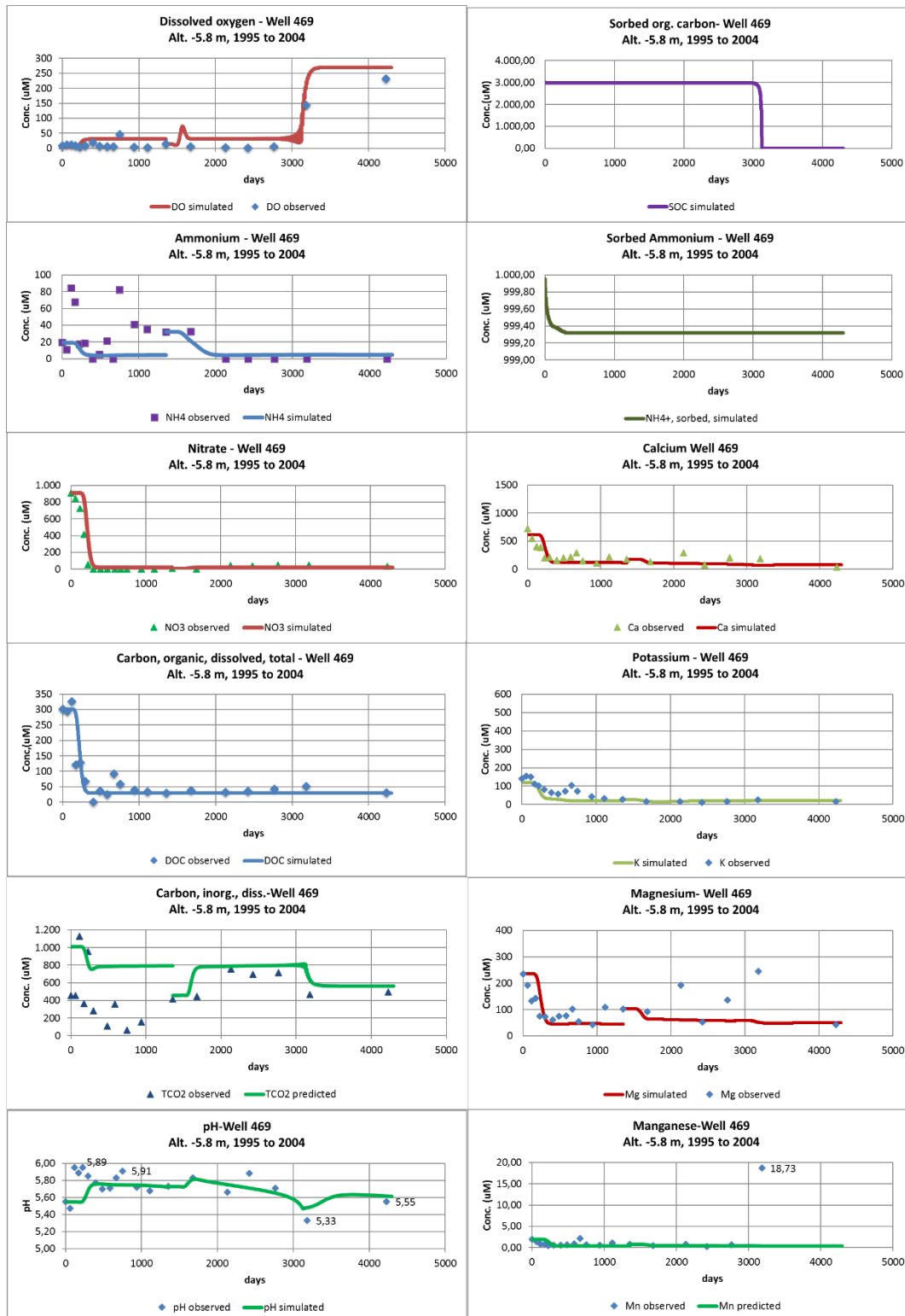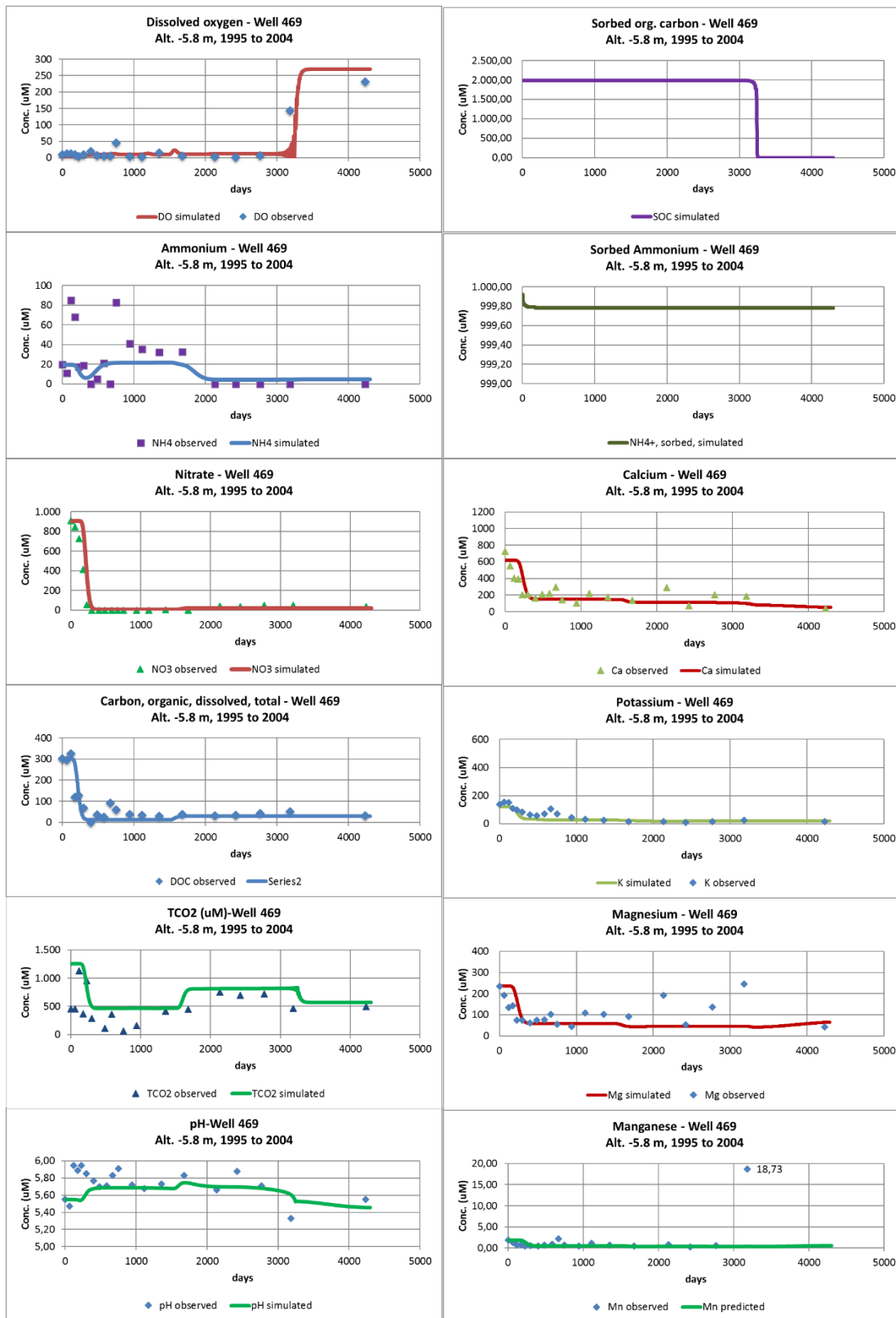
Figure 4-12 Observed and simulated concentrations for selected constituents at Well S469, for the -5.98 m altitude (referred to sea level), during 12 years (1995 to 2007), considering two successive injection concentrations and one background solution

4.2.2   Investigation of parameters

In this section, a discussion about the variability in the parameters from the small-scale model, and the applicability of these parameters to the large scale simulations is presented. The parameters were grouped into physical and geochemical parameters, and for the geochemical parameters, they were classified in sorption parameters, ammonium oxidation parameters, and carbon oxidation parameters.

4.2.2.1 Physical parameters

Among the model´s physical parameters, the dispersivity and the flow velocity were adjusted for the large scale applications. In Table 4-4, physical parameters from the small-scale model, and adjusted parameters for large scale application are shown. The physical parameters applied for each of the four large scale model configurations were the same.

Table 4-4 Physical parameters from small scale model, and corresponding parameters applied to large scale

Parameter	Unit	Small-scale	Large scale
Diffusion coefficient		1×10^{-9}	1×10^{-9}
Dispersivity	M	0.08	1.50
Flow velocity	m/day	0.67	0.50

Source: small-scale parameters after Mathisen et al. (in prep.); Large scale dispersivity selected based on previous tracer tests at the site (Hess, et al., 2002), and large scale flow velocity based on Smith et al. (2013) and Bohlke et al. (1999).

4.2.2.2 Geochemical parameters

Table 4-5 displays the geochemical parameter values for the large scale model after calibration, the parameter values for the original small-scale model, and reference values from different sources. As for the geochemical parameters, the initial sediment bound organic carbon content, and the growth and decay rates for the organic carbon oxidation process were adjusted after calibration.

Table 4-5 Geochemical parameters from the small-scale model, calibrated parameters from large scale model and reference values

	Parameter	Unit	Small-scale*	Large scale – calibr. (1 and 2)	Large scale – calibr. (3)	Large scale – calibr. (4)	Reference
	Sorption						
1	K-NH_4^+	Log K	-1.1	-1.1	-1.1	-1.1	
2	K-Na^+	Log K	-2.6	-2.6	-2.6	-2.6	
3	K-K^+	Log K	-1.0	-1.0	-1.0	-1.0	
4	K-Ca^{2+}	Log K	+1.0	+1.0	+1.0	+1.0	
5	K-Mg^{2+}	Log K	+1.5	+1.5	+1.5	+1.5	
6	K-Mn^{2+}	Log K	+1.5	+1.5	+1.5	+1.5	
7	K-Zn^{2+}	Log K	+3.0	+3.0	+3.0	+3.0	
8	Cation site density (T_s)	M	7.1×10^{-3}	7.1×10^{-3}	7.1×10^{-3}	7.1×10^{-3}	8.3×10^{-3} [a]
9	Specific area (A_s)	m^2/g	0.44	0.44	0.44	0.44	0.40 [a]
10	Solid mass/volume (S_s)	g/L	4177	4177	4177	4177	4140 [a]
	Ammonium oxidation						
11	$[NH_4^+]_0$	M	1×10^{-3}	1×10^{-3}	1×10^{-3}	1×10^{-3}	1×10^{-3} [b]
12	X_{n0}	g/L	6×10^{-6}	6×10^{-6}	6×10^{-6}	6×10^{-6}	6×10^{-6} [b]
13	K_n	μM	80	80	80	80	80 [b]
14	$K_{o,n}$	μM	40	40	40	40	72 [b]
15	μ_n	day^{-1}	0.01	0.01	0.01	0.01	1.0 [b]
16	Y_n	g VSS/mol_N	1.40	1.40	1.40	1.40	3.6 [b]
17	b_n	day^{-1}	0.001	0.001	0.001	0.001	0.05 [b]
	Carbon oxidation						
18	$[TOC]_0$	M	0.00136	**0.0034**	**0.0030**	**0.0020**	0.00136 [c]
19	X_{c0}	g/L	1×10^{-5}	1×10^{-5}	1×10^{-5}	1×10^{-5}	n/a
20	K_c	μM	40	40	40	40	35 [b]
21	$K_{o,c}$	μM	40	40	40	40	72 [b]
22	μ_c	day^{-1}	0.0249	**0.052**	**0.050**	**0.080**	5.00 [b]
23	Y_c	g VSS/mol_{TOC}	0.50	0.50	0.50	0.50	1.00 [b]
24	b_c	day^{-1}	0.01	0.01	0.01	**0.008**	0.06 [b]

Values in bold were adjusted for calibration

*Small-scale parameters after Mathisen et al. (in prep.)

[a] Stollenwerk et al. (1999)

[b] Estimated for wastewater (Mathisen, et al., in preparation)

[c] Smith et al. (2013)

Sorption coefficients. No adjustments were considered necessary for the sorption coefficients, because the major cation concentrations were captured well in all studied scenarios. Although for the ammonium concentrations the fit was not as good in scenarios 1 (background

S469-1995 and injection S474-1995) and 2 (background S469-1996 and injection S474-1995) compared to scenario 4 (background S469-1995 and two successive injection concentrations), for this last case a good fit was obtained without adjusting the sorption coefficient for ammonium, or any of these parameters. These values were also in the same range of values applied in other models, developed for the same wastewater plume, for different scales. The sorption coefficients (log K) were in a range of ± 1.8 to ± 5.6 for a previous one dimensional model, developed for a domain of 4000 m (Stollenwerk, et al., 1999); and a single value for log K of -1.8 was applied as sorption coefficient for Ca, Mg, Na, NH_4^+, Fe and Mn in a three dimensional model, for a domain of approximately 1600 m x 800 m x 45 m (Parkhurst, et al., 2003).

Ammonium oxidation parameters. The ammonium oxidation parameters from the small-scale model were not adjusted for the large scale calibration. The applied half saturation coefficient for O_2 ($K_{O,N}$) is about half from the corresponding value for wastewater, and this estimation was made for the small-scale calibration (Mathisen, et al., in preparation). For the set of parameters related to nitrifying microorganisms (μ_n, Y_n and b_n) the same values from small-scale were also maintained. These three values were decreased relative to the corresponding wastewater values, suggesting that the conditions for the nitrifying microorganisms are less favorable at the wastewater plume than in a wastewater treatment environment.

Carbon oxidation parameters. The carbon oxidation parameters that were adjusted in the large scale calibration are two of the parameters corresponding to aerobic respiring microorganisms: growth rate (μ_C), and decay rate (b_C). Also the initial amount of organic carbon in the sediments $[TOC]_0$ was adjusted.

The resulting values for the **growth rate** are in the range from 0.050 to 0.080 (day^{-1}), which is consistent compared to the estimated value for wastewater. These calibrated values indicate that

the growth rate in the plume's conditions ranges from 1% to 1.6% of the growth rate in wastewater. The large scale calibration values are about two to three times the value for the small-scale; this may be related to the representation of a highly contaminated zone for the large scale model domain, located completely beneath the former infiltration beds. Another possible explanation for these differences may be related to the fact that the small scale test was completed near the contaminant source, but after a long time the discharge was stopped. Thus, it may be possible that carbon was depleted by the time the small scale tracer test was completed, causing the parameters to be different.

In regards to the **microbial yield coefficient** (Y_c), the value from the small-scale calibration was maintained, and this value was half of the corresponding value for wastewater. This is likely related to the conditions that microorganisms experience at the study site, compared to the conditions in wastewater. Finally, the **decay rate** for microorganisms responsible for organic carbon oxidation from the small-scale was maintained in the large scale Configuration 1 (background S469-1995, injection S474-1995), Configuration 2 (background S469-1996, injection S474-1995) and Configuration 3 (backgrounds S469-1995 and S469-1999, injection S474-1995), and slightly decreased for calibrating Configuration 4 (background S469-1995, injections S473-1995 and S474-1995). These values are less than the corresponding value for wastewater, which may be explained by the different conditions in the two environments, and by the need to be consistent with the decreases in growth rate and microbial yield.

The **sorbed organic carbon pool** appears to be a key parameter for accurately representing oxygen consumption at the large scale. The large scale calibration values, in the range of 0.0020 to 0.0034 M, represent about 1.5 to 2.5 times the calibrated value from the small-scale. Parkhurst et al. (2003) estimated a maximum sorbed organic carbon concentration of 0.016 M after the treated

wastewater effluent discharge was stopped, which is about 5 to 8 times greater than the values obtained from calibration at the large scale.

Previous studies on this sediment cores analyses at this site indicated that the total carbon stored in the sediments may be in the range of <8 to 55.8 µmol (g dry wt)$^{-1}$, with most of this corresponding to organic carbon content. The same study showed that the content of water extractable organic carbon was about less than 10 to 50% (Smith, et al., 2013). Assuming a dry solids content of 1864 g dry wt./L and porosity of 0.39 (Smith, et al., 2013), the reported sorbed total carbon content represents about 0.04 to 0.27 M, which is quite higher than the calibration values obtained for both scales. However, the calibrated values may be interpreted as extractable organic carbon amounts, which is also consistent with the total utilization of sorbed organic carbon resulting from the large scale simulations.

4.2.3   Characterization of oxygen consumption processes

With respect to the characterization of the oxygen consumption processes, the obtained results suggest that and aerobic respiration is likely the dominant process taking place at the large scale. Nitrification also may be occurring, but any nitrification is likely consuming oxygen at a much lower rate. From the ammonium and nitrate simulations (see Figures 4-5 to 4-8), the nitrification process seems to stop in the first 400 days for Configurations 1 (Background 1995) and 2 (Background 1996). For Configurations 3 (Two background solutions) and 4 (Two injection solutions) oxygen consumption appears to occur in a short period between 1500 and 2000 days, and to be limited by the amount of ammonium desorbing from the sediments (see Figures 4-5 to 4-8).

Table 4-6 shows the oxygen consumption rates calculated from the large scale simulations, at the -5.8 m altitude from Well S469. The obtained rates for oxygen consumption, in a range of 1.10 to 1.17 µmol/($L_{aquifer} \times$ day), are lower than the corresponding rates calculated for the small

scale (8.9 to 12.8 µmol/($L_{aquifer} \times$ day) after units conversion, see Table 4-1). These values were expected to be lower than the corresponding values for the small-scale, because they represent the average of larger spatial and temporal conditions (Smith, et al., 1999). However, these values are very close to a similar rate of 1.1 µmol/($L_{aquifer} \times$ day), which was obtained through a natural gradient tracer test and reported in previous research (Smith, et al., 1999), and about two times greater than the results of ≤ 0.8 µmol/($L_{aquifer} \times$ day), reported in the same investigation and obtained applying oxygen isotope fractionation. Furthermore, a recent study developed at the same site, which made use of laboratory incubations of sediment cores, reported oxygen consumption rates that were in a range of 11.6 to 44.7 nmol (g dry wt.)$^{-1}$ day^{-1} (Smith, et al., 2013), which are roughly 50 times greater than the rates calculated here. Since the oxygen consumption rates obtained from the large scale simulations are in the range of 1.10 to 1.17 µmol/($L_{aquifer} \times$ day), they are considered to be within the range of similar values determined through different methods in previous research.

Table 4-6 Calculated oxygen consumption rates for Well S469, altitude -5.8 m, for four different large scale model configurations

	Altitude (m)	Distance from injection point (m)	Travel time (days) **	Maximum O_2 consumption (µmol/L)*	O_2 consumption rate (nmol *g dry sedim^{-1}*day^{-1})	O_2 consumption rate (µmol *L^{-1}*day^{-1})
Configuration 1	-5.80	111	222	245.01	0.23	1.10
Configuration 2	-5.80	111	222	257.54	0.24	1.16
Configuration 3	-5.80	111	222	260.20	0.25	1.17
Configuration 4	-5.80	111	222	259.66	0.24	1.17

*O_2 injection 270 µM for 1, 3 and 4; 281 µM for 2; ** based on flow velocity

Table 4-7 displays the nitrification rates calculated from the large scale simulations at the -5.8 m altitude of Well S469. Compared to the nitrification rates obtained from the small-scale, the nitrification rates obtained from the large scale applications are much lower, about 800 times smaller (for the small-scale, nitrification rates were in the range of 2.5 to 5.1 µmol ($L_{aquifer} \times$ day)$^{-1}$, after

units conversion; see Table 4-2). It is noted that, although the rates for the small scale were quite

different than those at the large scale, the ammonium oxidation parameters from the small-scale

yielded rates that were consistent with those observed for the large scale process. Nitrification rates

found in previous investigations applying single well injection tests were in the range of 0.02 to

0.28 µmol (L $_{aquifer}$ × h)$^{-1}$ (Smith, et al., 2006). The nitrification rates obtained for the four different

configurations for the large scale model, when converted to the corresponding units, are

approximately 1/100 of the values found by this previous research. Other investigations indicated

nitrification rates of 13 to 96 nmol (L $_{aquifer}$ × day)$^{-1}$, which were calculated based on a natural

gradient tracer test (Miller, et al., 1999).

Other reported values of 0.09 to 0.15 µmol (L $_{aquifer}$ × day)$^{-1}$, were indicated by an isotope

tracer test at the upper boundary of the plume (Bohlke, et al., 2006). The rates calculated from the

large scale simulations are approximately 500 times smaller than this value. Previous investigations

considered these rates to be small, and the nitrification reaction was suggested to be localized within

a zone where mixing of contaminated and uncontaminated ground-water was occurring (Bohlke, et

al., 2006), which may have been the situation at Well S469 in the first years after source removal.

On the other hand, ammonium oxidation reactions were indicated to be unimportant in the anoxic

portion of the wastewater plume, with rates ≤0.008 µmol (L$_{aquifer}$ × day)$^{-1}$ obtained through isotope

fractionation (Bohlke, et al., 2006). Other investigations suggested that nitrification might have

stopped after the contaminant source removal (at least before clean ground-water from up-gradient

entered the zone), because the oxygen consumed for the reaction was contained in the treated

effluent discharge (Repert, et al., 2006). The likely disappearance of nitrification in the time period

after the discharge was stopped may be related to the increase in ammonium concentrations that is

observed in the concentration profiles of field data for the first 400 days, which was captured by the simulations in scenario 4 (background W469-1995 and injections S473-1995 and S474-1995).

The O_2 consumption rate due to nitrification was obtained following equations 3-1 and 3-2, and these nitrification rates were considered to be consistent when compared to the O_2 consumption rates calculated from the simulations. According to these calculations, the nitrification process likely accounts for 0.5% to 0.8% of the dissolved oxygen consumption for the larger scale simulations.

Table 4-7 Calculated nitrification rates for Well S469, altitude -5.8 m, for four different model configurations

	Altitude (m)	Distance from injection point (m)	Travel time (days) **	Maximum NO_3^- generation (μmol/L)*	NO_3^- generation rate (nmol *g dry sedim $^{-1}$*day^{-1})	NO_3^- generation rate (μmol *L $^{-1}$*day^{-1})
Configuration 1	-5.80	111	222	1.02	9.64E-04	4.61E-03
Configuration 2	-5.80	111	222	0.96	9.07E-04	4.33E-03
Configuration 3	-5.80	111	222	0.98	9.26E-04	4.43E-03
Configuration 4	-5.80	111	222	0.70	6.61E-04	3.16E-03

*NO_3^- injection 19.31 μM

** based on flow velocity

Table 4-8 shows organic carbon oxidation rates, calculated from the large scale simulations, at the -5.8 m altitude from Well S469. The rates were based on generation of dissolved inorganic carbon, and resulted in a range of 0.59 to 0.71 nmol (g $_{dry\ sediment}\times$day)$^{-1}$. The TCO$_2$ generation rates obtained from the large scale are lower than the corresponding values from the small-scale simulations, but are still of the same order (TCO$_2$ generation rates from the small-scale resulted in a range of 1.1 to 2.8 nmol (g $_{dry\ sediment}\times$day)$^{-1}$; see Table 4-3). This may be interpreted as the result from averaging the conditions over a larger distance and time frame, because the large scale

application involves depletion of O_2 throughout the extent of the region. These rates may vary and may be limited due to depletion of O_2.

Oxygen consumption rates for the large scale simulations were estimated based on dissolved inorganic carbon generation (see equation 3-3). The oxygen consumption rates attributed to organic carbon oxidation, obtained from the large scale simulations, were in a range of 0.30 to 0.36 nmol (g dry sediment $\times$ day)$^{-1}$.

These values are smaller than the lowest value for oxygen consumption derived from laboratory experiments with aquifer sediment cores (11.6 nmol (g dry sediment $\times$ day)$^{-1}$), which was attributed to organic carbon oxidation (Smith, et al., 2013). However, the calculated oxygen consumption rates are nearly two times greater than the 1.1 μmol (L aquifer $\times$ day)$^{-1}$ based on a natural gradient tracer test within a 20 μmol oxygen horizon (Smith, et al., 1999).

Finally, the oxygen consumption rates due to organic carbon oxidation were compared with the oxygen consumption rates obtained from the large scale simulations. The oxygen consumption rates based on the inorganic carbon generation were about 1.5 times the total oxygen consumption rates derived from the simulations. It was expected that the organic carbon oxidation process accounted for nearly the 99% of the oxygen consumption, based on the oxygen consumption rates obtained from nitrification at the large scale, and considering the model´s assumptions. However, the observed difference may be attributed to an overestimation of the TCO_2 generation in the model or, to a lesser extent, to other processes responsible of TCO_2 generation being in development.

Table 4-8 Calculated organic carbon oxidation rates for Well S469 at altitude -5.8 m, for four different model configurations

	Altitude (m)	Distance from injection point (m)	Travel time (days) **	Maximum TCO_2 generation (μmol/L)*	TCO_2 generation rate (nmol *g dry sedim $^{-1}$*day^{-1})	TCO_2 generation rate (μmol *L^{-1}*day^{-1})
Configuration 1	-5.80	111	222	742.73	0.70	3.35
Configuration 2	-5.80	111	222	626.90	0.59	2.82
Configuration 3	-5.80	111	222	736.56	0.69	3.32
Configuration 4	-5.80	111	222	753.78	0.71	3.40

*TCO_2 injection 61.49 μM

** based on flow velocity

Other oxygen consuming processes, which may be driven by the presence of oxidizable inorganic compounds, such iron and manganese oxyhydroxides, in the sediments (Stollenwerk, et al., 1999; Parkhurst, et al., 2003), were not considered for the small-scale and for the large scale models. Based on the assumption that the studied locations are in the close vicinity of the former infiltration beds (Wells S473 to S469), the oxygen consumption attributed to other processes than nitrification and aerobic respiration is likely to be small compared to these processes (Smith, et al., 2013). The low concentrations of such compounds (Fe(II) and Mn) at the studied altitude of Well S469, indicated by field data (Savoie, et al., 2006; Savoie, et al., 2012), and reproduced well by the simulations support this assumption as well.

Another process not accounted for in this model is denitrification. Several studies at the Massachusetts Military Reservation's wastewater plume have indicated that denitrification was possibly occurring within the anoxic portion of the plume (Smith, et al., 2004; Smith, et al., 2001; Smith, et al., 1988), and that nitrate, oxygen and ammonium gradients in this plume favor the nitrifying microorganisms (Miller, et al., 2009). The low nitrate concentrations observed at Well S469 after the first 200 days (see Figures 4-9 to 4-12), may be related to denitrification. Previous

research suggests that denitrification may be the result of a change to an alternate metabolism of active nitrifying communities. This change may occur when the dissolved oxygen gets depleted at an altitude where relevant ammonium and dissolved oxygen concentrations coexisted (Miller, et al., 2009). The very low nitrite concentrations at -5.8 m for Well S469 throughout the selected time frame, were considered an indicator about the unlikely occurrence of denitrification at this location and altitude. However, is recognized that the heterogeneities of this wastewater plume and this aquifer may be related to development of different processes for different locations and altitudes.

The spatial variability of the subsurface characteristics, including the variability in hydraulic conductivity and the typical dimension of the heterogeneities, affect the behavior of flow in an aquifer (Gelhar, 1993). Thus, it is recognized that the development of a three dimensional model for the large scale application will likely be an appropriate approach for attaining accurate predictions. However, the main goal of this investigation was not the development of a full three-dimensional model; rather, the study was intended to assess the variability in the parameters and main oxygen consuming processes from small-scale to large scale. Furthermore, the performance of this study maintaining the existing model´s dimensionality may be seen as a first step for developing considerations about parameters and processes that will be likely useful for the development of a three dimensional large scale model.

4.3 Sensitivity Analysis

A sensitivity analysis was performed as described in section 3.5, with consideration to the results from the sensitivity analysis developed for the small-scale version of the model (Mathisen, et al., in preparation) as a basis. Table 4-9 presents the summary of the perturbations to the parameters, the maximum oxygen consumption obtained in response to each perturbation, and the percentage of variation in oxygen consumption referred to the base case (Configuration 2). The

reference oxygen consumption was 257.54 μM. The parameters selected for this analysis were the ammonium sorption coefficient (K-NH$_4^+$), the half saturation coefficient for nitrogen (K$_N$), the maximum specific ammonium utilization or growth rate (μ$_N$), and the microbial yield for ammonium oxidation (Y$_N$). Furthermore, the effects of perturbations on the half saturation coefficient for oxygen carbon oxidation (K$_{O,C}$), the maximum specific organic carbon utilization or growth rate (μ$_C$), the microbial yield for carbon oxidation (Y$_C$), the first order biomass decay coefficient for carbon oxidation (b$_C$), and the initial sorbed organic carbon pool (SOC) were studied.

Table 4-9 Changes in maximum consumed oxygen, in response to perturbations in sorption equilibrium and microbial oxidation-reduction reaction parameters

	Maximum consumption of O2 simulated at Well S469, -5.80 m altitude			
	Parameter increased by 20%		Parameter decreased by 20%	
	O$_2$ (μM)	% change	O$_2$ (μM)	% change
Sorption parameters				
K-NH$_4^+$	257,70	0,06%	257,44	-0,04%
Ammonium oxidation parameters				
K$_N$	257,52	-0,01%	257,39	-0,06%
μ$_N$	257,46	-0,03%	257,65	0,04%
Y$_N$	257,76	0,08%	257,40	-0,05%
Carbon oxidation parameters				
K$_{O,C}$	251,12	-2,49%	264,11	2,55%
μ$_C$	266,07	3,31%	241,22	-6,34%
Y$_C$	266,10	3,32%	241,12	-6,38%
b$_C$	245,15	-4,81%	266,73	3,57%
Sediment characteristics				
SOC	254,74	-1,09%	274,32	6,51%

The maximum oxygen consumption for Well S469, observed at the -5.8 m altitude, was not very dependent on sorption and ammonium oxidation parameters, and varied less than 1% for an increase or decrease in these parameters by 20%.

The oxygen consumption was dependent to some extent on the organic carbon oxidation parameters, varying from 2.5% to near 6.5% when these parameters were varied by ±20%. The decreases in microbial growth rate (μ$_C$) and microbial yield (Y$_C$) for carbon oxidation resulted in

decreases of oxygen consumption of around 6.4%; and the increase in decay rate (b_C) produced a decrease in the oxygen consumption of near 5%.

The initial sorbed organic carbon content (SOC) in the sediments was the parameter to which the model presented higher sensitivity. The increase in SOC by 20% resulted in a decrease of oxygen consumption of 1.09%, and the decrease in SOC by 20% showed an increase of 6.51% in oxygen consumption. Variations in this parameter also modified the simulated arrival time of the oxygen breakthrough. Thus, for the large scale model, the most relevant uncertainty may be the initial sediment´s organic carbon content, representative of the particular altitude and location.

It is important to indicate that more than one good fit was possible to be found with variations within the set of carbon oxidation parameters that represent the characteristics of the microorganisms involved in the organic carbon oxidation (i.e. growth rate, decay rate and bacterial yield). On the other hand, the use of a single calibration value for the sorbed organic carbon content for each model configuration essentially fixed the time for the oxygen breakthrough arrival, accommodated a match between dissolved oxygen concentration distribution and field data.

The results obtained from this sensitivity analysis indicate that the characterization of the microbial communities responsible for the organic carbon oxidation is relevant for the selection of consistent parameters, and thus may contribute to obtain accurate simulations. However, defining a representative value for the sorbed organic carbon content can be considered essential to obtain a good fit between the simulations and the concentration profiles from the field data.

5   Conclusions and recommendations

The goal of this research was to characterize the main processes contributing to oxygen consumption and controlling natural attenuation of the wastewater plume at the area of the Massachusetts Military Reservation in Cape Cod. An existing small-scale model, developed for this site in previous research (Mathisen, et al., in preparation), was used in further model applications, extended to a larger spatial and temporal scale, in order to investigate the variability in the parameters from the small-scale and the applicability of these parameters to fit the large scale applications.

5.1 Small-scale variability

As a first step, before the model extension, the variability in the parameters for different altitudes at the small-scale was investigated. Overall, the simulations presented a good fit to the concentrations distribution from the small-scale tracer test field data, and no variation of the model´s geochemical parameters was required to match simulations to field data for the different locations. Based on this small-scale simulations, it was concluded that both biodegradation processes assumed in the model, nitrification and organic carbon oxidation, were contributing to oxygen consumption. However, for one of the studied altitudes, a manganese oxidation process may also be occurring. This process was not included in the model, and is recommended for future study.

5.2 Model extension

Considerations about model up-scaling, developed in previous research (Carrera, 1993; Heuvelink, 1998), were observed for the configuration of the extended model. These considerations included maintaining the model support (i.e. the selection of similar cell-size), maintaining the configuration of the conceptual model, the use of reliable input data in accordance to the large scale and the variation of the dispersivity according to the large scale application.

For simulating the conditions of the wastewater plume at the large scale, four different representations were applied. The differences were based on the selection of the background and injection ground-water, on the temporal nature of the injection (steady or variable), and on considerations of relevant background solutions. The first configuration included a background solution from 1995 at Well S469, and an injection solution also from 1995 but based on a sample taken at Well S474, up-gradient from the former infiltration beds; the second configuration included the same injection solution, but a background solution from 1996, at Well S469. The third configuration was based on the same injection solution, and included two different background solutions based on samples at Well S469 from 1995 and 1999; and the fourth configuration was based on a background solution collected at Well S469 in 1995, including two successive injection solutions, the first based on a sample from Well S473 in 1995, and the second from Well S474 in 1995.

The extended applications presented an overall good fit to the concentrations distribution profiles from field data after calibration, particularly for the fourth configuration. The successful match for this configuration is likely because the two successive injections used in this case represent the actual conditions of the ground-water entering the zone beneath the former infiltration beds more closely. The organic carbon oxidation process was interpreted to be accounting for the main part of the oxygen consumption at the large scale. Nitrification was suggested to be present, but it was likely occurring at very low rates.

5.3 Investigation of parameters

In regards to the parameters for the extended version of the model, physical parameters were adjusted based on previous research at the Cape Cod site. Among the geochemical parameters, sorption coefficients from the small-scale version were maintained; parameters related to ammonium oxidation from the small-scale model were not varied, and parameters controlling the

organic carbon oxidation process were considered to be fitting parameters and adjusted in calibration. The initial sorbed organic carbon was increased, the growth rate related to the microorganisms responsible of organic carbon oxidation was increased as well, and the decay rate of these microorganisms was decreased after the large scale model calibration.

The large scale model presented high sensitivity to the initial sorbed organic carbon content in the sediments, and moderate sensitivity to growth rate, decay rate and microbial yield of microorganisms responsible for organic carbon oxidation. These results indicated that the main uncertainties for simulating the oxygen consuming processes in development at the large scale are the intial organic carbon content in the sediments, and the features related to the microorganisms responsible for the organic carbon oxidation.

5.4 Characterization of biodegradation processes

The characterization of each of the assumed biodegradation processes (i.e. nitrification and organic carbon oxidation) was supported by the calculation of oxygen consumption rates related to these processes and based on the results obtained in the simulations. The oxygen consumption rates obtained from the large scale simulations were in a range of 1.10 to 1.17 $\mu mol/(L_{aquifer} \times day)$, and was estimated that the nitrification process was accounting for 0.5 to 0.8% of the oxygen consumption, attributing the remaining oxygen consumption to organic carbon oxidation. These results are consistent with the conclusions of Bohlke et al. (2006), where nitrification was suggested to occur in localized zones of mixing of contaminated and uncontaminated ground-water, and to be unimportant in the anoxic zone of the wastewater plume. The former interpretation may represent the situation at the studied location (Well S469) before the contaminant source was removed, because the treated effluent discharge was likely oxic in the lasts 12 years of operation (Parkhurst, et al., 2003), and also after the discharge was stopped and uncontaminated ground-water from up-

gradient began to enter the zone. The nitrification process considered negligible in the anoxic zone may likely represent the conditions after source removal, but before the oxygen breakthrough arrival. Thus, conditions interpreted from the large scale simulations were different from the small-scale situation, where the oxygen consumption rates resulted in a range of 8.9 to 12.8 $\mu mol/(L_{aquifer} \times day)$, and the nitrification process was suggested to account for 57% to 80% of the oxygen consumption, attributing the remaining fraction to organic carbon oxidation.

The smaller-scale conditions associated with the small-scale tracer test likely describes the initial times when ground-water with high dissolved oxygen concentrations enters an anoxic zone of the wastewater plume and, in this situation, nitrification is the dominant process in regards to oxygen consumption. When oxygen concentrations get low, nitrification occurs only at very low rates, possibly because the related microorganisms become dormant, or due to a change in their metabolism (Miller, et al., 2009). This relates to the results obtained for the large scale, where organic carbon oxidation is suggested to be the dominant biodegradation process, at least for a steady situation characterized by low oxygen concentrations. Another possible explanation for the variability in the processes from the small-scale to the large scale may be that the small-scale tracer test was completed a long time after the discharge was stopped, which may be related to sorbed organic carbon being depleted at the studied location by the time of the development of the small-scale tracer test.

In conclusion, the interpretation of the processes observed at both scales suggest that, when the oxic ground-water initially arrived, organic carbon oxidation is likely the dominant oxygen consuming process, and it continues to be dominant until a great portion of the extractable organic carbon gets depleted from the sediments. After this major organic carbon depletion, the nitrification

process may become more relevant, and both biodegradation processes are important once the dissolved oxygen levels are allowed to remain near oxic conditions.

5.5 Recommendations for further research

Recognizing research as an ongoing process, a few considerations about possible needs of further research related to the present study is included next. First, other possible occurring processes, such as denitrification and oxidation of inorganic compounds, may be considered in the model for representing the aquifer´s restoration process at larger scales. Although the oxidation of inorganic compounds will likely not affect the results obtained for the studied location at the large scale, the inclusion of denitrification may refine and give a broader scope to the results obtained in this investigation. Other recommendations for further research include the assessment of the variability in the model parameters, when applied to an active discharge situation of treated wastewater. Finally, the extension of the presented model to three dimensions may be considered, based on the variability observed through the representation of the conditions at different scales.

The results of this thesis should provide a basis for addressing research to characterize the rates and variability of natural attenuation processes associated with wastewater- contaminated subsurface discharges.

6 References

Bedient P.B., Rifai H.S. and Newell C.J. Ground water contamination: transport and remediation [Book]. - [s.l.] : Prentice Hall, 1997. - p. 604.

Bekins B., Rittman B. E. and MacDonald J. A. Natural attenuation strategy for groundwater cleanup focuses on demonstrating cause and effect [Journal]. - [s.l.] : Eos. Transactions American Geophysical Union, 2001. - 5 : Vol. 82. - pp. 53-58.

Bohlke J. K. [et al.] Recharge conditions and flow velocities of contaminated and uncontaminated ground waters at Cape Cod, Massachusetts. Evaluation of $\delta2H$, $\delta18O$, and dissolved gases [Report] : Water Resources Investigation Report / US Geological Survey. - 1999. - pp. 337-348. - 99-4018C.

Bohlke J. K., Smith R. L. and Miller D. N. Ammonium transport and reaction in contaminated groundwater: Application of isotope tracers and isotope fractionation studies [Journal] // Water Resources Research. - 2006. - 5 : Vol. 42.

Bundschuh J., Zilberbrand M. and WATERnetBASE Geochemical modeling of groundwater, vadose and geothermal systems [Book]. - Leiden, The Netherlands : CRC Press/Balkema, 2012.

Carrera J. An overview of uncertainties in modeling groundwater solute transport [Journal] // Journal of contaminant hydrology. - 1993. - 1 : Vol. 13. - pp. 23-48.

Christensen T. H., Bjerg P. L. and Kjeldsen P. Natural attenuation: a feasible approach to remediation of groundwater pollution at landfills? [Journal] // Groundwater Monitoring and Remediation. - 2000. - 1 : Vol. 20. - pp. 69-77.

Duncan J. J. Use of Modflow to simulate the effects of model parameters on groundwater flowpaths near surface water bodies [Report] : Thesis / Worcester Polytechnic Institute. - 1997.

Fitts C. R. Uncertainty in deterministic groundwater transport models due to the assumption of macrodispersive mixing: evidence from the Cape Cod (Massachusetts, U.S.A.) and Borden (Ontario, Canada) tracer tests [Journal] // Journal of Contaminant Hydrology. - 1996. - 23. - pp. 69-84.

Gelhar L. W. Stochastic subsurface hydrology [Book]. - [s.l.] : Prentice-Hall, 1993.

Gordon A. Effects of grid and pond geometry resolution on fluxes and flow paths into surface water bodies [Report] / Civil and Environmental Engineering Department ; Worcester Polytechnic Institute. - 2001.

Hess K. M. [et al.] Multispecies reactive tracer test in an aquifer with spatially variable chemical conditions, Cape Cod, Massachusetts: Dispersive transport of bromide and nickel [Journal] // Water Resources Research. - 2002. - 8 : Vol. 38.

Hess K. M. [et al.] Natural restoration of a sewage-contaminated aquifer, Cape Cod, Massachusetts [Conference] // Hydrology and hydrogeology of urban and urbanizing areas, proceedings of the conference. - Boston, Mass. : [s.n.], 1996.

Heuvelink G. B. Uncertainty analysis in environmental modeling under a change of spatial scale [Journal] // Nutrient cycling in Agroecosystems. - 1998. - 1-3 : Vol. 50. - pp. 255-264.

Kennedy L., Everett J. W. and Gonzalez J. Aqueous and mineral intrinsic bioremediation assessment: natural attenuation [Journal] // Journal of environmental engineering. - 2004. - 9 : Vol. 130. - pp. 942-950.

Kent D. B., Wilkie J. A. and Davis J. A. Modeling the movement of a pH perturbation and its impact on adsorbed zinc and phosphate in a wastewater-contaminated aquifer. [Journal] // Water Resources Research. - 2007. - 7 : Vol. 43.

Khan F.I., Husain T. and Hejazi R. An overview and analysis of site remediation technologies [Journal] // Journal of environmental management. - 2004. - 2 : Vol. 71. - pp. 95-122.

LeBlanc D. R. Sewage plume in a sand and gravel aquifer, Cape Cod, Massachusetts [Report]. - [s.l.] : USGPO, 1984. - No. 2218.

Mathisen P. P. [et al.] Natural-gradient injection experiment and reactive-transport modeling to assess processes leading to oxygen consumption in an anoxic, wastewater-contaminated aquifer, Cape Cod, MA [Report]. - in preparation. - pp. 1-2.

Mathisen P.P. and Chang N. B. Considerations regarding geochemical transformations downstream of subsurface wastewater effluent disposal facilities [Book Section] // Effects of urbanization on groundwater: an engineering case-based approach for sustainable development. - 2010.

Meile C. and Tuncay K. Scale dependence of reaction rates in porous media [Journal] // Advances in Water Resources. - 2006. - 1 : Vol. 29. - pp. 62-71.

Miller D. N. and Smith R. L. Microbial characterization of nitrification in a shallow, nitrogen contaminated aquifer, Cape Cod, Massachusetts and detection of a novel cluster associated with nitrifying Betaproteobacteria [Journal] // Journal of contaminant hydrology. - 2009. - 3 : Vol. 103. - pp. 182-193.

Miller D.N., Smith R. L. and Bohlke J.K. Nitrification in a shallow, nitrogen-contaminated aquifer, Cape Cod, Massachusetts [Report]. - Charleston, South Carolina : U.S. Geological Survey Toxic Substances Hydrology Program. Proceedings of the Technical Meeting, 1999. - pp. 329-335. - Vol. 3.

NRC Natural Attenuation for groundwater remediation [Report] / Committee of Intrinsic Remediation ; National Research Council US. - [s.l.] : National Academies Press, 2000.

Parkhurst D. L., Stollenwerk K. G. and Colman J. A. Reactive-transport simulation of phosphorus in the sewage plume at the Massachusetts Military Reservation, Cape Cod, Massachusetts [Report]. - [s.l.] : US Department of the Interior, US Geological Survey, 2003.

Parkhurst D.L. and Appelo C. A. J. Description of input and examples for PHREEQC version 3-A computer program for speciation, batch-reaction, one-dimensional transport, and inverse geochemical calculations [Book Section] // U.S. Geological Survey Techniques and Methods, book 6. - 2013.

Repert D. A. [et al.] Long-term natural attenuation of carbon and nitrogen within a groundwater plume after removal of the treated wastewater source [Journal] // Environmental science and technology. - 2006. - 4 : Vol. 40. - pp. 1154-1162.

Savoie J. G. [et al.] Groundwater-quality data for a treated-wastewater plume near the Massachusetts Military Reservation, Ashumet Valley, Cape Cod, Massachusetts, 2006-2008 [Report] : U.S. Geological Survey Data Series 648. - 2012. - pp. 11, CD-ROM.

Savoie J.G. [et al.] Ground-water-quality data for a treated-wastewater plume undergoing natural restoration, Ashumet Valley, Cape Cod, Massachusetts, 1994-2004 [Report] / U.S. Geological Survey Data Series 198. - 2006.

Schirmer M. [et al.] Evaluation of biodegradation and dispersion as natural attenuation processes of MTBE and benzene at the Borden field site [Journal] // Physics and Chemistry of the Earth, Part B: Hydrology, Oceans and Atmosphere. - 1999. - 6 : Vol. 24. - pp. 557-560.

Smith R. L. [et al.] Assessing denitrification in groundwater using natural gradient tracer tests with 15N. In situ measurement of a sequiential multistep reaction [Journal] // Water Resources Research. - 2004. - 7 : Vol. 40.

Smith R. L. [et al.] Assessment of nitrification potential in ground water using short term, single-well injection experiments [Journal] // Microbial ecology. - 2006. - 1 : Vol. 51. - pp. 22-35.

Smith R. L. [et al.] In situ stimulation of groundwater denitrification with formate to remediate nitrate contamination [Journal] // Environmental Science and Technology. - 2001. - 1 : Vol. 35. - pp. 196-203.

Smith R. L. [et al.] Long-term groundwater contamination after source removal - The role of sorbed carbon and nitrogen on the rate of reoxygenation of a treated-wastewater plume on Cape Cod, MA, USA [Journal] // Chemical Geology. - 2013. - Vol. 337. - pp. 38-47.

Smith R. L. and Duff J. H. Denitrification in a sand and gravel aquifer [Journal] // Applied and Environmental Microbiology. - 1988. - 5 : Vol. 54. - pp. 1071-1078.

Smith R.L. [et al.] In situ assessment of the transport and microbial consumption in groundwater, Cape Cod, Massachusetts [Conference] // Proceedings of the Technical Meeting / ed. Program US Geological Survey Toxic Substances Hydrology. - Charleston, SC : [s.n.], 1999. - Vol. 3. - pp. 317-322.

Stollenwerk K.G. and Parkhurst D. L. Modeling the evolution and natural remediation of a ground-water sewage plume [Conference] // US Geological Survey Toxic Substances Hydrology Program. Proceedings of the Technical Meeting. - Charleston, South Carolina : [s.n.], 1999. - Vol. 3.

USEPA A citizen´s guide to Monitored Natural Attenuation [Report] / Office of Solid Waste and Emergency Response ; US Environmental Protection Agency. - 2001. - Publication # EPA 542-F-01-004.

USEPA A citizen´s guide to natural attenuation [Report] / Office of Solid Waste and Emergency Response ; US Environmental Protection Agency. - Washington, DC : [s.n.], 1996. - Publication # EPA 542-F-96-016.

van der Heijde P. K. [et al.] Spatial and temporal scales in groundwater modelling [Book]. - [s.l.] : John Wiley and Sons, 1988. - pp. 195-223.

Vermeulen P. T. M., Te Stroet C. B. M. and Heemink A. W. Limitations to upscaling of groundwater flow models dominated by surface water interaction [Journal] // Water resources research. - 2006. - 10 : Vol. 42.

Appendix A

Small-Scale Tracer Test: Summary of Calibration/Verification Simulations at 4.72 m

This research presented in thesis evaluates the processes governing natural attenuation in a subsurface plume of wastewater-contaminated groundwater. The approach involves the analysis of field data collected by the United States Geological Survey (USGS) from an existing wastewater effluent plume at the Toxic Substances Hydrologic Research Site in Cape Cod, Massachusetts. Five years after the cessation of the wastewater effluent discharge at this site, a field experiment consisting of a small-scale tracer test was completed by P. Mathisen and a number of USGS researchers in which clean groundwater was injected in the subsurface below one of the sewage disposal beds that was the original source of the contaminant plume. For this previous research, a reactive transport model was used to characterize the geochemical transport processes at this site. (Mathisen et al., in preparation). Since this research made use of the results from this previously completed field experiment and the transport model (with slight adjustments to the original calibration parameters), some of the basic results are included here. More specially, selected results from the simulations performed for the calibration altitude are presented in this Appendix in order to provide a basis to establish comparisons between the simulations for the original calibration altitude and the results obtained from the application of the small-scale model at different altitudes and locations. The format of plots in this section is consistent with the plots presented in this thesis. Descriptions of the sampling (and associated simulation) locations are included in this thesis. A more detailed description of the tracer test configuration, monitoring, and analysis are provided in Mathisen et al. (in preparation).

Figures A-1 and A-2 show observed and simulated concentration distributions for selected constituents for the original calibration altitude for the small-scale model (4.73 m, referenced to mean sea level), at locations of 4.6 m and 6.2 m from the injection point for the small-scale tracer

test experiment, as well as plots from field data for specific conductance and bromide injection concentrations. These locations were considered representative of a single flow path in previous research (Mathisen et al., in prep.).

The simulations accurately match the dissolved oxygen concentrations for the location at 4.6 m. They also closely match observed dissolved oxygen concentrations at 6.2 m, although a slight underestimation of oxygen consumption is shown for the first days at the location at 6.2 m. The decrease in ammonium concentrations and the corresponding increase in nitrate concentrations indicate that nitrification was occurring at the locations considered to be within the plume. The simulated distributions correspond closely with the observations, and it may be concluded that the nitrification process is likely contributing to oxygen consumption at these locations. The simulations of dissolved inorganic carbon concentrations present a good fit to the field data for all considered locations. Moreover, for these three locations, simulated and observed pH concentrations match closely, which supports the likely development of organic carbon oxidation. In addition, the simulations of sorbed organic carbon concentrations indicate that organic carbon is being utilized throughout the duration of the tracer test. In summary, the results at the altitude of 4.72 m suggest that both, nitrification and organic carbon oxidation, are required to account for the observed oxygen consumption. The results of this test are described in more detail in Mathisen et al. (in preparation).
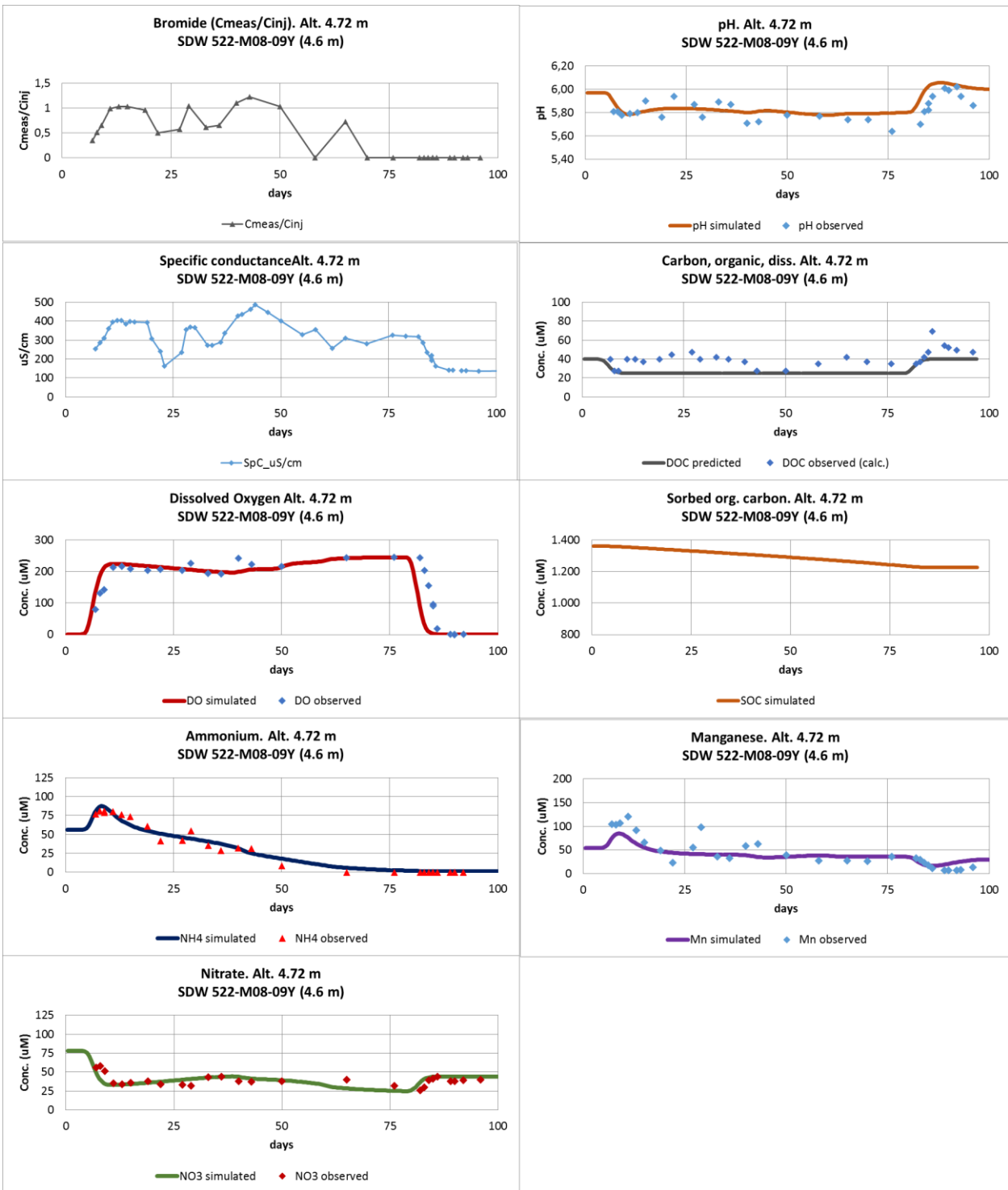
Figure A-1 Simulated and observed concentrations for selected constituents during the experiment's time course, at altitude 4.72 m, for the location at 4.6 m from the injection well
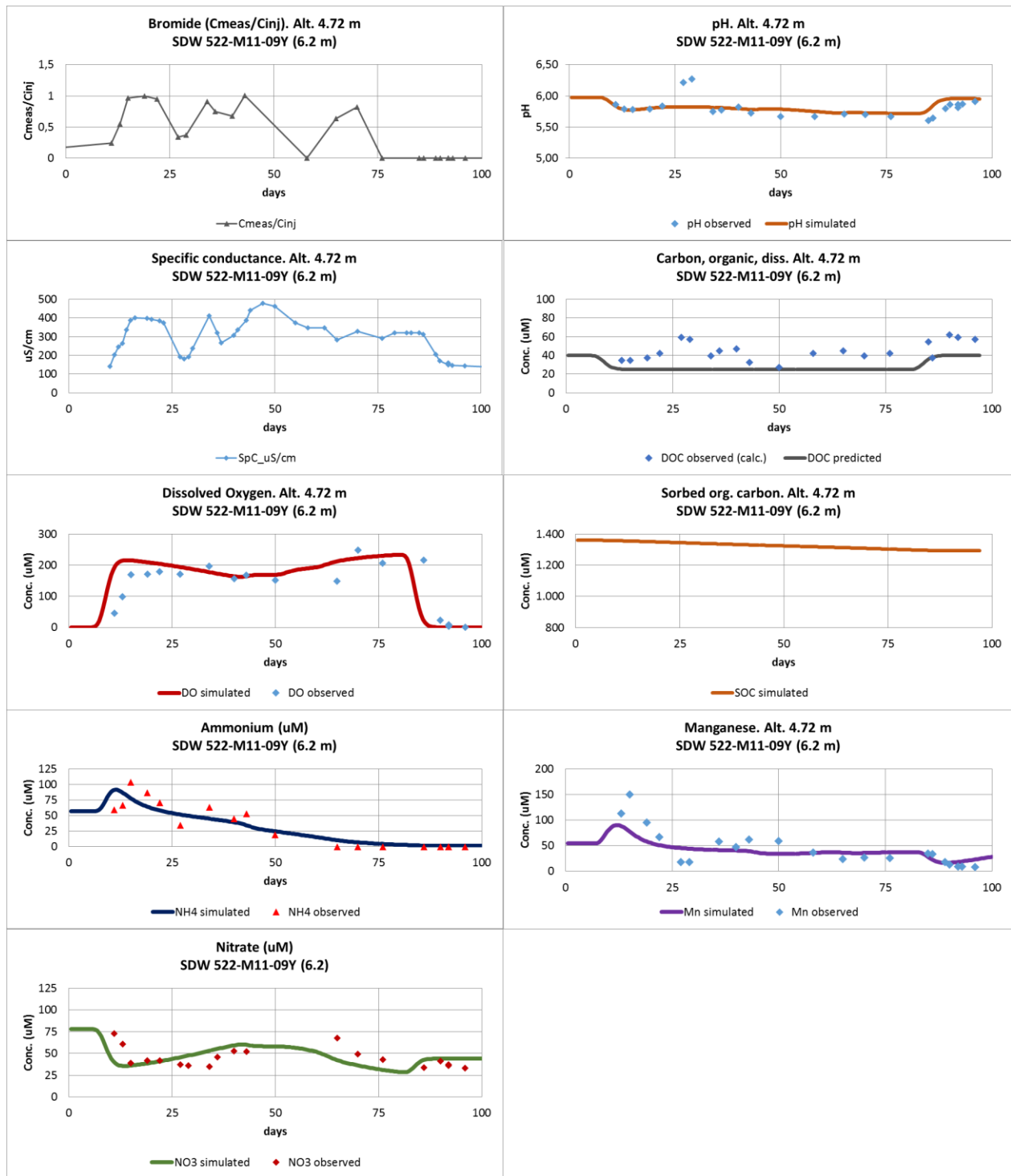
Figure A-2 Simulated and observed concentrations for selected constituents during the experiment's time course, at altitude 4.72 m, for the location at 6.2 m from the injection well

Using the simulation results, the rates corresponding to total oxygen consumption, nitrate generation and inorganic carbon generation are presented here for the calibration altitude and location of 4.6 m from the injection point. It is intended that these rates serve as a basis for comparing the corresponding values obtained for the different altitudes selected for the small-scale variability study.

Table A-1 presents the total oxygen consumption rate, the nitrification rate and the organic carbon oxidation rate, calculated for the 4.72 m altitude at the location at 4.6 m from injection point, based on the simulations. The estimated travel time for these calculations was 5 days. The rates obtained from the small-scale tracer test developed in previous research were reported to be in the range of 0.0017 to 0.0025 μmol (g dry sediment × day)$^{-1}$ (Mathisen, et al., in preparation), which is consistent with these calculations.

Table A-1 Calculated oxygen consumption rates, nitrification rates and organic carbon oxidation rates based on simulated concentrations, for calibration location at the altitude of 4.72 m

	Maximum O_2 consumption (μmol/L)*	O_2 consumption rate (μmol g dry sedim $^{-1}$*day^{-1})	Max NO_3^- generation (μM)**	NO_3^- generation rate (μmol *g dry sedim $^{-1}$*day^{-1})	Max TCO_2 generation (μM)***	TCO_2 generation rate (μmol g dry sedim $^{-1}$ day^{-1})
Simulations Alt. 4.72 m	60.74	**0.0025**	21.00	**0.0009**	90.69	**0.0038**

*maximum consumption corresponding to minimum concentration during the simulation, compared to the injection concentration, shifted with bases on travel time
** based on injection concentration of the model, 27.00 μmol/L
*** based on concentration of S522-0054, 246.10 μmol/L (Mathisen et al., in prep.)

In summary, for the 4.72 m altitude the simulations indicated that ammonium and carbon oxidation account for the oxygen consumption observed in the tracer test. Moreover, one fourth to one third of the oxygen consumption for the different examined locations at this altitude was attributed to nitrification (Mathisen et al., in prep.).